# Antimicrobial proteins for human health

Nahom Ahferom Berhane

Thesis submitted to the

Faculty of Graduate and Postdoctoral Studies

in partial fulfillment of the requirement for

the MSc degree in

Cellular and Molecular medicine

Department of Cellular and Molecular Medicine

Faculty of Medicine

University of Ottawa

## Authorization

**Journalpermissions** Nov 20 (11 days ago)

to me

Dear Nahom,

Thank you for your email. This work is licensed under a Creative Commons Attribution 4.0 International License. **You may reuse this material without obtaining permission from Nature Publishing Group, providing that the author and the original source of publication are fully acknowledged, as per the terms of the license.** The images or other third party material in this article are included in the article's Creative Commons license, unless indicated otherwise in the credit line; if the material is not included under the Creative Commons license, users will need to obtain permission from the license holder to reproduce the material. To view a copy of this license, visit http://creativecommons.org/licenses/by/4.0/.

Kind regards,
Oda

**Oda Siqveland**
Permissions Assistant

**SpringerNature**
The Campus, 4 Crinan Street, London N1 9XW,
United Kingdom
T +44 (0) 207 014 6851

http://www.nature.com
http://www.springer.com
http://www.palgrave.com

**Abstract**

Bacteria are one of the largest causes of human disease, with millions of deaths every year attributed to bacterial infections, and they have become more difficult to tackle with the widespread emergence of antibiotic resistance. In this thesis, I describe my studies that pursued two approaches: one focus was on using antimicrobial histones as an alternative to treatment for antibiotic resistant bacteria; in another approach the recombinant version of an eggshell cuticle protein was expressed and purified for testing against food-safety pathogens.

One major pathogen that is contributing to this challenge of antibiotic resistance is *Staphylococcus aureus*. The methicillin-resistant strain of *S. aureus* leads to increased hospital stays and increased mortality in patients. The impact of such pathogens is worsened when bacteria form surface-attached aggregates known as biofilms. Development of new approaches to eradicate antibiotic- resistant biofilms will benefit human health. This study looked at an alternative method to eradicate bacteria compared to traditional antibiotics. Histones with antimicrobial activity were extracted from chicken blood and tested against methicillin-sensitive and methicillin-resistant strains of *Staphylococcus aureus* biofilm (MSSA and MRSA). The histone mixture completely eradicated both strains in biofilm form at relatively low concentrations. In addition, the histone mixture also displayed fast kill kinetics against planktonic forms of the two strains. Finally, the interaction of the histone mixture with the bacterial membrane in MRSA biofilms was observed by scanning electron microscopy (SEM). Bacteria treated with the histone mixture showed clear morphological changes, including pore formation and cell collapse. Therefore, the histone mixture purified from chicken red blood

cells could prove to be a good alternative to traditional antibiotics for protection against antibiotic-resistant strains of bacteria in their planktonic and biofilm forms.

Reduction of food-borne illness is another important aspect in the promotion of human health. A significant contributor to food-borne illness is contaminated table eggs. The unfertilized egg can be contaminated by a variety of pathogens including *Salmonella* spp. and *Bacillus* spp. The egg is protected by the eggshell which is traversed by respiratory pores that are normally covered by a cuticle plug to restrict pathogen entry. This cuticle consists of several proteins including ovocaxlyin-32 (OCX-32). OCX-32 has a large number of naturally occurring haplotypes due non-synonymous single nucleotide polymorphisms (SNPs). In this study, the goal was to express five of the most common haplotypes of OCX-32 in *Escherichia coli* and purify the recombinant protein for assay of its antimicrobial activity. Five constructs that contain the cDNA of common OCX-32 haplotypes (A, B, C, D, and O) with a histidine tag at the C-terminus were generated. The constructs were subcloned into pGEX4T-1 vector which encodes Glutathione-S-transferase (GST) upstream of the multiple cloning site. My study developed methods to optimize the expression conditions, and to increase the solubility of the recombinant protein. Various expression strains of *E. coli* and solubility buffers were tested. In addition, the construct was subcloned into a plasmid containing the small ubiquitin-like modifier (SUMO) fusion tag; the solubility of the new SUMO-OCX-32 haplotype A recombinant fusion protein was evaluated. The best results were obtained by slow dialysis refolding of denatured SUMO-OCX-32 fusion protein. This recombinant protein showed almost complete solubility with minimal precipitation and was tested against the egg-related pathogen, *Bacillus*

*cereus.* Unfortunately, the SUMO-OCX-32 recombinant protein did not inhibit growth of *B. cereus*.

In my studies reported in this thesis, two very different approaches were taken. A histone mixture was isolated from an abundant starting material, which proved to be highly effective and promising in the eradication of *S. aureus* biofilms at relatively low concentrations. Alternatively, expression of a soluble recombinant protein for functional activity assay was very challenging and required the optimization of a number of methods to prepare soluble protein for testing. One of the methods tested proved effective in obtaining large amounts of soluble protein. However, further developmental work will be essential to determine if this approach is a viable strategy in acquiring functional protein.

## Table of contents

**Authorization** ... ii
**Abstract** ... iii
**Table of contents** ... vi
**List of Figures** ... ix
**List of abbreviations** ... xii
**Acknowledgments** ... xiv
**Chapter 1** ... 1
**General introduction** ... 1
**1.1 Bacterial structure and impacts in human health** ... 2
**1.2 Antibiotic resistance** ... 4
**1.3 Bacterial Biofilms** ... 5
**1.4 Cationic antimicrobial peptides** ... 7
**1.5 Histones** ... 8
**1.6 Importance of the pathogen-free table egg** ... 12
**1.7 Ovocalxyin-32, an eggshell cuticle protein** ... 18
**1.8 Protein expression and refolding** ... 19
**1.9 Hypothesis and objectives** ... 24
**1.10 Outline of the thesis** ... 24
**Chapter 2** ... 26
**A Histone mixture from chicken erythrocytes inhibits Methicillin-resistant and methicillin-sensitive *Staphylococcus aureus* biofilms** ... 26
**1. Materials and methods** ... 27
1.1 Histone mixture extraction ... 27
1.2 Determination of minimum biofilm eradication concentration ... 28
1.3 Time kill kinetics for planktonic MSSA and MRSA ... 29
1.4 Scanning electron microscopy ... 29
1.5 Statistical analyses ... 30
**2. Results** ... 30
2.1 Minimum biofilm eradication concentration and log inhibition for MSSA and MRSA ... 30
2.2 Kill kinetics for planktonic MSSA and MRSA treated with histone mixture ... 36
2.3 Effect of histone mixture on MRSA bacterial surface ... 39

**Chapter 3** ..... 41
**Expression and purification of recombinant Ovocalyxin-32 for antimicrobial testing** ..... 41
**1. Materials and methods** ..... 42
1.1 Ovocalxyin-32 fusion protein constructs ..... 42
1.2 Optimization of expression for OCX-32 fusion protein ..... 42
1.3 His-tag purification using on-column refolding ..... 43
1.4 Bacterial transformation procedure ..... 45
1.5 Solubility testing of induced recombinant protein ..... 45
1.6 Protein tag change through plasmid subcloning ..... 46
1.7 His-tagged recombinant protein purification in denaturing conditions ..... 49
1.8 Dialysis Procedure ..... 49
1.9 Protein quantification ..... 50
1.10 Determination of Minimum inhibitory concentration (MIC) through broth microdilution assay ..... 50
**2. Results** ..... 52
2.1 Optimization of expression conditions ..... 52
2.2 On-column refolding ..... 57
2.3 Evaluation of change in expression strain ..... 60
2.4 Evaluation of fusion partner change to Small ubiquitin-like modifier (SUMO) ..... 64
2.5 Dialysis refolding for GST-OCX-32 ..... 67
2.6 SUMO-OCX-32 dialysis refolding and antimicrobial activity test ..... 73
**Supplementary** ..... 77
**Chapter 4** ..... 86
**General Discussion** ..... 86
**References** ..... 100

**List of Tables**

**Chapter 2**

**Table 1**. MIC and MBEC values of histone mixture against methicillin-sensitive and resistant *S. aureus*..... 32

**Chapter 3**

**Table S1**. Buffers used for Bugbuster mix ..... 84

**Table S2**. Nucleotide sequence of PCR primers used for DNA sequencing and verification of ligation. ..... 85

**List of Figures**

**Chapter 1**

**Figure 1**. 15% SDS-PAGE analysis for histone mixture extracted from chicken erythrocytes..... 11

**Figure 2**. Eggshell structure in cross-section view with major components labelled. ..... 17

**Figure 3**. Protein sequence for the OCX-32 constructs used in the study. ..... 22

**Figure 4**. The vector used for expressing the OCX-32 haplotypes which are inserted between BamHI and EcoRI site ..... 23

**Chapter 2**

**Figure 5**. Dose-dependent growth inhibition of Methicillin-sensitive *Staphylococcus aureus* (MSSA) biofilm by increasing concentrations of histone mixture. ..... 33

**Figure 6**. Dose-dependent growth inhibition of Methicillin-resistant *Staphylococcus aureus* (MRSA) biofilm by increasing concentrations of histone mixture. ..... 34

**Figure 7**. Inhibition of MSSA and MRSA biofilms by the histone mixture ..... 35

**Figure 8**. Time Kill kinetics for planktonic MSSA treated with histone mixture. ..... 37

**Figure 9**. Time Kill kinetics for planktonic MRSA treated with the histone mixture. ..... 38

**Figure 10**. Scanning electron microscopy of MRSA biofilms. ..... 40

**Chapter 3**

**Figure 11**. Schematic depiction of OCX-32 construct in pSMT3 plasmid. ..... **Error! Bookmark not defined.**

**Figure 12**. Western blot analysis of protein expression at various incubation temperatures following induction. ..... 54

**Figure 13**. Western blot analysis of protein expression for various IPTG concentrations. ..... 55

**Figure 14**. Western blot analysis of protein expression for various incubation times following induction. ..... 56

**Figure 15**. SDS-PAGE analysis for elutions of GST-OCX-32 haplotype O and B from on-column refolding. ..... 58

**Figure 16.** Coomassie Blue stained SDS-PAGE (12.5%) to evaluate elution of GST-OCX-32 under denaturing conditions from nickel affinity column. ..... 59

**Figure 17**. Coomassie Blue-stained SDS-PAGE (12.5%) solubility analysis for *E. coli* RIL (1ml cultures) transformed with GST-OCX-32 haplotype A construct..... 61

**Figure 18**. Coomassie Blue-stained SDS-PAGE (12.5%) solubility analysis for *E. coli* Rosetta (1ml cultures) transformed with GST-OCX-32 haplotype A construct..... 62

**Figure 19**. Coomassie Blue-stained SDS-PAGE (12.5%) solubility analysis for *E. coli* Origami 2 (1ml cultures) transformed with GST-OCX-32 haplotype A construct. ..... 63

**Figure 20**. 2% agarose gel analysis for PCR samples for OCX-32 insert ligated into pSMT3 plasmid, no insert control positive control and no template negative control. ..... 65

**Figure 21**. Coomassie Blue-stained SDS-PAGE (12.5%) solubility analysis for *E. coli* Rosetta (1ml cultures) transformed with SUMO-OCX-32 haplotype A construct. ..... 66

**Figure 22**. SDS-PAGE analysis for dialysis refolding of GST-OCX-32 haplotype A. ..... 69

**Figure 23**. SDS-PAGE analysis for dialysis refolding of GST-OCX-32 haplotype A. ..... 70

**Figure 24**. SDS-PAGE analysis for dialysis refolding of GST-OCX-32 haplotype A. ..... 71

**Figure 25.** Time-dependent growth of Gram-positive *B. cereus* under different conditions and at 2 concentrations of GST-OCX-32 haplotype A. ..... 72

**Figure 26.** SDS-PAGE analysis for dialysis refolding of SUMO-OCX-32 haplotype A. ..... 74

**Figure 27.** SDS-PAGE analysis for dialysis refolding of SUMO-OCX-32 haplotype A. ..... 75

**Figure 28.** Dose-dependent growth inhibition of Gram-positive *B. cereus* bacteria versus SUMO-OCX-32 haplotype A. ..... 76

**Supplementary**

**Figure S1.** Proteomics analysis for all 5 haplotypes of 50kDa GST-OCX-32 recombinant protein band. ..... 77

**Figure S2.** Dose-dependent effect of imidazole on *Salmonella enterica* serovar Enteritidis growth. ..... 78

**Figure S3.** Western blot analysis labelled with anti-GST antibody for *E. coli* Rosetta solubility test with various buffers. ..... 79

**Figure S4.** Western blot analysis labelled with anti-GST antibody for *E. coli* RIL solubility test with various buffers. ..... 80

**Figure S5.** Time-dependent growth of Gram-positive *S. aureus* bacteria in presence of GST-OCX-32 haplotype A. ..... 81

**Figure S6.** Time-dependent growth of Gram-positive *B. cereus* bacteria in presence of GST-OCX-32 haplotype A. ..... 82

**Figure S7.** Effect of EDTA on *B. cereus* growth ..... 83

**List of abbreviations**

AAFC – Agriculture and Agri-food Canada

AMP – antimicrobial peptide

ANOVA – Analysis of Variance

ATCC – American Type Culture Collection

BCA – Bicinchoninic Acid

BME – β-mercaptoethanol

BSA – Bovine Serum Albumin

CAMA - cecropin (1-7)–melittin A (2-9) amide

CAMP – Cationic Antimicrobial Peptide

CDC – Centers for Disease Control and Prevention

cDNA – Complementary Deoxyribonucleic Acid

CFIA – Canadian Food Inspection Agency

CFU – Colony forming unit

DNA – Deoxyribonucleic Acid

DTT – Dithiothreitol

EDTA – Ethylenediaminetetraacetic Acid

EPS – Extracellular Polymeric Substance

FDA – Food and Drug Administration

GnHCl – Guanidine Hydrochloride

GST – Glutathione-S-Transferase

HCl – Hydrochloric Acid

HMDS – Hexamethyldisilizane

LB – Luria-Bertani

LPS – Lipopolysaccharides

LTS – Lipoteichoic Acid

MBEC – Minimum Biofilm Eradication Concentration

MIC – Minimum Inhibitory Concentration

MRSA – Methicillin-resistant *Staphylococcus aureus*

MSSA – Methicillin-sensitive *Staphylococcus aureus*

NETs – Neutrophil Extracellular Traps

NIH – National Institutes of Health

OCX– Ovocalyxin

OD – Optical density

PBS – Phosphate Buffered Saline

R & D – Research and Development

RARRES1 – Retinoic Acid Receptor Responder 1

RBC – Red Blood Cells

SD – Standard Deviation

SDS – Sodium Dodecyl Sulfate

SDS-PAGE – Sodium Dodecyl Sulfate-Polyacrylamide Gel Electrophoresis

SEC – Size Exclusion Chromatography

SEM – Scanning Electron Microscopy

spp. – Species

SUMO – Small Ubiquitin-like Modifier

SNP – Single Nucleotide Polymorphism

TCA – Trichloroacetic Acid

tRNA – Transfer Ribonucleic Acid

Ulp1 – Ubiquitin-like-specific protease 1

WHO – World Health Organization

**Acknowledgments**

First of all, I would like to thank my thesis supervisor and mentor, Dr. Maxwell Hincke. Without his unending support and guidance, none of this would have been possible. I would like to offer him my sincerest gratitude for allowing me to work in his lab and gain valuable experience as a co-op student and later as a graduate student.

I would also like to thank the members of my thesis advisory committee, Dr. Laura Trinkle-Mulcahy and Dr. Jean-François Couture for their great advice and comments that helped guide the project.

I would like to offer my sincere thanks to Dr. Garima Kulshreshtha and Dr. Megan Rose-Martel for their mentorship and help in my project. Their guidance has been invaluable. I am also grateful to fellow my lab mates and friends; Joelle Jodoin, Garima Kulshreshtha and Nicholas Calvert for making the graduate school experience more entertaining and encouraging. I would also like to thank Samantha Brixi and Harold Lu for their help in the project through their great ideas and late afternoons. I would also like to thank Dr. Tamer Ahmed for his encouragement and support throughout my studies.

Next, I would like to thank Dr. Jean-François Couture for his comments and suggestions on possible avenues of the project. I am also grateful for his generous gift of *E. coli* expression strains and plasmid. I would also like to thank members of his lab, and especially Monika Joshi and Sabina Sarvan for their assistance with troubleshooting and plasmid ligation.

I would also like to thank Tom Henderson's Meats and Abattoir Inc. and Laplante Poultry Farms Ltd. for their generous donation of fresh poultry blood which was essential for the project. The

research was funded by US Poultry, Canadian Poultry Research Council (CPRC), Natural Sciences and Engineering Research Council of Canada (NSERC), Livestock Research Innovation Corporation (LRIC) with help from Burnbrae farms and Hy-Line International.

Finally, I am thankful for my friends and family especially my mom, Sara, who made great sacrifices to ensure my success in life. This accomplishment wouldn't have been possible without her tireless support. I am also grateful to my sister, Saba, for her friendship and keeping me sane throughout the experience. I would also like to thank my brother, Sirak, for all the laughs and being a great roommate all these years. I would also like to thank my dad, Ahferom, for getting us to Canada and instilling the value of education.

# Chapter 1

# General introduction

**1.1 Bacterial structure and impacts in human health**

Bacteria are amongst the most numerous organisms in the world, with an estimated $10^7$-$10^9$ species, of which less than 100 are known human pathogens (Schloss and Handelsman, 2004). Bacteria can be classified into two major classes according to their structure: Gram-positive and Gram-negative. Gram-positive bacteria retain Gram stain due to their thick peptidoglycan layer and contain surface protein such as lipoteichoic acid (LTA) that can interact with the immune system (Akira, 2001). Gram-positive bacteria result in many common infections such as otitis media (*Streptococcus pneumoniae*), skin infections (*Staphylococcus aureus*) and necrotizing fasciitis (*Streptococcus pyogenes*). Gram-negative bacteria do not retain the Gram stain after washing and contain an outer membrane layer over a thin peptidoglycan layer. These bacteria contain surface proteins known as lipopolysaccharides (LPS) which can act as an endotoxin through the Lipid A component (Ramachandran, 2014). Gram-negative bacteria are implicated in many infections such as the water borne illness, cholera, transmitted by *Vibrio cholerae.* Other examples include food borne bacteria such as *E. coli* that can result in diarrhea and other symptoms as well as the sexually transmitted *Neisseria gonorrhoeae* which is responsible for the disease gonorrhea (NIH, 2016).

Bacteria are one of the largest causes of human illness worldwide, with the Gram-positive *Clostridium difficile* alone leading to about 14,000 deaths per year in the United States according to the Centers for Disease control and Prevention (CDC) (CDC, 2013b). Prevalence of certain bacterial disease such as diarrhea, which are caused by various Gram-negative bacteria such as *E. coli* and *Campylobacter jejuni,* can be attributed to poor levels of sanitation leading to

increased infant mortality (Gavazzi et al., 2004). Other bacterial infections such as methicillin-resistant *Staphylococcus aureus* (MRSA) have become more problematic in hospital settings where resistance to established antibiotics is prevalent (CDC, 2016b). According to the CDC, antibiotic resistance adds an extra $20 billion per year to the US healthcare system and leads to 23,000 deaths per year (CDC, 2013a, 2013b). Thus, infectious diseases remain a major problem worldwide, whether the issues arise due to inadequate sanitation for treatable infections or through the healthcare setting for antibiotic resistant infections.

Another major problem associated with bacteria is food safety. There are about 4 million cases of food-related illness each year in Canada, which include major pathogens such as *E. coli, Salmonella* spp.*,* and *Listeria* spp. (CFIA, 2013). These contaminants affect many food products including red meat, poultry, eggs, dairy, and seafood. Salmonella alone causes 88,000 illnesses and 17 deaths per year in Canada, while *E. coli* O157:H7 causes 12,800 illnesses and 8 deaths (Public Health Agency of Canada, 2016). The problem of ensuring food safety is challenging due to the widespread nature of bacterial contamination.

This thesis will focus on two topics of infectious antibiotic resistant bacteria affecting human health, as well as protection of the egg from food-safety pathogens. Chapter 2 looks at methicillin-sensitive and resistant strains of *Staphylococcus aureus* affecting human health directly through antibiotic resistance, as well as via formation of biofilms. The study focused on antimicrobial histone mixture isolated from chicken erythrocytes as a possible treatment against these pathogenic bacteria. Chapter 3 focuses on bacterial pathogens affecting food safety, mainly *Bacillus cereus.* This section of the project emphasized the protection of egg

sterility by investigating the antimicrobial activity of haplotype of an eggshell cuticle protein, Ovocaxlyin-32.

### 1.2 Antibiotic resistance

Antibiotic resistance is the major reason that various bacteria are re-emerging as a health problem in recent years. This has been due to overuse of antibiotics in agriculture as well as improper usage in humans, including over-prescription, and incomplete dosages. Bacteria acquire resistance mostly through horizontal transfer, mutations or conjugative transposons in their chromosomes (Neu, 1992). This resistance to a growing number of antibiotics leads to higher mortality rates as well as extra costs in healthcare (Health Canada and Public Health Agency of Canada 2014). In recent years, there have been problems with pathogens such as *Neisseria gonorrhoeae,* which has shown resistance to last resort antibiotics in at least 10 countries including Canada (WHO, 2017).*Neisseria gonorrhoeae,* along with *Clostridium difficile* and Carbapenem-resistant Enterobacteriaceae, are considered urgent threats according to the CDC (CDC, 2017a). Another pathogen of major concern is the Gram-positive bacterium *Staphylococcus aureus*, with the CDC classifying it as serious threat; it is associated with 11,285 deaths per year in the US (CDC, 2017a). This pathogen rapidly acquired resistance to β-lactam antibiotics such as penicillin in the 1940s, which forced the development of a semi-synthetic antibiotic version, methicillin, to combat the problem in the 1960s (Lyon and Skurray, 1987). However, methicillin-resistant *Staphylococcus aureus* (MRSA) emerged widely in the 1980s (Neu, 1992). The methicillin-resistant strain of *S. aureus,* compared to the methicillin-sensitive strain, leads to longer hospital stays as well as increased mortality rates (Lodise and McKinnon, 2007). In Canadian hospitals, there has been a 17-fold increase in MRSA infections between

1995-2007 (Simor et al., 2010). The methicillin-resistant strain can cause skin infections as well as lung infections. In addition, the pathogen can be problematic in hospital settings leading to central line-associated bloodstream infections and pneumonia (Centers for Disease Control and Prevention, 2016).

Moreover, there has been a large decrease in the rate of discovery of new antibiotics over the last few decades, with a 56% reduction in new Food and Drug Administration (FDA) approved antibiotics comparing 1998-2002 to 1983-1987 (Conly and Johnston, 2005). This decline in research into new antibiotics has been attributed to the nature of antibiotics which are only taken until the infection clears and then completely stopped (Conly and Johnston, 2005). Thus, pharmaceutical companies face difficulty in recovering R & D investment, compared to other pharmaceuticals. In addition, when a new class of antibiotics with potent activity is approved, they are often not used widely in order to save them for a last resort treatment (Conly and Johnston, 2005). This further decreases the incentives for companies to develop new antibiotics, particularly for new classes of antibiotics with novel bacterial targets.

### 1.3 Bacterial Biofilms

Antibiotic resistance is further exacerbated in surface aggregates of bacteria. Such aggregates are known as biofilms and consist mainly of a matrix of Extracellular Polymeric Substance (EPS) that is highly hydrated. The EPS contains polysaccharides, proteins and extracellular DNA (Flemming et al., 2007). The matrix make up to 90% of the mass of the biofilm and is responsible for bacterial adhesion to a surface (Flemming and Wingender, 2010). The rest of the mass is made up of the microbes themselves. Other functions of the EPS include, but are not limited to, aggregation of bacterial cells and cohesion of biofilms; it can also serve as a

nutrient source (Flemming and Wingender, 2010). Motile bacteria encased in biofilms move in a different manner, and their growth is slower than their planktonic counterparts (O'Toole et al., 2000). The change in their type of movement is due to expression of a gene that regulates pili instead of the regular flagellar gene. For example, *Pseudomonas aeruginosa* uses pili type IV when it is in biofilm form to move along a surface in a twitching motion, in contrast with flagellar motion when in planktonic form (O'Toole et al., 2000). The pili type IV also helps late colonizers, as these bacterial cells climb over the existing biofilm and settle on the top (Høiby et al., 2010).

In addition, bacterial metabolism in biofilms becomes heterogeneous, leading to slower activity within the interior of the biofilm compared to cells in the outer zones (Ciofu et al., 2017). Therefore, the interior bacteria tend to be more anaerobic while the faster growing bacteria on the outside are aerobic. This can affect the efficacy of antibiotics directed against these biofilms. For example, β-lactams, aminoglycosides and fluoroquinolones are not effective against bacteria growing in a low oxygen environment (Bjarnsholt et al., 2013). Thus, bacteria in biofilm form can be more resistant to antibiotics by 100-1000 fold when compared to planktonic bacteria (Høiby et al., 2010). Therefore, treatment is very difficult, especially when the growth occurs in medical devices such as catheters, prosthetic heart valves and orthopaedic devices (Stewart and Costerton, 2001). In many cases, the only way to completely eradicate the biofilm becomes removal of the device. As a result, many antibiotic options are not available when treating chronic biofilm infections. Therefore, the discovery of alternative antibacterial solutions for treating biofilms is a priority.

### 1.4 Cationic antimicrobial peptides

One alternative to traditional antibiotics is antimicrobial peptides, which are constituents of the natural innate defence system found in many organisms (eg. LL-37 in humans, indolicidin in cattle, and magainins in amphibians have been identified) (Brogden, 2005). These belong to a major class of compounds known as cationic antimicrobial peptides (CAMPs). Such peptides interact strongly with the negatively charged head groups of bacterial membranes, including phosphatidyl serine, phosphatidyl glycerol and phosphoethanolamine, through electrostatic interactions, as opposed to the neutral head groups that predominate in eukaryotic membranes (Zasloff, 2002; Band and Weiss, 2015). Through similar electrostatic interactions, CAMPs can bind to the major outer membrane component of Gram-negative bacteria, lipopolysaccharides (LPS) (Matsuzaki, 1999). They also have similar interaction with lipoteichoic acid (LTA), a major constituent of the Gram-positive cell wall (Scott et al., 1999). CAMP peptides also contain hydrophobic residues which can allow them to enter the lipid bilayer (Brogden, 2005). In addition, CAMPs act as host immunomodulation compounds without direct effect on the bacteria (Peschel and Sahl, 2006). Some CAMPs such as nisin can directly bind to bacterial receptors, such as lipid II which is important in peptidoglycan synthesis, in addition to forming specific pores (Yeaman and Yount, 2003; Sass et al., 2008). Therefore, nisin inhibits peptidoglycan synthesis, which can explain why it is more active against Gram-positive bacteria (Yeaman and Yount, 2003; Sass et al., 2008). It is thought that bacteria have more difficulty in developing resistance to such molecules since changes in the fundamental properties of their membrane would be required. CAMPs such as magainins from the skin of African clawed frog and buforin from the stomach lumen of the Asian toad display broad-spectrum antimicrobial

activity *in vitro* versus various pathogens such as *E. coli., Salmonella typhimurium, Streptococcus pyogenes, Bacillus subtilis,* and *Staphylococcus aureus* ( Zasloff, 1987; Zasloff et al., 1988; Kim et al., 2000; Park et al., 2000). The type of interaction of such peptides with the cell membrane depends on the ratio of peptide molecules to lipids in the membrane of the bacteria. At high peptide concentrations, the peptides bind in a perpendicular manner to the membrane bilayer and form pores. At lower ratio of peptide to lipid, the peptide molecules insert into the bilayer directly, becoming inactive but leading to physical thinning of the bilayer (Brogden, 2005). In addition to bacterial membrane damage or insertion, CAMPs can also reduce bacterial viability through inhibition of nucleic acid synthesis, inhibition of proteases or inhibition of protein synthesis (Kawasaki and Iwamuro, 2008).

**1.5 Histones**

The class of antimicrobial peptides with positive charges also includes histones. Histones are major components of the nucleosome that are organized in an octameric fashion and function to package DNA. Histones structures are also dynamic since they can be modified in many ways such as lysine methylation or acetylation to change levels of access to DNA during transcription (Zentner and Henikoff, 2013). Histones isolated from calf thymus were first shown to have antimicrobial activity (Hirsch, 1958). The study looked at lysine rich histone A and arginine rich histone B. Histone B fraction showed antimicrobial activity against diverse bacteria including *E. coli* K12, *Klebsiella pneumoniae* C, *S. typhimurium, S. aureus* and *P. aeruginosa* (Hirsch, 1958). Histones with antimicrobial activity have since been isolated from various sources such as shrimp, fish, frogs as well as mammals (Kawasaki and Iwamuro, 2008). They share many characteristics of CAMPs such as an overall positive charge and amphipathic α-helical structures

(Zasloff, 2002). Histones are also a large component of neutrophil extracellular traps (NETs) that form when neutrophils release their granule contents, including histones and cytoplasmic proteins, at the site of infection (Brinkmann and Zychlinsky, 2012). NETs are part of the innate immune response, as neutrophils respond to pathogens such as *S. aureus* and *E. coli* by trapping them and preventing the spread of infection (Brinkmann and Zychlinsky, 2012).

Histones can be isolated from any nucleated cell. Non-mammalian vertebrate erythrocytes contain a nucleus, unlike fully differentiated mammalian erythrocytes, which lose their nucleus after final maturation (Schwartz and Stansbury, 1954). This feature permits mammalian RBCs to squeeze through the smaller capillary beds found in the mammalian vascular system. Mammalian red blood cells are biconcave in overall shape, while nucleated erythrocytes from avian, amphibian, fish, and reptile species are biconvex (Cohen, 1982; Götting and Nikinmaa, 2015). Therefore, nucleated RBCs from blood of these vertebrates can be a good source for the purification of histones. One convenient source is chicken blood, which is normally an abattoir waste product, from which up to 50mg of histones per 200ml of blood can be prepared (Peterson and Hansen, 2008). Histones isolated from chicken nucleated erythrocytes contain H2A, H2B, H3 and H4 as core histones in addition to the linker histones, H1 and H5 (Rose-Martel et al., 2017) (**Figure 1**). This histone mixture displays broad-spectrum antimicrobial activity against both Gram-positive and Gram-negative bacteria (Rose-Martel and Hincke, 2014). This histone mixture also binds to lipoteichoic acids (LTA) of Gram-positive bacteria and lipopolysaccharides (LPS) of Gram-negative bacteria (Rose-Martel and Hincke, 2014). In the first section of this study (Chapter 2), we investigated a defined histone mixture (H1, H2A, H2B, H3, H4 and H5), extracted from chicken RBCs, as a biofilm eradication compound against both

methicillin-sensitive and methicillin-resistant species of *S. aureus.* In addition, the kinetics of bactericidal activity of the histone mixture against planktonic forms of the two strains was investigated. Lastly, the mechanism of the histone effect on the bacterial surface when encased in biofilm EPS was studied through scanning electron microscopy.

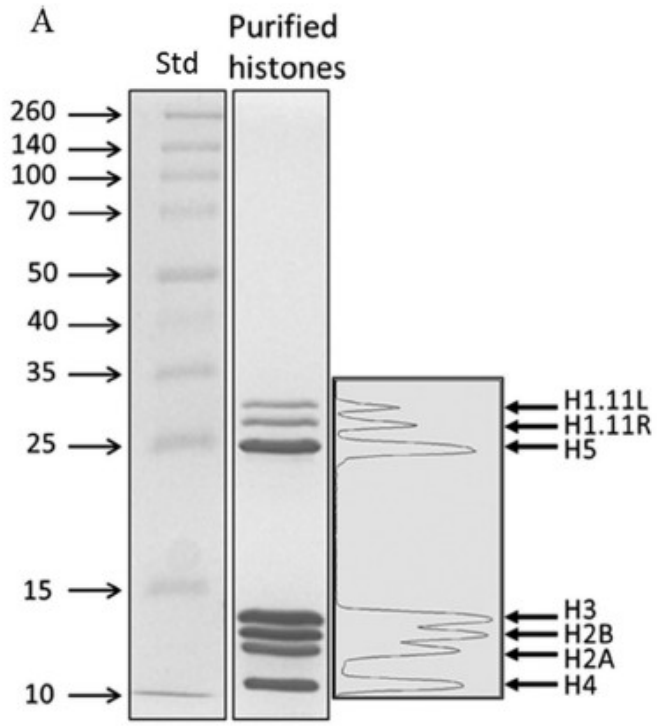


**Figure 1. 15% SDS-PAGE analysis for histone mixture extracted from chicken erythrocytes.** The densitometry for each of the bands is also shown. Figure adapted from Figure 1 of Rose-Martel et. al 2017.

### 1.6 Importance of the pathogen-free table egg

The chicken egg is a major food product with a rich nutritional content, including proteins, cholesterol, essential fatty acids as well as vitamins and minerals. It is a widely consumed food in Canada with per capita consumption of 238.8 eggs per year (AAFC, 2017). Compared to egg white, the yolk provides higher amounts of nutrition in most categories except for potassium, magnesium and sodium (Iannotti et al., 2014). Structurally, the avian egg consists of several layers starting with the innermost yolk, albumen, eggshell membranes, mammillary cone layer, palisades, vertical crystal layer and cuticle (Hincke et al., 2012). The eggshell is traversed with thousands of respiratory pores that permit gaseous exchange of metabolic oxygen and carbon dioxide associated with the developing embryo (Sparks and Board, 1984). The respiratory pores are covered by a plug of cuticle material, which constitutes the uncalcified outermost layer of the eggshell (Hincke et al., 2012).

Eggshell formation is a strictly controlled process during the passage of a forming egg along the length of the oviduct. The yolk is first formed in the ovary and progresses through the infundibulum to acquire the vitelline membrane which surrounds it. The albumin is deposited as the forming egg passes through the magnum, followed by the assembly of the eggshell membranes in the white isthmus segment. The eggshell membranes become the foundation upon which eggshell mineralization occurs. The final process of mineralization occurs in the uterus where the mammillary cones, palisade layer, vertical crystal layer and the cuticle are sequentially deposited (Hincke et al., 2012; Rose-Martel and Hincke, 2017). The mineralization process takes place in the uterine fluid during about 20h (Gautron et al., 2001). The acellular environment of the uterine fluid contains the inorganic components of the eggshell as well as

the precursors of eggshell matrix. The protein profile of the uterine fluid varies according to the stage of eggshell formation, with egg white proteins such as ovalbumin and ovotransferrin at higher concentration in the initiation phase, whereas lysozyme, ovocleidin-17, ovocalyxin-21, ovocalyxin-32, ovocalyxin-36, and ovocledin-116 are enriched at the growth stage (Dominguez-Vera et al., 2000). The cuticle material is finally deposited during the terminal phase of mineralization. Finally, the egg is expulsed from the vagina (oviposition) (Hincke et al., 2012).

The chicken egg contains innate physical and chemical barriers at every layer to protect the embryo from pathogens (Rose-Martel and Hincke, 2017). Unlike the rest of the eggshell, the cuticle is not completely mineralized; its outer layer is non-mineralized, and the inner layer contains hydroxyapatite-containing vesicles (Rose-martel et al., 2012). The non-mineralized outer layer contains mainly proteins as well as polysaccharides and lipids (Rose-Martel and Hincke, 2017). The cuticle of the chicken eggshell has a thickness between 0 and 10µm (Rose-martel et al., 2012). Eggs laid with incomplete cuticle have an increased vulnerability to bacterial penetration (Bruce and Drysdale, 1994). Another function of the eggshell cuticle is to control water movement by forming a plug which blocks the mouth of each respiratory pore and restricts the loss of water from the egg interior. This also prevents water uptake that could transfer bacteria to the interior when eggs are stored in cooler humid conditions (Bruce and Drysdale, 1994; Wellman-Labadie et al., 2008). Proteomics studies have demonstrated that the most abundant cuticle proteins include: ovocalyxin-32 (OCX-32), ovocalyxin-36 (OCX-36), ovocalyxin-25(OCX-25), ovocleidin-116, clusterin, and lysozyme C (Rose-martel et al., 2012). The function of some of these proteins have already been studied. For example, OCX-36 possesses antimicrobial activity against *Staphylococcus aureus* and exhibits significant dose-

dependent binding of *E. coli* O111:B4 lipopolysaccharide (LPS) (Cordeiro et al., 2013). OCX-25 has sequence similarities to Kunitz-like protease inhibitor, which is predicted to display antimicrobial activity by inhibiting bacterial proteases (Rose-martel et al., 2012). Lysozyme C is found in both the outer eggshell as well as the cuticle (Wellman-Labadie et al., 2008). Lysozyme C has antimicrobial activity against Gram-positive food-borne bacteria such as *Clostridium botulinum* and *Listeria monocytogenes* (Hughey and Johnson, 1987). Ovocleidin-116 is found abundantly in the palisades and plays a role in eggshell mineralization (Dunn et al., 2009). The palisade layer contains more than 500 proteins, including ovocleidin-116, ovocleidin-17, osteopontin, ovocalyxin-36, ovocaxlyin-21 and clusterin (Hincke et al., 2012). Ovalbumin, lysozyme, ovotransferrin, ovocalyxin-36 and clusterin are among the proteins found in the mammillary cones and the eggshell membranes (Rose-Martel et al., 2012; Ahmed et al., 2017).

Chicken eggs are a key feature in the development of therapeutics such as the growth of viruses used in vaccines. For example, the flu vaccine against seasonal influenza is grown in fertilized eggs, to prepare both the inactivated vaccine and the live attenuated vaccine. Eggs are injected with the virus which is allowed to replicate and then later harvested (CDC, 2016a). The chicken egg is also useful since its yolk contains large amounts of IgY immunoglobulin (Marcq et al., 2013). The hen produces these specific antibodies to protect the chick against environmental pathogens. The hen is injected with specific antigens in order to produce large quantities of specific IgYs that are deposited in the egg yolk. The whole yolk, or the purified IgY fraction can be used in feed for passive immunization of other animals (Marcq et al., 2013). Therefore, due to the economic, nutritional and health benefits of the chicken egg, it is very important to have an egg that is reliably free of pathogens.

Egg contamination is a common cause of food poisoning, with 1.02 million cases of *Salmonella* infections estimated in the US every year (Scallan et al., 2011). The egg and especially the yolk is a source of nutrients that support bacterial growth; consequently, if a contaminated egg is not cooked properly, it can lead to food poisoning. There are two possible routes for egg contamination by *Salmonella.* Bacterial colonization within the hen oviduct can occur prior to the egg acquiring the eggshell (vertical transmission). These bacteria originate within reproductive system of the contaminated chicken or migrate from other organs (Berrang et al., 1999). This mechanism allows more efficient colonization of the yolk compared to other possible routes of infection. Infection can also occur immediately after oviposition (egg expulsion from the body of the hen) before the cuticle hardens on the freshly laid egg (horizontal transmission). Such contamination can be due to bacteria from the alimentary canal contaminating the cloaca, the orifice which is the common endpoint of the digestive, reproductive and urinary tracts (Keller et al., 1995). Horizontal transmission from environmental bacteria can also occur. This may arise due to contaminated feces and other particles on the surface where the eggs are deposited after laying (Gantois et al., 2009). *Salmonella* and other pathogens found in feces and in the egg production environment may penetrate the eggshell through microcracks on the shell surface, or through the eggshell respiratory pores that span the entire eggshell (Hincke et al., 2012). The penetration of pathogens can be enhanced when there is a temperature difference between the body temperature of the hen (42$^{o}$C) and the environment. This differential temperature after the egg is laid creates a negative pressure across the eggshell, where contraction of the egg contents pulls surface moisture and bacteria into the interior (Berrang et al., 1999). The cuticle covers

these pores and can protect against pathogen entry. Commercial eggs for human consumption in North America, Australia and Japan are washed to remove surface contamination (Gole et al., 2014). The washing process damages the cuticle layer and may contribute to *Salmonella* contamination if drying and storage is not conducted appropriately. The amount of total cuticle proteins present on washed eggs was found to be about 1/3 of unwashed eggs (Rose-martel et al., 2012; Kulshreshtha et al., 2018). However, washing does not reduce the thickness of the cuticle uniformly over the eggshell surface. While the problem of contamination in the production environment has been greatly reduced by implementation of stricter policies for egg producing facilities, contamination can still occur during egg washing and food processing (Patrick et al., 2004). Other pathogens that have been detected in eggs include *Staphylococcus* spp., *Pseudomonas* spp., *Bacillus* spp., *Micrococcus* spp., and *Escherichia* spp. Gram-negative bacteria are more commonly found in the interior of decaying eggs, whereas Gram-positive bacteria can tolerate the dry exterior environment of the egg (Board and Tranter, 1986). Thus, an intact cuticle and eggshell are dramatically important barriers to reduce bacterial penetration.

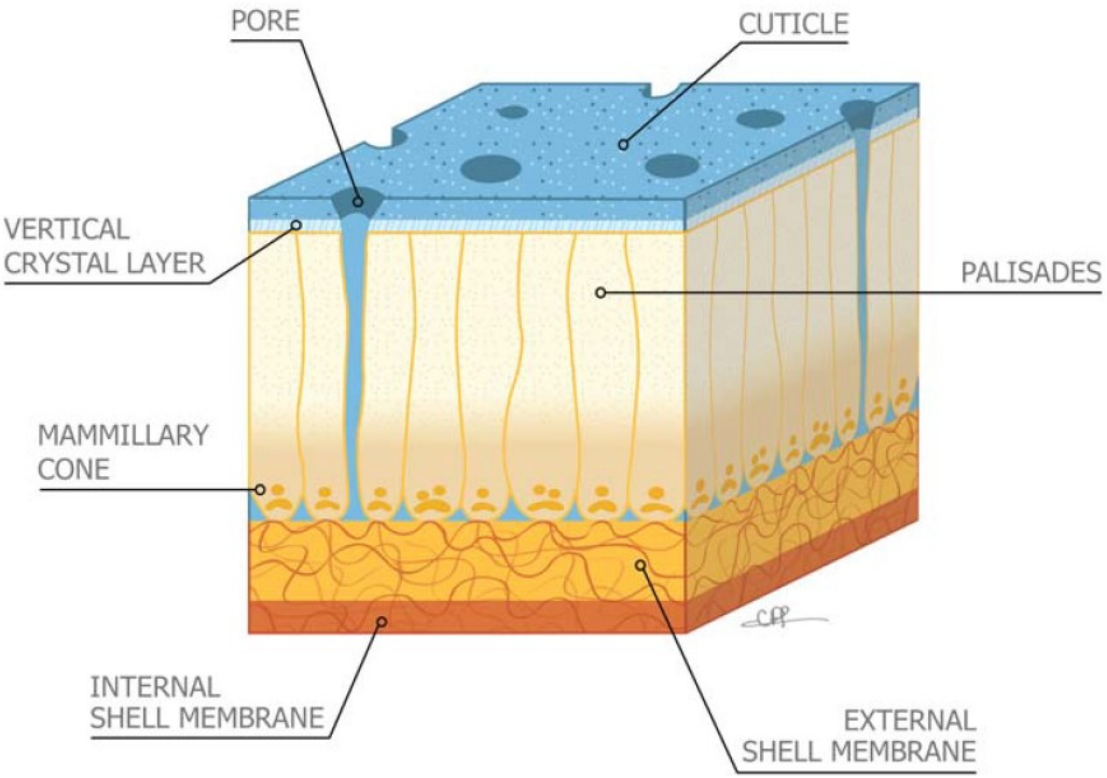


**Figure 2. Eggshell structure in cross-section view with major components labelled.** Adapted from Figure 4 of Hincke et al. 2012.

### 1.7 Ovocalxyin-32, an eggshell cuticle protein

Ovocalyxin-32 (OCX-32) is one of the most abundant cuticle proteins and is also found in the vertical crystal layer as well as the outer palisade layer (Gautron et al., 2001). It is encoded by the *Gallus gallus* (chicken) gene, *RARRES1* (NCBI, 2017). OCX-32 has 32% amino acid identity with its human ortholog, retinoic acid receptor-responsive gene (*TIG1*) (Gautron et al., 2001). Due to its abundance in the cuticle, OCX-32 has been proposed as a potential candidate to defend against invading pathogens.

OCX-32 also possesses partial amino acid sequence similarity to latexin (an inhibitor of carboxypeptidase A activity) (Hincke et al., 2003). In previous work, it was shown that recombinant Glutathione S-tranferase-OCX-32 inhibits bovine carboxypeptidase A activity. In addition, GST-OCX-32 also significantly inhibited the growth of Gram-positive *Bacillus subtilis* at 100 µg/ml, compared to the GST negative control (Xing et al., 2007). Therefore, it was proposed that through its role as a peptidase inhibitor, OCX-32 may serve as an antimicrobial protein by inhibiting bacterial proteases. This is important since peptidases such as metallopeptidases found in bacteria have key roles in the life cycle of bacteria; finding new ways of targeting and inhibiting these peptidases could be one approach to control bacterial pathogens (Supuran, 2012). In addition, proteases can boost the pathogenicity of bacteria by improving its survival capacity in the infected host through breakdown of immunoglobulins and components of the complement system in the host (Maeda and Yamamoto, 1996; Travis and Potempa, 2000).

As many as 28 total single nucleotide polymorphisms (SNPs) have been identified within the OCX-32 gene. Of these, 21 are within the exons and 18 are non-synonymous (Fulton et al.,

2012a). SNPs that are associated together within the same exon allow the identification of haplotypes through complete or partial linkage disequilibrium. OCX-32 polymorphisms have been correlated with egg weight, puncture score and other factors that are important egg production variables, although differences in cuticle properties were not assessed or reported (Fulton et al., 2012a).

**1.8 Protein expression and refolding**

The most common protein expression system that is currently used is *Escherichia coli*, which is very low-cost to maintain and grow, as well as to produce at very high cell density (Rosano and Ceccarelli, 2014). In addition, *E. coli* is one of most thoroughly studied organisms with its full genome published in 1997 (Blattner et al., 1997). Many lab and pathogenic strains of this bacterium are currently in widespread use in laboratories. Thus, it is a good candidate system for heterologous expression of proteins. However, *E. coli* also has a major drawback due to absence of any post translational modification machinery. In addition, production of a heterologous protein in large quantities can lead to sequestration of the recombinant protein in inclusion bodies (Hannig and Makrides, 1998). These bodies are made up of insoluble protein and contain the over-expressed protein of interest in relatively pure form. The over-expressed protein is in aggregated form and can be separated from the rest of the soluble bacterial proteins through cell lysis and centrifugation to harvest inclusion bodies in the pellet. However, during inclusion body purification, insoluble contaminants may also be present such as outer membrane proteins, which can be removed using low concentration chaotropic agents and detergents following cell lysis (Vallejo and Rinas, 2004). Purified inclusion bodies are soluble in high concentrations of chaotropic agents such as urea and guanidine hydrochloride. However,

expressed proteins from inclusion bodies then need to be effectively refolded to obtain native protein for subsequent activity assays.

A major problem during refolding is formation of aggregates due to non-native disulfide bond formation between cysteines that can be intermolecular or intramolecular, the latter of which is usually the rate-limiting step (Okumura et al., 2011). Thus, reducing agents are required to inhibit the formation of non-native disulfide bridges. The reducing agents are usually removed from the solution before final refolding steps to allow the native disulfide bonds to form. The addition of oxidized and reduced glutathione during refolding can be beneficial, as the oxidized form can act as oxidizing agent in forming disulfide bonds while the reduced glutathione acts as reducing agent that can break non-native disulfide bonds, leading to disulfide shuffling that permits correct protein folding (Okumura et al., 2011). In addition, the intermediate step between denatured and native protein heavily favors the aggregated state. This is especially the case where the starting concentration of protein is relatively high. In terms of kinetics, the correct folding towards native protein is first order reaction while the misfolding reaction is second order or higher. Thus, the aggregated state tends to be favored. Due to this issue, the starting concentration of protein needs to be as low as possible. However, a limitation for using very low concentration of protein can be the requirement of vast amounts of dialysis buffer to get any useful amounts of protein (Okumura et al., 2011).

In the second section of the thesis (Chapter 3), I describe my project to express and purify recombinant GST-OCX-32 fusion proteins representing the 4 most prevalent haplotypes (A-D) of ovocalyxin-32, as well as the originally described variant (O) (Fulton et al., 2013; Xing *et al.* 2007) (**Figure 3**). Several methods were evaluated to increase the solubility of the expressed

protein including changes in bacterial expression strain and an alternative protein tag. The expressed protein was refolded using both on-column refolding and dialysis to evaluate whether speed of denaturant removal affects protein solubility. Potential antimicrobial activity of a purified recombinant protein was tested against a food-safety pathogen, *B. cereus*.

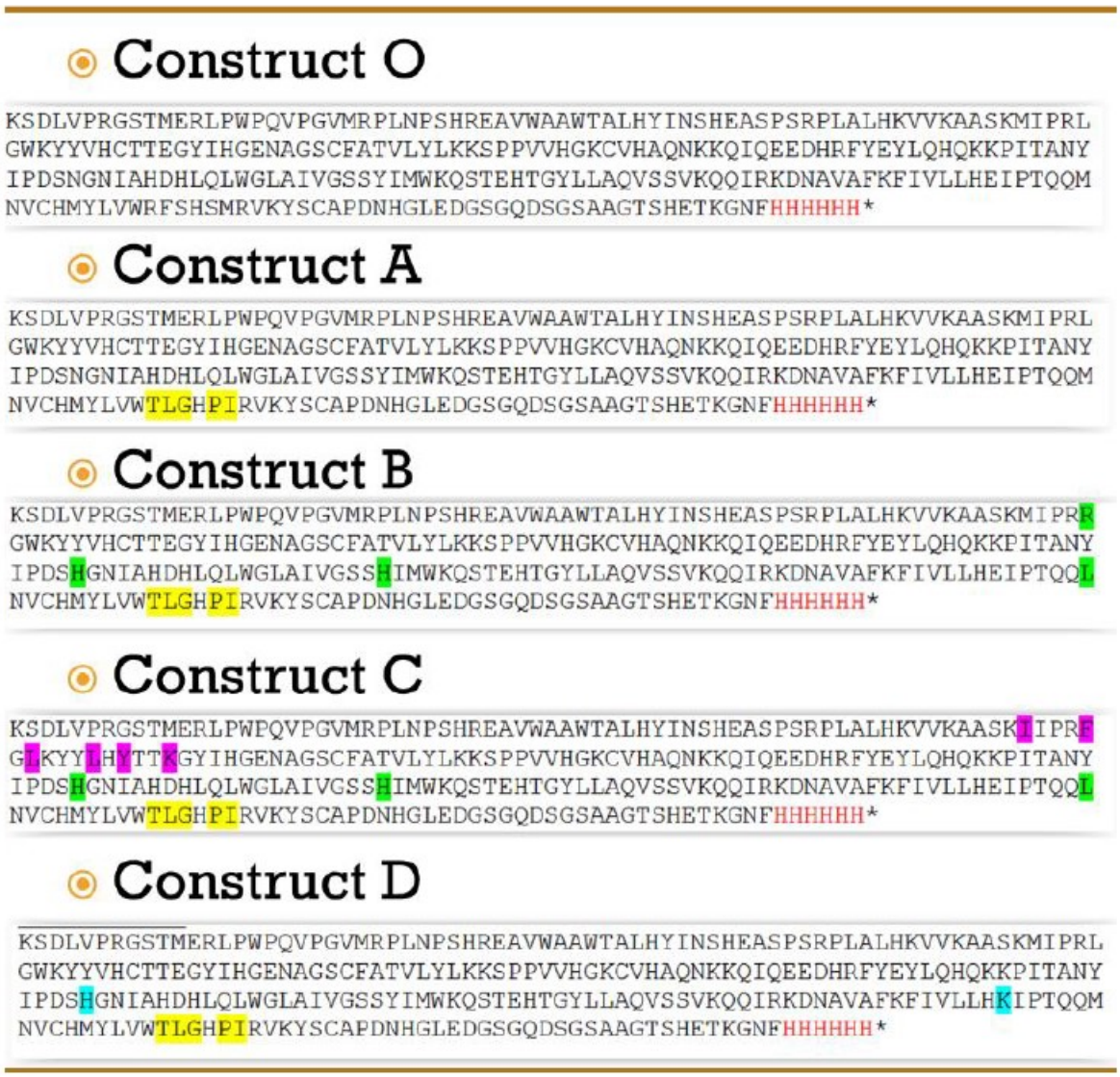


**Figure 3. Protein sequence for the OCX-32 constructs used in the study.** Construct O corresponds to the recombinant protein initially purified by (Xing et al., 2007). The 6xHis sequence is encoded at the C-terminus (red text) while the N-terminus shows the last 10 residues of the glutathione S-transferase(GST) tag. The highlighted residues were obtained by site directed mutagenesis (Mutagenex Inc.) and correspond to the various haplotypes arising from non-synonymous SNPs (Fulton et al., 2012b). Asterisk (*) indicates stop codon.

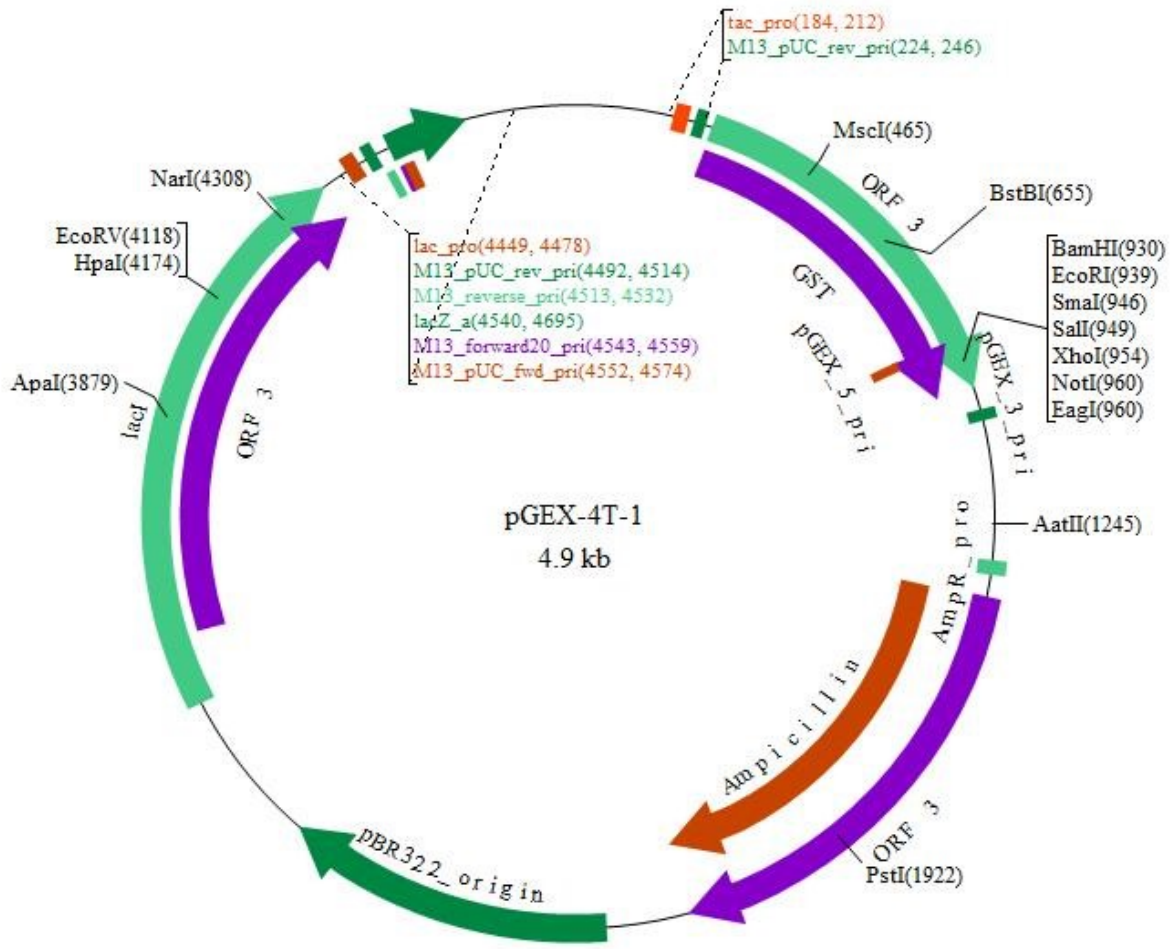


**Figure 4. The vector used for expressing the OCX-32 haplotypes which are inserted between BamHI and EcoRI sites.** Note the GST encoded sequence on the top right which flanks the N terminus of the OCX-32 cDNA. The ampicillin resistance gene is in orange. Figure adapted from BVTech Plasmid, 2017.

### 1.9 Hypothesis and objectives

Hypothesis 1: The histone mixture extracted from chicken erythrocytes is a source of antimicrobial molecules that are effective against antibiotic-resistant bacteria. This hypothesis was tested by comparing histone activity against methicillin-sensitive and resistant *Staphylococcus aureus* species.

Objectives: (1) Determine the minimum biofilm eradication concentration of histone mixture against methicillin-sensitive and resistant *Staphylococcus aureus.* (2) Assess the biocidal activity of the histone mixture against planktonic methicillin-sensitive and resistant *Staphylococcus aureus* by using kill kinetics assays. (3) Observe possible interaction of the histone mixture with the bacterial membrane using scanning electron microscopy, to determine a possible mechanism of action.

Hypothesis 2: Naturally occurring haplotypes of ovocalyxin-32 have differences in antimicrobial activity.

Objectives: (1) Optimize the expression conditions of recombinant ovocalyxin-32 in *E. coli*. (2) Purify soluble protein following over-expression of the protein. (3) Test antimicrobial activity against the food pathogen, *Bacillus cereus*.

### 1.10 Outline of the thesis

The first part of the thesis (Chapter 2) will describe my role in the investigation of the antibiofilm activity of histone mixture extracted from chicken erythrocytes. My focus was to determine the minimum biofilm eradication concentration (MBEC), and study kill kinetics

against planktonic forms of methicillin-sensitive and resistant *Staphylococcus aureus*. In addition, I investigated the histone mixture interaction with the bacterial membrane, as assessed by scanning electron microscopy.

The second part of the thesis (Chapter 3) will report my work to optimize the expression and purification of soluble recombinant ovocalyxin-32 in *E. coli*. My main focus consisted of investigating issues of solubility using different refolding methods, as well as various expression strains of *E. coli,* in addition to testing alternative protein fusion partners.

The final part of thesis (Chapter 4) is a general discussion describing the importance of developing novel antimicrobial agents that are effective against antibiotic – resistant against proteins. Moreover, I discuss the difficulties faced in heterologous expression of recombinant proteins in the bacterial expression system.

# Chapter 2

# A Histone mixture from chicken erythrocytes inhibits Methicillin-resistant and methicillin-sensitive *Staphylococcus aureus* biofilms

**(The results in this chapter have been published in Scientific reports in April 2017 under "Histones from Avian Erythrocytes Exhibit Antibiofilm activity against methicillin-sensitive and methicillin-resistant *Staphylococcus aureus*).**

Rose-Martel, M., Kulshreshtha, G., Berhane, N.A., Jodoin, J. and Hincke, M.T. (2017) Histones from Avian Erythrocytes Exhibit Antibiofilm activity against methicillin-sensitive and methicillin-resistant Staphylococcus aureus. Scientific Reports, 2017 Apr 5; 7: 45980. doi: 10.1038/srep45980.

## 1. Materials and methods

### 1.1 Histone mixture extraction

The first part of the thesis focuses on utilizing histone mixture from chicken erythrocytes to be used as an antimicrobial agent against antibiotic resistant bacteria. The following protocol was developed in a previous study (Rose-Martel and Hincke, 2014). Blood was collected from white rock chickens that were euthanized at a local slaughterhouse in accordance with Canadian Food Inspection Agency (CFIA) regulations. The blood was immediately mixed with 1.5mg/ml EDTA. The collected whole blood was centrifuged, and the erythrocytes pelleted. The erythrocytes were washed with PBS. The red blood cells (RBC) from 100ml of blood were lysed with total of 1L of hypotonic lysis buffer (10mM Tris-HCl, 1mM KCl, 1.5mM $MgCl_2$, 1mM DTT pH 8.0) for 1h at 4$^{o}$C. The sample was centrifuged at 10,000 x g for 10min at 4$^{o}$C and resuspended in hypotonic lysis buffer. Following 3-4 rounds of resuspension in lysis buffer, the hemoglobin and other soluble proteins were removed. The absence of hemoglobin was verified through spectral scan of samples from each round of centrifugation (300-500nm). The pellet from the final round was resuspended in 400ml of 0.4N $H_2SO_4$ and agitated for 1h at 4$^{o}$C. Following complete re-suspension in the acid, the histones were precipitated by addition of 133ml 100% trichloroacetic acid (TCA) drop-wise (Fisher Scientific). The mixture was incubated at 4$^{o}$C for 1h and centrifuged to pellet the precipitated histones at 16,000xg for 10min at 4$^{o}$C. The histones were washed with cold acetone three times and finally centrifuged at 16,000xg for 5min at 4$^{o}$C. The histone pellet was dissolved in 100ml of sterile water and passed through 3kDa MWCO Amicon ultra centrifugal unit (Millipore Sigma). Following filtration, the retained protein was freeze dried overnight using a VirTis BenchTop Freeze dryer (SP Scientific).

1.2 Determination of minimum biofilm eradication concentration

MSSA (ATCC 6538) and MRSA (ATCC 29247) were obtained from Centre for Research and Environmental Microbiology, University of Ottawa (CREM).

Single colonies were taken from LB agar plates and grown in LB broth overnight at 37$^{o}$C and 250rpm. The overnight culture was regrown in 1:50 dilution in LB broth until exponential phase was obtained ($OD_{600}$=0.2). The bacteria were pelleted and resuspended in LB broth to obtain $10^5$ – $10^6$ CFU/ml. 150 µl of the culture was plated on MBEC plate containing pegs on the lid and grown for 24h at 37$^{o}$C and 100rpm (Innovotech). The biofilm on the lid of plate was washed in 96-well plate containing PBS pH 7.4. The lid was immersed in 96-well plate containing 200µl histone mixture dissolved in sterile water pH 7.4, kanamycin, and sterile water for 2h at 37$^{o}$C and 100rpm. The histone mixture concentration was determined using the bicinchoninic acid (BCA) assay (Pierce, Thermofisher). The biofilm on the pegs was washed twice in PBS as described above. The peg-laden biofilms were immersed in the wells of a 96-well plate containing 200 µl of LB broth and sonicated for 10min to dislodge any bacteria. The lid with pegs was replaced with a sterile lid and the LB plate was incubated for 24h with continuous shaking and measuring absorbance at 600nm every 30min using an Eon microplate spectrophotometer (BioTek). Serial dilutions of uninhibited control were used to generate standard curves. The standard curves were used to calculate log bacterial inhibition for each histone concentration.

1.3 Time kill kinetics for planktonic MSSA and MRSA

Bacteria were grown until exponential phase as described in section 2.2. After centrifugation, the bacterial pellet washed in PBS, and finally re-suspended in PBS pH 7.4. The bacteria were diluted in PBS to obtain $10^5 – 10^6$ CFU/ml and incubated at a 1:1 ratio (100µl total) with increasing concentrations of histone mixture at 37$^o$C and 200rpm. Indolicidin was a positive control for inhibition, at its previously determined minimum inhibitory concentration. Sterile water was used as a negative control for inhibition. The bacteria were incubated for various durations (0, 5, 22.5, 45, 90, 180 min) and plated in 96-well plates. LB broth (100µl) was added to each well after the incubation periods and the plates were monitored for 16h with continuous shaking and measuring of absorbance at 600nm every 30min using Eon microplate spectrophotometer (BioTek). Serial dilutions of uninhibited control bacteria generated standard curves used to calculate the CFU/ml values. Each trial had their own independent standard curve.

1.4 Scanning electron microscopy

Bacteria were grown in the same protocol as section 2.2. Instead of growing biofilm in pegs, the adjusted bacterial suspension in LB (250 µl) was pipetted into the wells of a48-well plate that contained filter membranes (0.22 µm pore size, MilliporeSigma). The plate containing the filters were incubated for 24h at 37$^o$C and 150 rpm. The LB broth was removed, and the filters were rinsed with PBS to remove planktonic bacteria. Histone mixture dissolved in water (128 µg/ml) was added to the filters, with sterile water alone as a negative control (300µl). The filters were incubated for 2h at 37$^o$C and 100rpm. The histone mixture was removed, and the sample was rinsed twice with PBS as described above. The filters were removed from the 48-well plate,

placed in small glass flasks, and fixed with 5% glutaraldehyde in 0.1M sodium cacodylate, pH 7.5 (VWR) at 4$^{o}$C overnight. The glutaraldehyde was aspirated, and the filters were dehydrated using ethanol washes of 20, 40, 60, 80, 90, 95 and twice in 100% for 10 min each. The filter membranes were chemically dried using 1:2 hexamethyldisilizane (HMDS):100% ethanol, 2:1 and 100% HMDS for 10min each, followed by air drying overnight. The next day, the filters were gold coated and visualized using a Tescan Vega-II XMU VPSEM instrument (Nano Imaging Facility, Carleton University, Ottawa).

1.5 Statistical analyses

Statistical analysis was done using Student's T-test to analyze significance for log inhibition of biofilm bacteria with various concentrations of histone mixture. Student's T-test was also used to determine statistical significance between MIC and MBEC values of histone mixture treatment against planktonic and biofilm forms of the two strains.

For the time kill kinetics, the data distribution was analyzed using MINITAB 17 (PA, USA). Data showing normal distribution were compared using ANOVA. Tukey's test was used to compare the differences between least square means. Standard deviation (SD) was reported with the mean values. A p value of ≤ 0.05 was necessary for statistical significance.

**2. Results**

2.1 Minimum biofilm eradication concentration and log inhibition for MSSA and MRSA

Following acid extraction of histone mixture, mature biofilms were challenged with serially diluted concentrations of histones and monitored for an additional 24h. For MSSA, the histone mixture showed large increases in lag time at 8 and 16 µg/ml histone mixture, indicating

bacterial growth inhibition (**Figure 5**). The biofilm was completely eradicated at 32 μg/ml histone mixture or higher. The methicillin-resistant strain showed similar susceptibility, with 8 and 16 μg/ml histone mixture showing inhibited growth curves compared to untreated control, and complete eradication at 32 μg/ml (**Figure 6**)**.** Three trials were performed; the MBEC for MSSA was determined to be 21±5 μg/ml while the MBEC for MRSA was 23±5 μg/ml (**Table 1**). These MBEC values were significantly higher than the previously determined minimum inhibitory concentrations (MICs) for planktonic forms of the two strains. MSSA had a MIC of 6±1 μg/ml and MRSA had a similar MIC of 8±2 μg/ml (Rose-Martel and Hincke, 2014) (**Table 1**). Sterile water was used as a control for uninhibited growth and kanamycin 2mg/ml was used as a positive control for inhibition. All MBEC experiments were done using 3 biological replicates, as well as 3 technical replicates for each trial. The MBEC curves shown are representative curves from one trial of each strain (**Figures 5 and 6**).

MSSA biofilms were significantly inhibited at 8 μg/ml ($p \leq 0.002$) (**Figure 7**). At 32 μg/ml and higher, there was no bacterial growth detected (>9 $\log_{10}$ reduction compared to untreated bacteria). MRSA showed significant inhibition at 16 μg/ml of histone mixture ($p \leq 0.0001$) (**Figure 7**). At 32 μg/ml and higher, MRSA showed no bacterial growth (>5$\log_{10}$ reduction compared to untreated bacteria). Thus, the MRSA shows more resistance at lower concentration of histones (8 μg/ml) while both strains show similar susceptibility at higher concentrations.

**Table 1. Minimum inhibitory concentration (MIC) values of histone mixture against methicillin-sensitive and resistant S. aureus** (Rose-Martel and Hincke, 2014**). Minimum biofilm eradication concentration (MBEC) values of histone mixture against MSSA and MRSA.** The results are average of 3 independent trials in triplicate (average ± SD).

| | **MIC (µg/ml)** | **MBEC (µg/ml)** |
|---|---|---|
| **MSSA** | 6±1 | 21±5 |
| **MRSA** | 8±2 | 23±5 |

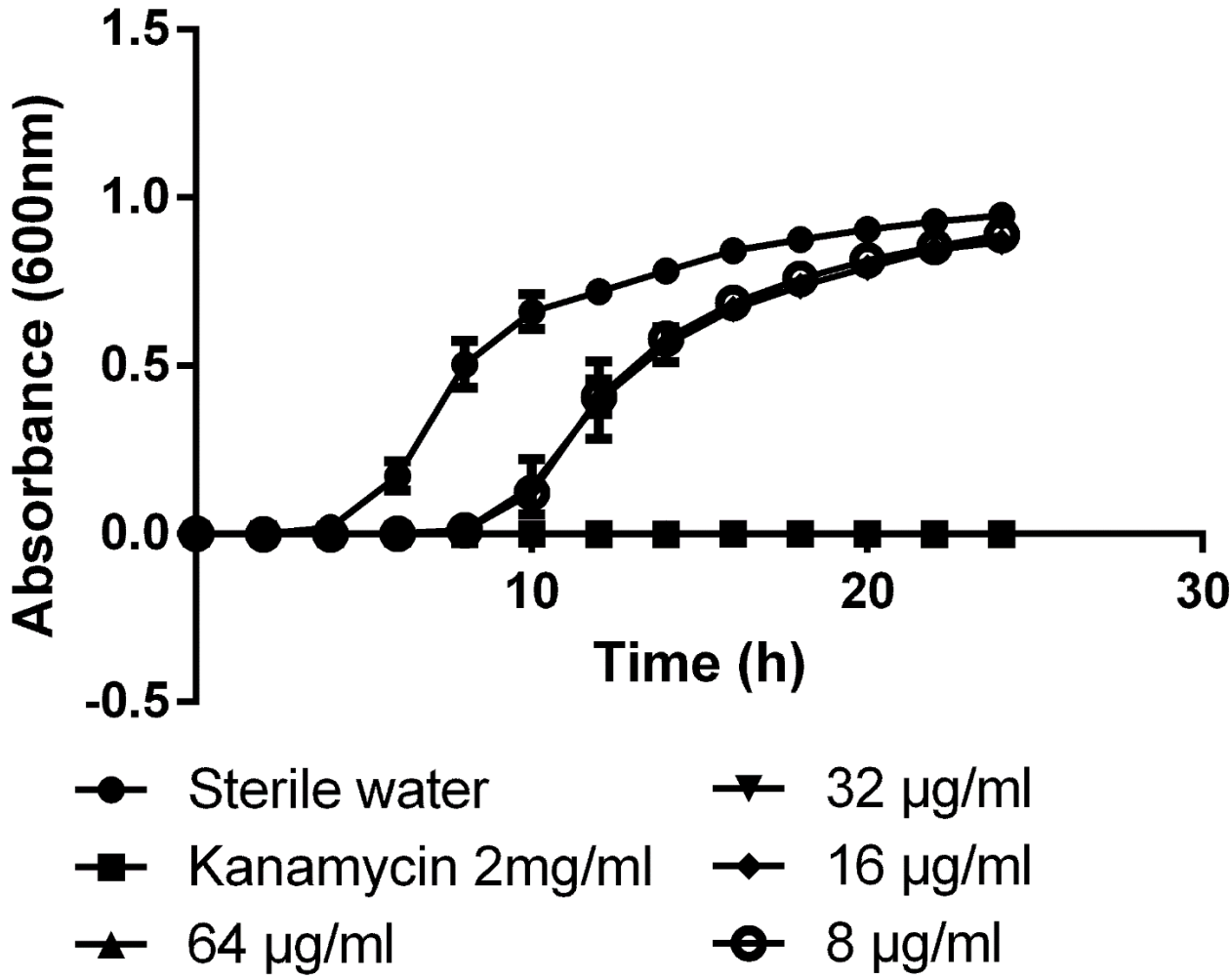


**Figure 5. Dose-dependent growth inhibition of Methicillin-sensitive *Staphylococcus aureus* (MSSA) biofilm by increasing concentrations of histone mixture.** The histones were dissolved in sterile water pH 7.4 which was also used as a negative control. Kanamycin was used as a positive control for inhibition. Error bars represent the standard deviation of technical replicate values.

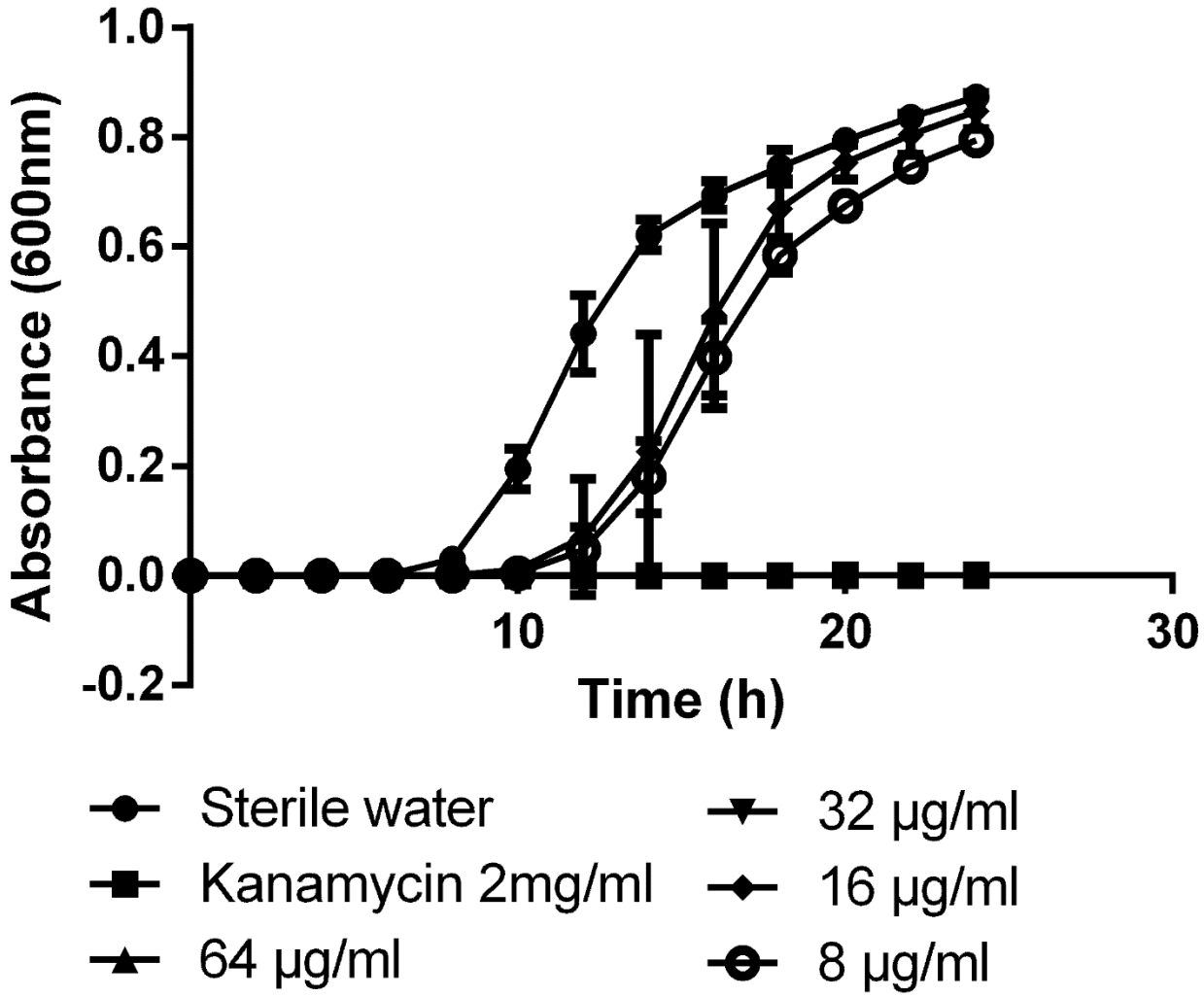


**Figure 6. Dose-dependent growth inhibition of Methicillin-resistant *Staphylococcus aureus* (MRSA) biofilm by increasing concentrations of histone mixture.** The histones were dissolved in sterile water pH 7.4 which was also used as negative control for inhibition. Kanamycin was used as a positive control. Error bars represent the standard deviation of technical replicate values.

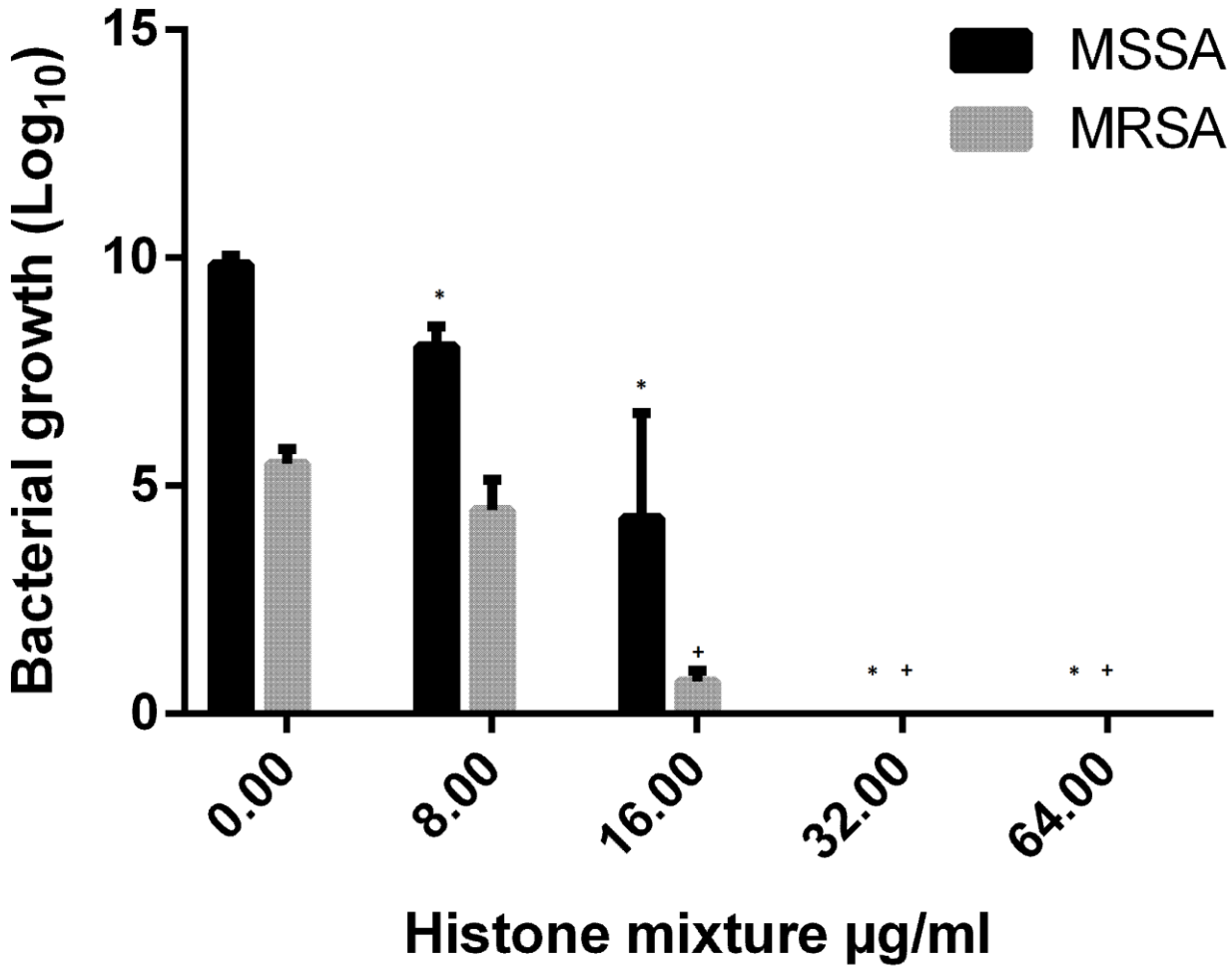


**Figure 7. Inhibition of MSSA and MRSA biofilms by the histone mixture.** The inhibition values are based on 3 trials, each in triplicate and n=3. On the abscissa, 0 indicates incubation with negative control (sterile water pH 7.4). *, p≤0.002 compared to negative control. +, p≤0.0001 compared to negative control.

2.2 Kill kinetics for planktonic MSSA and MRSA treated with histone mixture

The kill kinetics for inhibition of planktonic MSSA growth showed about 0.5 $\log_{10}$ reduction with 5 min incubation at the minimum inhibitory concentration (8 μg/ml). However, this reduction was much faster at 2XMIC (1.5 $\log_{10}$ reduction) and at 4XMIC (~3.5 $\log_{10}$ reduction) for histones at 5 min incubation (**Figure 8**). There was stronger growth reduction with 22.5 min incubation at 1XMIC of histones showing ~1 $\log_{10}$ reduction and higher concentrations of histones showing almost complete inhibition (5.5 to 6 $\log_{10}$ reduction, $p \leq 0.001$) (**Figure 8**). Following 45 min incubation, 2XMIC or higher showed full inhibition of MSSA and no growth during subsequent monitoring for 16 h. Indolicidin was used as a positive control for inhibition, with its MIC determined to be 16 μg/ml (data not shown). The kill kinetics was much faster for MRSA against histone mixture, showing >2 $\log_{10}$ inhibition at 5 min incubation for 1XMIC (8 μg/ml) and higher concentrations showing bactericidal effects (>3 $\log_{10}$ reduction) within 5 min (**Figure 9**). Indolicidin was used as positive control of inhibition with the MIC determined to be 32 μg/ml (data not shown). Incubation with indolicidin led to large reduction for both strains within 5 min (5.5 to 6 $\log_{10}$, $p \leq 0.001$). All the experiments were done in 3 biological replicates, with three technical replicates in each trial.

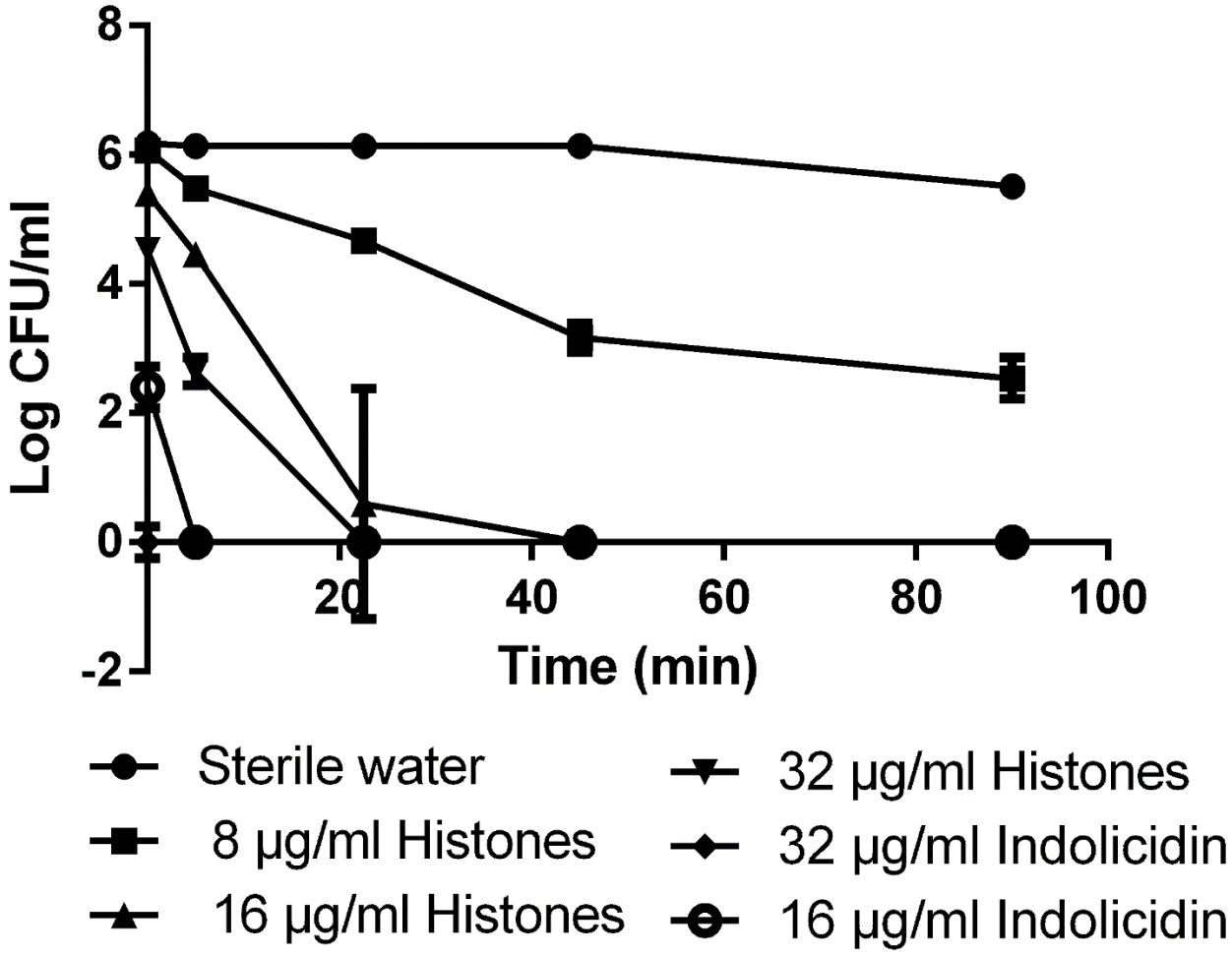


**Figure 8. Time Kill kinetics for planktonic MSSA treated with histone mixture.** The bacteria were also treated with sterile water pH 7.4 as a negative control. Indolicidin was used as a positive control, with its MIC determined in a prior experiment (16 µg/ml).

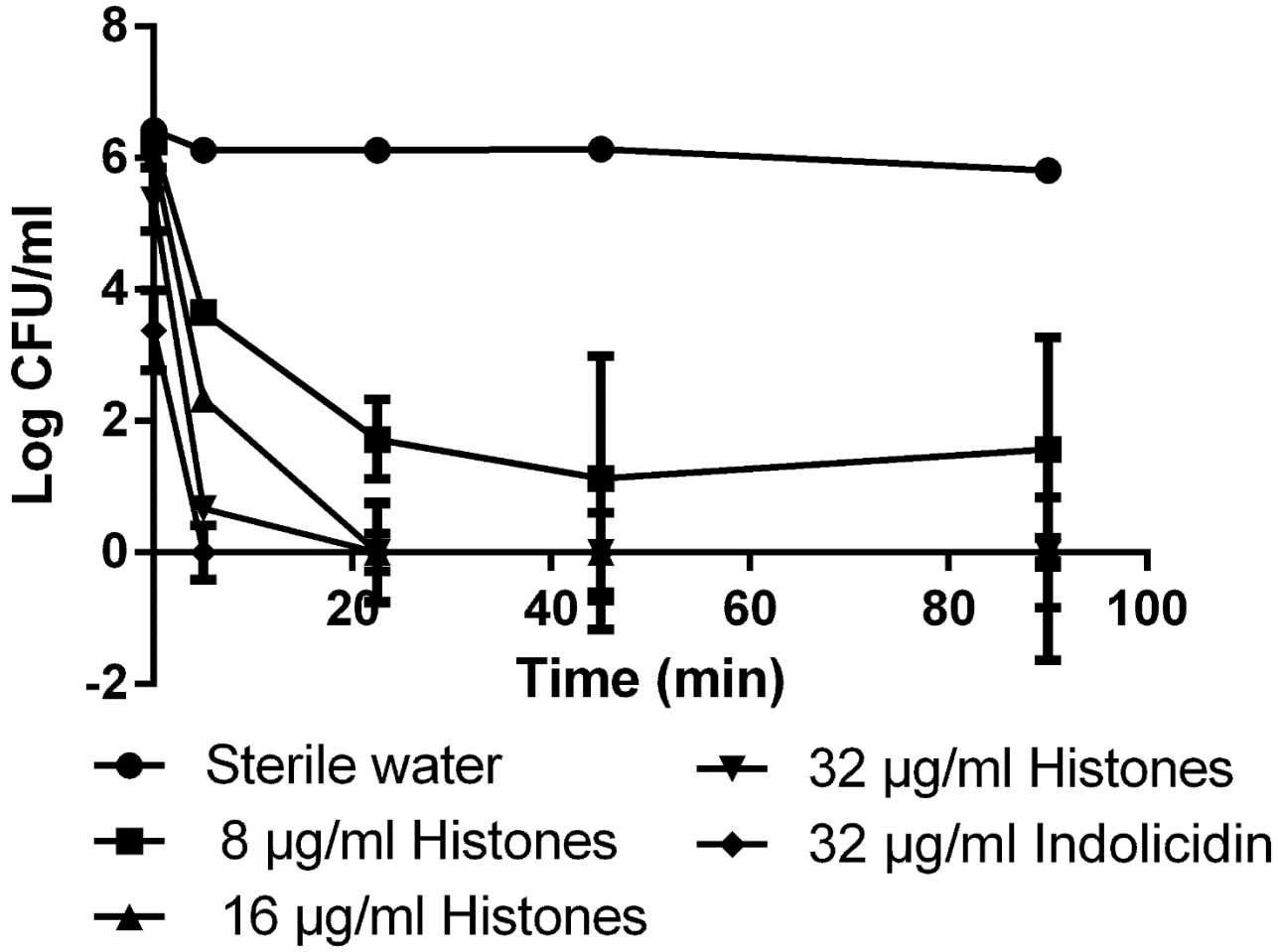


**Figure 9. Time Kill kinetics for planktonic MRSA treated with the histone mixture.** Bacteria were treated with sterile water pH 7.4 as a negative control for inhibition. Indolicidin was used as a positive control, with its MIC determined in a prior experiment (32 µg/ml).

2.3 Effect of histone mixture on MRSA bacterial surface

The effect of the histone mixture on the bacterial surface of methicillin-resistant *Staphylococcus aureus* (MRSA) was determined using scanning electron microscopy. Bacterial biofilms were grown on filter membranes and treated with histone mixture, or with sterile water as a negative control. The water-treated bacteria displayed smooth surfaces with no visible damage. MRSA treated with 128 μg/ml histone mixture showed clear morphological changes. Bacteria treated with histone mixture showed signs of blebbing as well as pore formation, collapse and indentations on the surface (**Figure 10**). Thus, the histone mixture appears to be directly affecting the bacterial membrane.

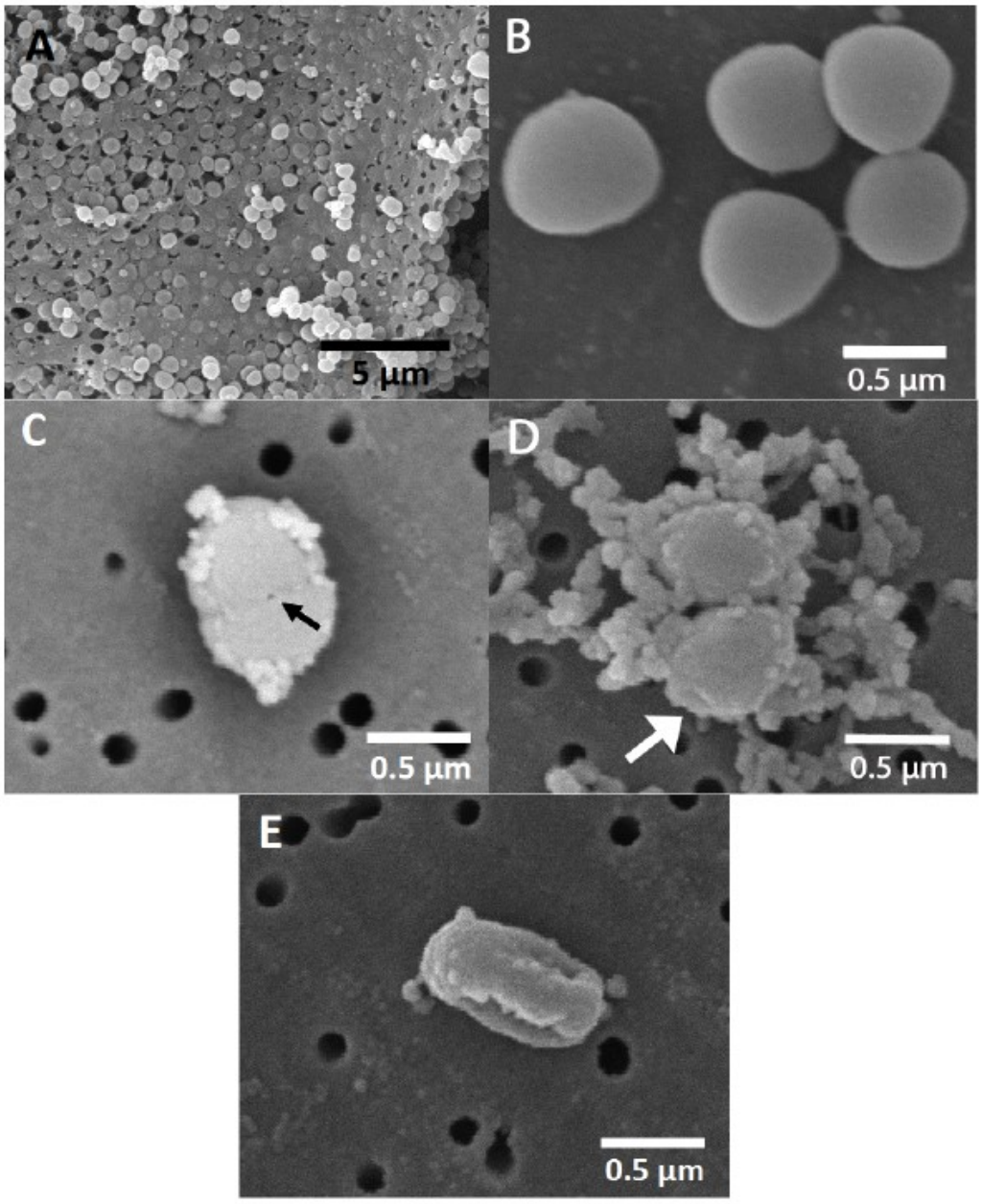


**Figure 10. Scanning electron microscopy of MRSA biofilms.** A) and B) 5000X and 40 000X magnification of bacteria treated with negative control (sterile water pH 7.4). C), D) and E) show 40 000X magnification of MRSA treated with 128 µg/ml histone mixture. C) arrow indicates pore on the surface of the bacteria. D) arrow indicates indentation. Figure reprinted from supplementary Figure 4 (Rose-Martel et al., 2017).

# Chapter 3

# Expression and purification of recombinant Ovocalyxin-32 for antimicrobial testing

## 1. Materials and methods

### 1.1 Ovocalxyin-32 fusion protein constructs

The second part of the thesis focuses on expressing and purifying five haplotypes of an eggshell cuticle protein, ovocalyxin-32, as away of protecting human health by increasing the natural antimicrobial defence of the egg. The five haplotypes of OCX-32 were subcloned into the pGEX-4T-1 vector. The vector contains an ampicillin resistance gene and encodes bacterial glutathione S-transferase (GST) upstream of the multiple cloning site (**Figure 4**). Thus, the final construct contained GST in the same reading frame as the N-terminus of the protein. In addition, a 6xhistidine tag was added prior to the stop codon, also in the same reading frame as the inserted cDNA (OCX-32). Each plasmid was purified using Qiagen plasmid miniprep kit and submitted for sequencing in order to verify the construct sequence at the DNA Sequencing Facility, StemCore, Ottawa Hospital Research Institute. The recombinant protein is 468 amino acids in length (~58kDa predicted size), including the GST, mature OCX-32 and 6xHis-tag (Xing et al., 2007; Pierce Protein Methods, 2017). The recombinant protein (50kda band) from all five haplotypes were also ran on pre-cast 4-12% Bis-Tris protein gels (Invitrogen). The bands were sent for proteomics analysis at the Quebec Genomics Center (Laval, QC). The proteomics analysis displays the full construct including the N-terminal GST, OCX-32 insert with all SNPs and the C-terminal histidine tag (**Figure S1**).

### 1.2 Optimization of expression for OCX-32 fusion protein

A single colony of *E. coli* BL-21 pLysS containing OCX-32-6xHis construct within pGEX-4T1 expression plasmid (**Figure 4**) was picked from an LB agar plate containing 100µg/ml of ampicillin and grown overnight in 3ml of LB broth (containing 100µg/ml ampicillin) in a 37°C

incubator at 250rpm. The overnight culture strain was grown in at 37°C and 250rpm in 100mL of LB broth with ampicillin for plasmid selection. When the bacterial suspension reached exponential growth phase ($OD_{600}$= 0.5), six samples of 3mL culture were aliquoted and IPTG induction was tested at increasing concentrations (0, 0.1mM, 0.5mM, 0.75mM, 1mM). The cultures were grown for an additional 3 hours. Then 1ml aliquot of each culture was centrifuged at 13,000xg for 10 min for a preliminary evaluation for successful expression. The bacterial pellets were dissolved in 5% SDS and protein concentration was determined using the bicinchoninic acid (BCA) assay (Pierce, Thermofisher). Western blotting after transfer to nitrocellulose was performed with either anti-OCX-32 (1:5000, 1 hr) or anti-GST (Abcam) (1:5000, 1 hr) polyclonal antibodies, following separation by 12.5% SDS-PAGE, to confirm the expression of the GST-OCX-32 fusion protein. The Spectra™ Multicolor Broad Range Protein Ladder (Thermofisher) was used.

Blots were incubated with goat anti-rabbit secondary antibody (1:5000, 30 min) (Promega) and visualized through chemiluminescence with Western Lighting Plus-ECL (PerkinElmer). The anti-OCX-32 antibody was a gift from our collaborator at the French National Institute for Agronomic Research (INRA), Dr. Joël Gautron. The optimization protocol was repeated at various incubation times (1, 3, 6, 12, 18h) as well as at different induction temperatures (15, 22, 30°C). In each case, the other variables were kept constant. The final optimal conditions were: 0.5mM IPTG concentration, induction for 6h at 15°C.

1.3 His-tag purification using on-column refolding

The inclusion body purification protocol was developed by our collaborator at College of Animal Science and Technology, China Agricultural University, Yahui Gao and Dr. Zhuo-Cheng Hou. The

nickel affinity binding protocol is based on the manufacturer instructions from GE Healthcare Life sciences HiTrap™ Chelating HP (GE Healthcare Life Sciences, 2017).

The *E. coli* BL21 pLysS culture was grown with the same protocol as section 2.2. The induction was conducted at the optimal conditions: 0.5mM of IPTG for 6h, 15$^{o}$C. Following induction, the bacterial pellet was harvested by centrifugation and re-suspended in 20mM Tris-HCl, pH 8. The suspension was sonicated for 3 cycles of 15s with 30s pauses at 4°C using 120W, 20kHz with an Ultrasonic Processor (Fisher Scientific) at 40% amplitude. The suspension was then centrifuged, and the pellet was re-suspended in 3ml of 2 M urea, 20 mM Tris-HCl, 0.5 M NaCl, 2% Triton™ X-100 pH 8.0 per 100ml of starting culture and sonicated as above. After one round of washing with urea and another round lacking urea, the pellet was re-suspended in 5ml of 20 mM Tris-HCl, 0.5 M NaCl, 5 mM imidazole, 6 M guanidine hydrochloride (GnHCl), 10 mM 2-mercaptoethanol (BME), pH 8 (resuspension buffer). This suspension was stirred for 90min at room temperature, centrifuged at 16,000xg, 15min, 4$^{o}$C to remove remaining undissolved particles, and the supernatant was then filtered through a 0.22 µm filter (MilliporeSigma). A 1ml resin HiTrap Chelating column (GE healthcare life sciences) was prepared by washing with 10ml of distilled water and then charged with 0.5ml of 0.1M $NiSO_4$. The column was equilibrated with 10ml of resuspension buffer at 1ml/min. Next, 5ml of the protein sample dissolved in re-suspension buffer was loaded at 1ml/min onto the column. It was then washed with 10ml of resuspension buffer. The buffer was changed to 10ml of wash buffer (20 mM Tris-HCl, 0.5 M NaCl, 20 mM imidazole, 1 mM oxidized and 2 mM reduced glutathione, 6M urea pH 8.0). The column was then successively washed with 10ml each of wash buffer containing 5, 4, 3, 2, 1 and 0 M urea at flow rate of 1ml/min to refold the bound protein. The protein was then

eluted by 5ml of 20 mM Tris-HCl, 0.5 M NaCl, 50 mM imidazole, pH 8. The imidazole concentration in the buffer was increased to 100mM, 200mM and 250mM (5ml each) at a flow rate of 1ml/min. For each elution buffer, 1ml fractions were collected for a total of 20 fractions. The entire process was conducted at room temperature.

1.4 Bacterial transformation procedure

Plasmid DNA (pGEX4T-1) containing the GST-OCX-32 construct was extracted from an overnight culture of *E. coli* BL21 cells using a Qiagen miniprep kit according to the manufacturer's protocol. The insert in the purified plasmid DNA was sequenced to confirm the correct sequence of OCX-32 haplotypes. Other strains of *E. coli* were transformed with the purified plasmid (RIL, Rosetta or Origami 2). The transformation used 100ng of DNA to transform 50µl of chemically competent bacteria (RIL, Rosetta or Origami 2). The cells were incubated on ice for 30min and then heat shocked by incubating at 42$^{o}$C for 30s, followed by cooling on ice for 2 min. The cells were added to 950µl of LB broth with no antibiotic and incubated at 37$^{o}$C and 220 rpm for 1h. They were then plated on LB agar containing appropriate antibiotic: 50µg/ml chloramphenicol and 100µg/ml ampicillin for RIL and Rosetta, 12.5µg/ml tetracycline and 100µg/ml ampicillin for Origami 2. The plates were incubated overnight at 37$^{o}$C.

1.5 Solubility testing of induced recombinant protein

Overnight cultures were grown from a single colony in 3ml LB broth containing the appropriate antibiotic(s). The next day, 25ml of LB broth was inoculated with 500 µl of the overnight culture and grown until $OD_{600}$ = 0.5. The bacteria were induced with 0.5mM IPTG and

incubated for 6h at 15$^{o}$C and 250rpm. The bacteria were aliquoted into 1ml fractions and centrifuged and the resuspended in 100 µl of BugBuster Master Mix (MilliporeSigma) diluted in several buffers (**Table S1**). The BugBuster mix contains BugBuster protein extraction reagent as well as benzonase and lysozyme. Bacteria were gently rocked for 10min at 4$^{o}$C and a 30 µl sample was taken as total cell lysate. The rest of the sample (70 µl) was centrifuged and both soluble and insoluble fractions retained. Samples were analyzed by SDS-PAGE as well as Western blot to monitor recombinant protein presence in each fraction.

1.6 Protein tag change through plasmid subcloning

Following purification of plasmid DNA (pGEX4T-1) containing the GST-OCX-32 insert, 1 µg of plasmid the DNA was digested using 10 units each of BamHI-HF and SalI-HF for 1hr at 37$^{o}$C (New England Biolabs). The same amount of purified target plasmid (pSMT3) containing 6xHis-SUMO was also digested with the same enzymes (**Figure 11**). The insert and digested target plasmid were isolated from agarose gel and purified using Qiagen Gel extraction kit. The insert and plasmid were ligated using 1 Weiss U of T4 DNA ligase in 5:1 ratio of insert to plasmid (Thermofisher). The ligated DNA was transformed into DH5α cells (Thermofisher) following same protocol as section 2.4. A colony of transformed DH5α cells was grown and the plasmid DNA was purified using Qiagen plasmid miniprep kit; and the presence of the insert was verified by PCR and sequenced using pSMT3 primers (**Table S2**) to confirm the sequence of the open reading frame (ORF) and OCX-32 construct sequence with expected SNPs. The DNA sequencing was performed at the DNA Sequencing Facility, StemCore, Ottawa Hospital Research Institute. GoTaq Green Master mix (Promega) was used for the PCR amplification with manufacturer's suggested protocol PCR conditions and volumes (Promega, 2017). The new construct was

transformed into the desired expression bacterial strain (*E. coli* Origami 2 or Rosetta) through heat shock following same protocol as section 2.4.


**Figure 11. Schematic depiction of OCX-32 construct in pSMT3 plasmid.** The plasmid contains cDNA encoding small ubiquitin-like modifier (SUMO) along with OCX-32 gene inserted between the BamHI and SalI sites of the multiple cloning site. Plasmid was donated by Dr. Jean-François Couture, BMI, University of Ottawa.

1.7 His-tagged recombinant protein purification in denaturing conditions

Insoluble recombinant protein from inclusion bodies under denaturing conditions was purified using a HiTrap Chelating column (GE Healthcare Life Sciences) charged with 0.1M $NiSO_4$. The column was equilibrated in 6M GnHCl, 20mM Tris-HCl, 0.5M NaCl, pH 7.0 for 10 min. The sample was dissolved in 5ml of 6M GnHCl and applied to the nickel affinity column at a flow rate of 1ml/min. The column was washed with 5mL of the same buffer. Following this, the column was washed with the same buffer and then with 6M GnHCl, 20mM Tris-HCl, 0.5M NaCl, 50mM imidazole, pH 7. Finally, the column was eluted with 6M GnHCl, 20mM Tris-HCl, 0.5M NaCl, 250mM imidazole, pH 7.

1.8 Dialysis Procedure

In order to obtain a recombinant protein that was soluble under native conditions, the guanidine hydrochloride concentration was decreased by dialysis. Typical procedures were as follows: 1ml of protein dissolved in 6M Gn HCl, 20mM Tris-HCl, 0.5M NaCl pH 7 was placed in a dialysis tubing (FisherBrand 6-8 kDa MWCO) with ~20% of the bag's total volume being filled with air. The dialysis bag was first placed in a 200ml solution of 5M GnHCl, 0.5M NaCl, 20mM Tris-HCl, 1mM reduced glutathione, 0.1mM oxidized glutathione, 0.5mM BME, 0.2mM Ethylenediaminetetraacetic acid (EDTA), pH 7. The dialysis was performed at 4°C. After a minimum of 3 hours at each concentration, the dialysate was replaced with a 200ml solution of the same composition, but with reduction of the concentration of GnHCl by 1M at each stage, until reaching 2M. The dialysate was diluted with a solution containing the same components, except for GnHCl, to dilute the concentration of denaturant slowly. Typically, the solution was diluted by adding buffer at a rate of 0.2-0.4 mL/min using an EP-1 Econo Pump (Biorad), such

that a 1M change in GnHCl would take a minimum of 8 hours. All the dialysis steps were completed in the cold room (4$^{o}$C).

After observing the effects of EDTA and BME on bacterial growth, the dialysate was changed in later experiments to reduce the EDTA concentration from 0.2mM to 0.02mM and completely remove BME in the final stages of dialysis. For SUMO-OCX-32 refolding, the same protocol was used, with 0.02mM EDTA, and with removal of BME from the dialysis buffer after GnHCl reached 1M.

### 1.9 Protein quantification

The purified protein was quantified using SDS-PAGE analysis with bovine serum albumin (BSA) standard. The stock BSA standard (2mg/ml) was from the BCA assay kit (Thermofisher), which was further diluted known quantities of BSA were loaded on the gel, as well as the soluble protein and the resolubilized pellet following dialysis. The samples were run for 50min at 200V and stained with 0.25% Coomassie Brilliant Blue G-250 Dye. Following gel drying, the intensity of the bands was measured by densitometry using ImageJ software version 1.51 (National Institutes of health). The densitometry result for the BSA standards was used to create a standard curve and linear regression was performed. The protein quantities in the soluble and insoluble protein following dialysis were calculated by interpolating from the standard curve.

### 1.10 Determination of Minimum inhibitory concentration (MIC) through broth microdilution assay

*Staphylococcus aureus* (ATCC 6538), *Bacillus cereus* (ATCC 11778), *Salmonella enterica* serovar Enteritidis (ATCC 31194) were a kind gift from University of Ottawa's Centre for

Research on Environmental Microbiology (CREM).

Bacteria were grown on an LB agar plate overnight at 37°C. A single colony was selected and grown in 3ml of LB broth overnight at 250rpm and 37°C. The overnight culture was then diluted 1/50 in 25ml LB broth and incubated at 37°C in a 250rpm shaker until it the exponential growth phase was achieved ($OD_{600}$=0.2). Next, 3ml of culture was pelleted and washed in 3ml of PBS (pH 7.4) and finally re-suspended in a concentration of $10^5$ CFUs/mL in PBS. The final CFU was determined empirically for each bacterial species by colony counts in LB agar. The purified OCX-32 fusion protein was serially diluted in buffer (usually 0.5M NaCl, 20mM Tris-HCl, 1mM reduced glutathione, 0.1mM oxidized glutathione, 0.5mM BME, 0.2mM EDTA, pH 7). After observing antibacterial effect of EDTA and BME, the buffer contained 0.02mM and no BME in later experiments. Next, 50 µl of the serially diluted protein was mixed with 50µl of the bacterial dilution containing $10^5$ CFUs/mL in PBS. When the purified concentration of OCX-32 was very low (<50µg/ml), the ratio was increased to 150µl:50µl protein to bacteria with all controls also modified in the same manner (150 µl: 50µl buffer to bacteria). The mixture was incubated at 37°C, 200rpm for 3 h. Following the incubation, 100 µl of the mixture was loaded on 96-well microplate in triplicate and 100µl of LB broth was added to each well. The microplate was incubated overnight (18 h) at 37°C at 206 oscillations/min with monitoring every 30 min at 600nm for growth in an EON microplate reader (BioTek). For positive control of inhibition against *S. aureus* and *B. cereus,* chicken histone H5 was used at their minimum inhibitory concentration (Jodoin, 2017).

## 2. Results

### 2.1 Optimization of expression conditions

For the optimization of protein expression, my initial focus was to work with the supernatant after bacterial cell lysis to avoid a refolding step that would be necessary if using urea or guanidine hydrochloride to extract insoluble protein from inclusion bodies. This was done to obtain a fully folded and fully functional protein without the use of strong denaturants (6M urea or 6M GnHCl), since we assumed that soluble recombinant protein in the supernatant was properly folded and functional.

A potential problem was degradation of the recombinant protein when expression was induced at 37$^{o}$C. In order to troubleshoot this possibility, 3ml of bacterial culture were grown overnight at 37$^{o}$C, as described above, and induced with 0.5mM IPTG at several lower temperatures: 15$^{o}$C, 22$^{o}$C and 30$^{o}$C (**Figure 12**). In the Western blot using anti-GST, the intensity of the immunoreactive 50kDa band was higher in the supernatant obtained after expression at 15$^{o}$C compared to higher induction temperatures including 22$^{o}$C and 30$^{o}$C (**Figure 12**). The intensity of the lower molecular weight bands (assumed to be degradation products) was also lower in the 15$^{o}$C incubated sample, compared to the higher temperatures (22 and 30$^{o}$C). In addition, the concentration of IPTG was tested to optimize protein expression, using 0.1, 0.25, 0.5 or 1mM. The Western blot labelled with anti-OCX-32 antibody showed that induction with 0.5 mM IPTG led to the expression of highest intensity of soluble protein at 50kDa (**Figure 13**). The intensity of lower molecular weight bands for all IPTG concentrations tested were very similar. Another tested condition for optimization of the expression conditions was induction time. Induction times of 1, 3, 6, 12 and 18h were tested at 15$^{o}$C with 0.5mM of IPTG. There was

significantly more soluble GST immunoreactive protein present after 18h of incubation compared to the rest of the incubation times (**Figure 14**) ($p<0.05$). However, the Western blot indicated that 18h incubation also had more degradation which produced a 40kDa band detected with anti-GST antibody. Induction time of 6h led to higher amounts of degradation products compared to 1h and 3h but lower than 18h incubation. All the Western blots for induction times were performed 3 times and the average intensity was taken using Image Studio Lite Version 5.2. Statistical analysis was done using one-way ANOVA and the Tukey method. Therefore, the optimum conditions for the expression of immunoreactive GST-OCX-32 were: 0.5mM of IPTG, induction at 15$^{o}$C for 6h.

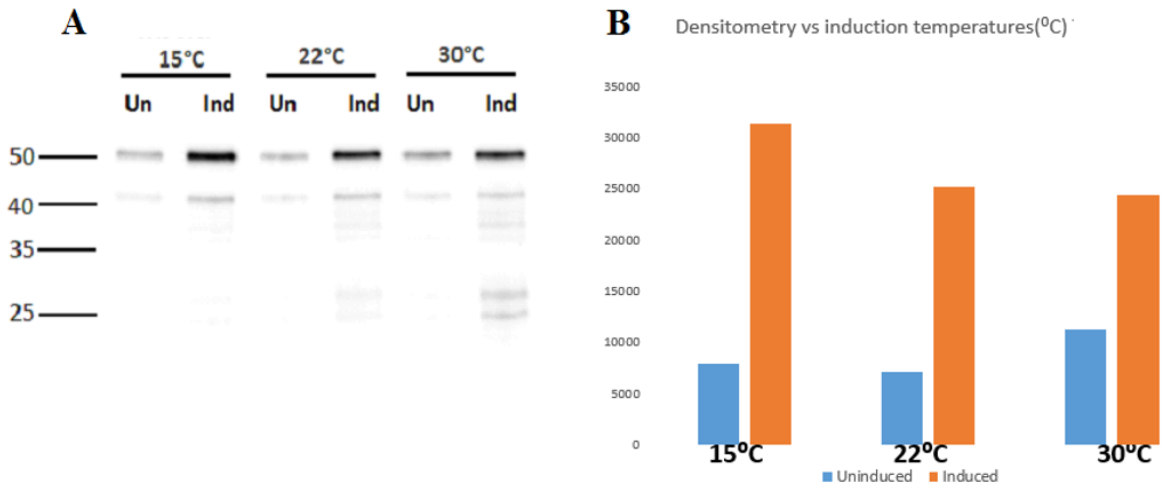


**Figure 12. Western blot analysis of protein expression at various incubation temperatures following induction.** A) Western blot for 2µg of protein supernatant expressed under different temperatures and in the presence (Ind) or absence (Un) of 0.5mM IPTG. The bands were labelled with anti-GST antibody. B) densitometry results for the 50kDa band comparing incubation temperatures.

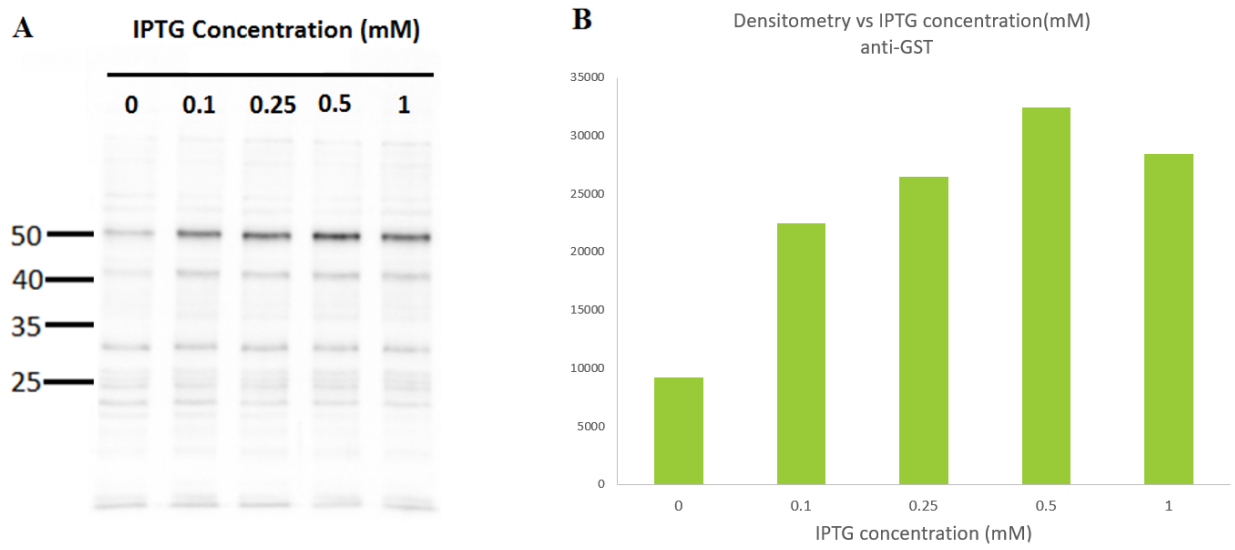


**Figure 13. Western blot analysis of protein expression for various IPTG concentrations.** A) Western blot labelled with anti-GST for 2µg of protein supernatant expressed for 3h at 15$^{o}$C using increasing concentrations of IPTG. B) Densitometry results for the 50kDa band comparing IPTG concentrations.

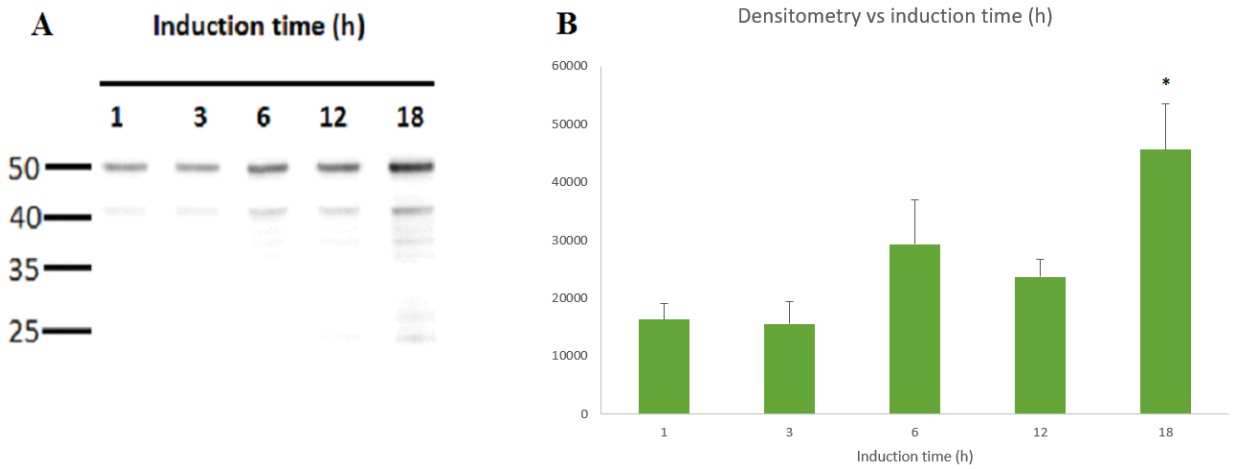


**Figure 14. Western blot analysis of protein expression for various incubation times following induction.** A) Western blot labelled with anti-GST for 2µg of protein supernatant expressed using 0.5 mM IPTG induction at 15$^{o}$C for various time points. B) Densitometry results for the 50kDa band comparing induction times. Asterisk (*) indicates significant ($p \leq 0.05$, n=3) different from all other induction times. No other induction times were significantly different.

2.2 On-column refolding

The GST-OCX-32 recombinant protein haplotype A was over-expressed in *E. coli* BL21 pLysS and the inclusion bodies purified as described in section 2.3. Inclusion bodies were dissolved in denaturing buffer (6M GnHCl, 20mM Tris-HCl, 0.5M NaCl, pH 7.0). The recombinant His-tagged protein was retained by nickel affinity column, and renatured while bound by reducing the urea concentration in a step-wise wash approach. This produced a concentration of 0.9µg/ml to 47.7µg/ml of purified recombinant protein from 200ml bacterial culture (**Figure 15**). The refolded protein was tested against a common egg pathogen, *Salmonella enterica* serovar Enteritidis by broth microdilution assay (described in section 2.10). However, the high imidazole concentration (200mM) in the elution buffer itself inhibited bacterial growth (**Figure S2**). The assay tested increasing imidazole concentrations (0, 50, 100, 200 and 250mM) in the elution buffer. The imidazole could not be removed from the purified protein using various methods that were tested, without losing the protein. These methods include: PD-10 desalting column (GE healthcare), buffer exchange through Vivaspin protein concentrator (GE healthcare) and amicon ultra-centrifugal filters (MilliporeSigma) (data not shown). The protein was no longer present after these various approaches that aimed to remove imidazole from the buffer.

Following on-column refolding, a large amount of recombinant protein could be subsequently eluted from the nickel affinity column under denaturing conditions. We assumed that this protein was precipitated during “on-column refolding” and retained on the column (**Figure 16**).

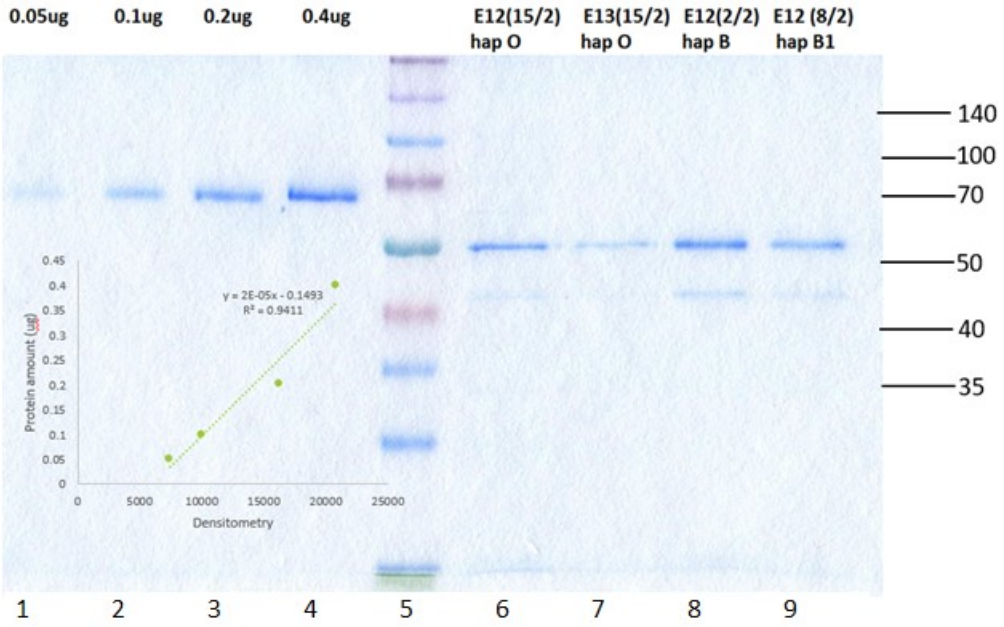


**Figure 15. SDS-PAGE analysis for elutions of GST-OCX-32 haplotype O and B from on-column refolding.** Lanes **1-4** show known amounts of bovine serum albumin (BSA) used for calculating standard curve. Lanes **6-9** show various purification batches for haplotype O and B.

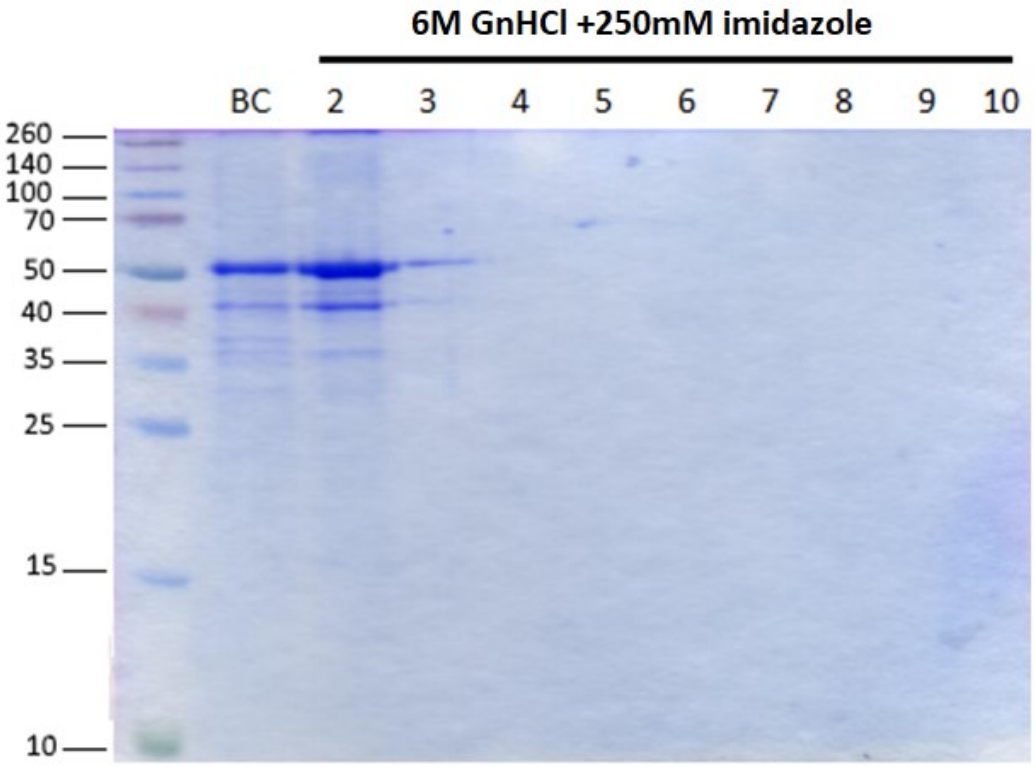


**Figure 16. Coomassie Blue stained SDS-PAGE (12.5%) to evaluate elution of GST-OCX-32 under denaturing conditions from nickel affinity column. BC:** Protein sample before applying to the nickel affinity column. **Lanes 2-10:** 1 mL fractions collected from elution of the column with 6M GnHCl and 250mM imidazole

2.3 Evaluation of change in expression strain

Several *E. coli* strains were evaluated: *E. coli* BL21 pLysS (initial strain), *E. coli* BL21 CodonPlus RIL, *E. coli* BL21 Rosetta (DE3), and *E. coli* Origami 2 (DE3). The RIL and Rosetta strains provide more copies of tRNA genes that were assumed to be a limiting factor in producing heterologous protein. Lysis of *E. coli* RIL bacteria following induction showed no recombinant GST-OCX-32 in the supernatant by SDS-PAGE (**Figure 17**)**.** The pellet following lysis showed a large band at 50kDa (**Figure 17**)**.** This was also confirmed through Western blotting with anti-GST (**Figure S4**). When the expression system was changed to Rosetta, the same results were obtained, (**Figure 18, Figure S3**). The final expression strain that was tested, *E. coli* Origami 2, had mutations in glutathione reductase and thioredoxin reductase that have been found to increase disulfide bond formation. This strain showed similar results to RIL and Rosetta, with only insoluble recombinant protein (**Figure 19**). The SDS-PAGE images only show buffers 1-4. The rest of the buffers evaluated (5-10) showed the same results for all strains tested with only insoluble recombinant protein detected (data not shown).

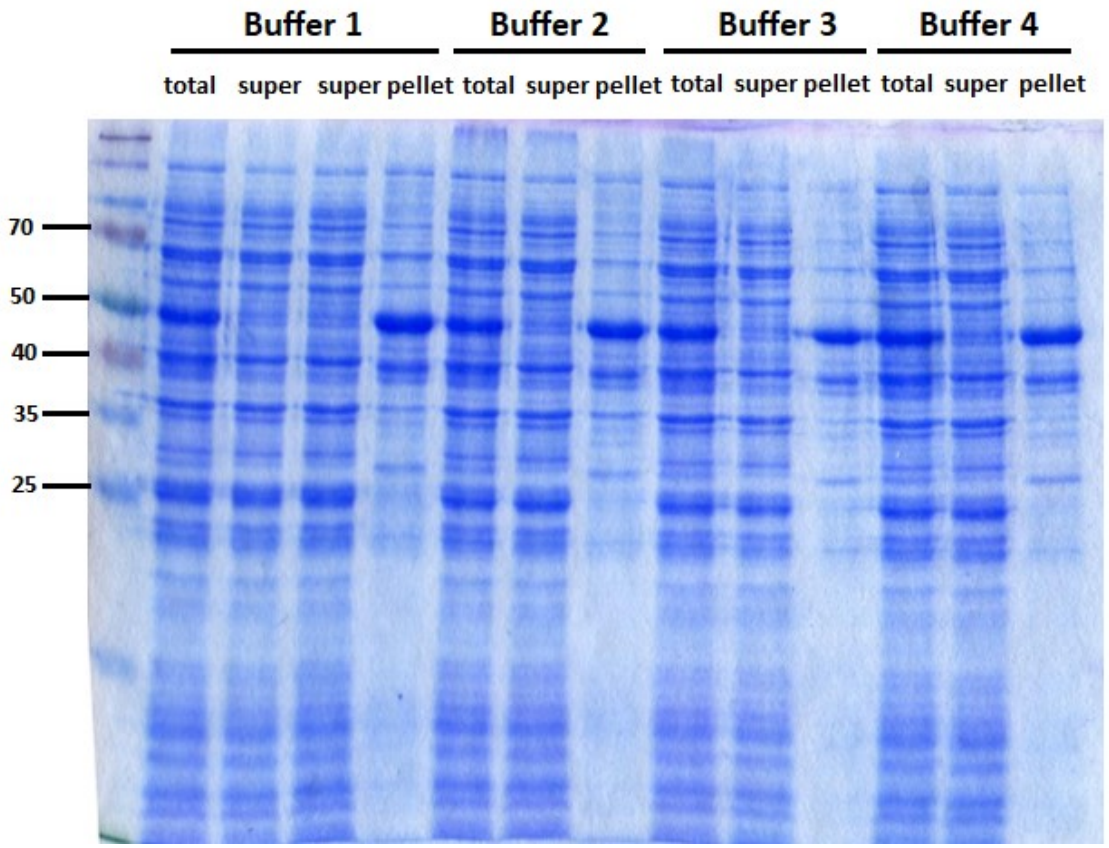


**Figure 17. Coomassie Blue-stained SDS-PAGE (12.5%) solubility analysis for *E. coli* RIL (1ml cultures) transformed with GST-OCX-32 haplotype A construct.** The solubility testing was done using BugBuster protein extraction reagent mixed with various buffers (**Table S1)**. The bacteria were induced with 0.1mM IPTG at 15$^{o}$C for 6h. Total: the total lysate before centrifugation, Super: supernatant following centrifuging of the total lysate, pellet: the pellet following centrifugation and dissolved in SDS.

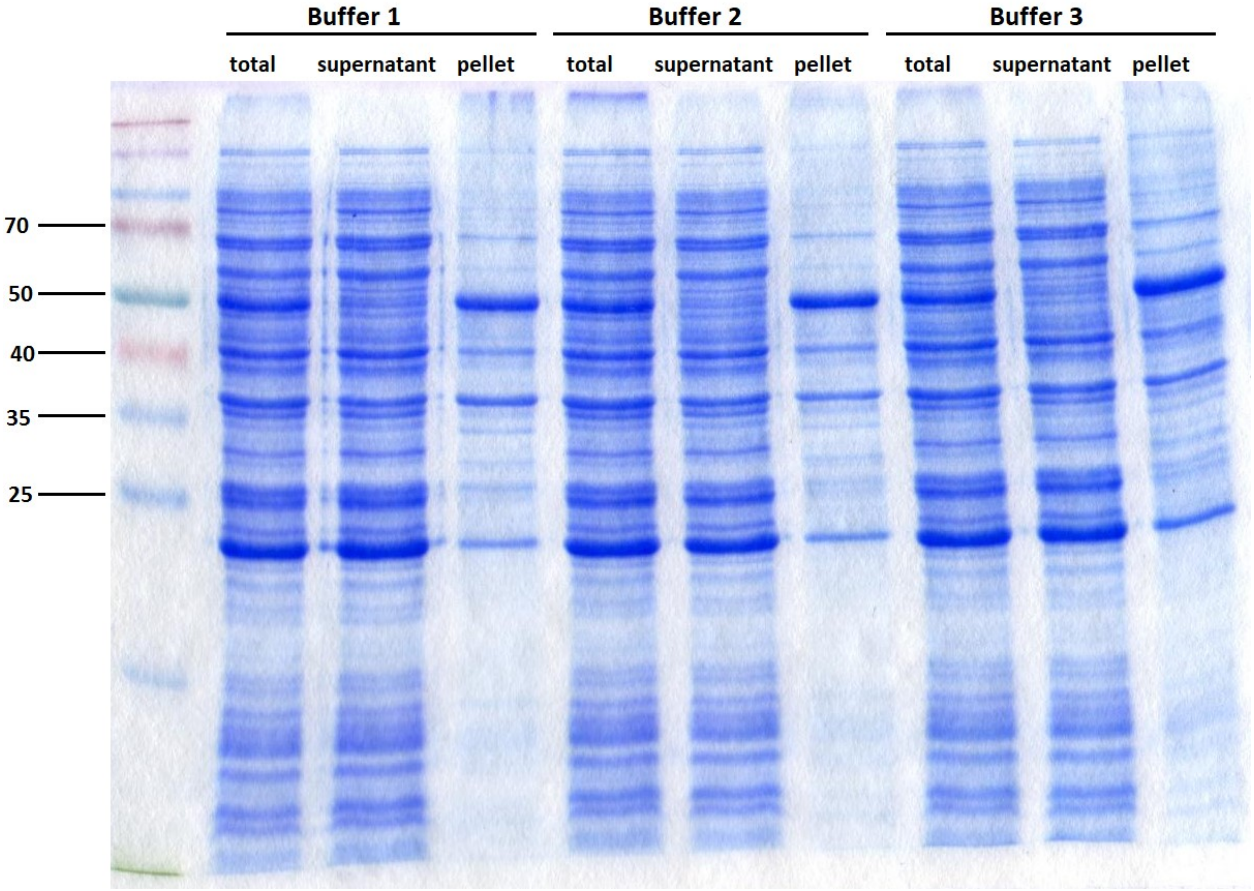


**Figure 18. Coomassie Blue-stained SDS-PAGE (12.5%) solubility analysis for *E. coli* Rosetta (1ml cultures) transformed with GST-OCX-32 haplotype A construct.** The solubility testing was done using BugBuster protein extraction reagent mixed with various buffers (**Table S1**). The bacteria were induced with 0.1mM IPTG at 15$^{o}$C for 6h. Total: the total lysate before centrifugation, Super: supernatant following centrifuging of the total lysate, pellet: the pellet following centrifugation and dissolved in SDS.

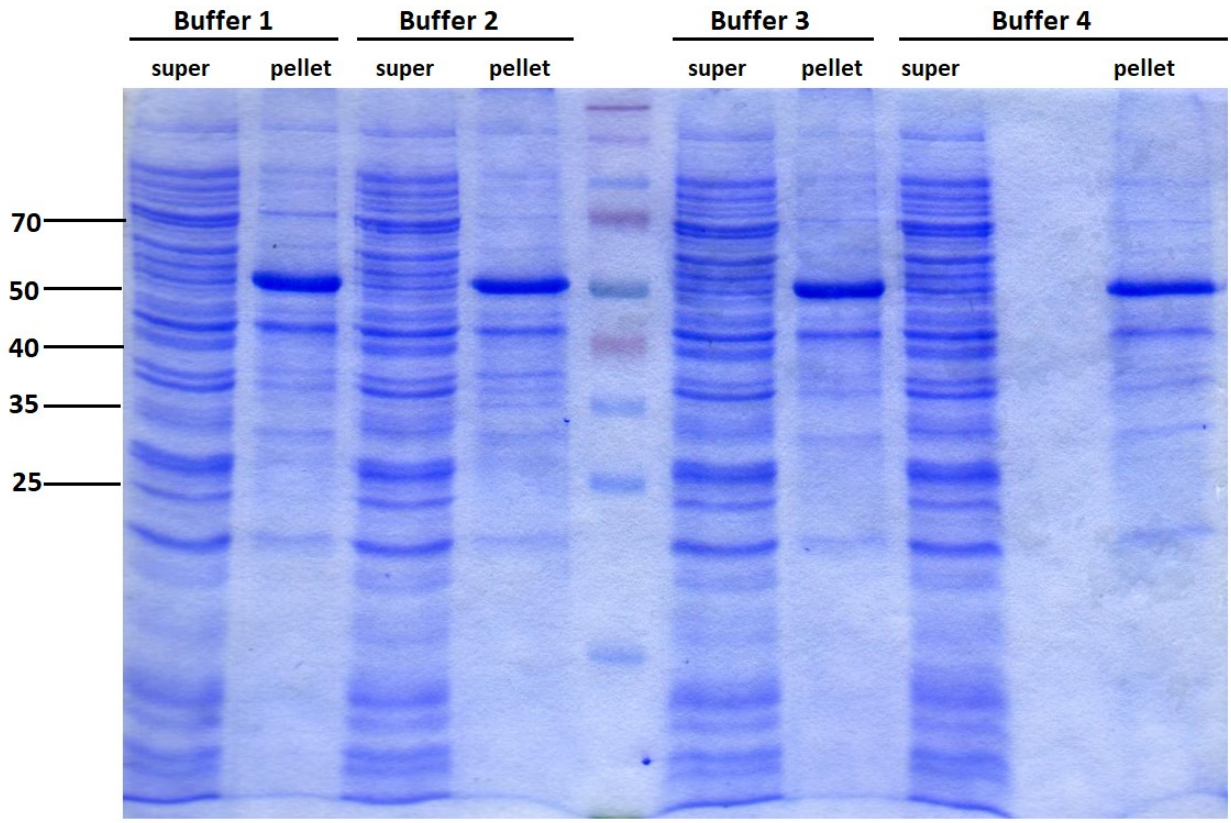


**Figure 19. Coomassie Blue-stained SDS-PAGE (12.5%) solubility analysis for *E. coli* Origami 2 (1ml cultures) transformed with GST-OCX-32 haplotype A construct.** The solubility testing was done using BugBuster protein extraction reagent mixed with various buffers (**Table S1**). The bacteria were induced with 0.1mM IPTG at 15$^{o}$C for 6h. Super: supernatant following centrifuging of the total lysate, pellet: the pellet following centrifugation and dissolved in SDS.

2.4 Evaluation of fusion partner change to Small ubiquitin-like modifier (SUMO)

The cDNA for haplotype A OCX-32 was inserted into pSMT3 plasmid containing 6xHis-SUMO and successful ligation was confirmed using agarose gel electrophoresis following PCR amplification using SUMO primers designed using NCBI primer design tool (**Figure 20**), (**Table S2**). The 'no insert' control containing only the pSMT3 plasmid showed the expected size of 218bp, whereas the amplicon with insert was 1001bp (**Figure 20**). The expected full-length sequence and correct reading frame for expression were also confirmed by DNA sequencing of the insert (data not shown). The ligated plasmid amplification was done in DH5α cells and the purified plasmid was transferred to an expression strain, *E. coli* Rosetta, for solubility testing. The solubility testing using various buffers and BugBuster mix showed no protein in the supernatant while a large amount of insoluble protein at the predicted size for SUMO-OCX-32 recombinant protein was detected (**Figure 21**).

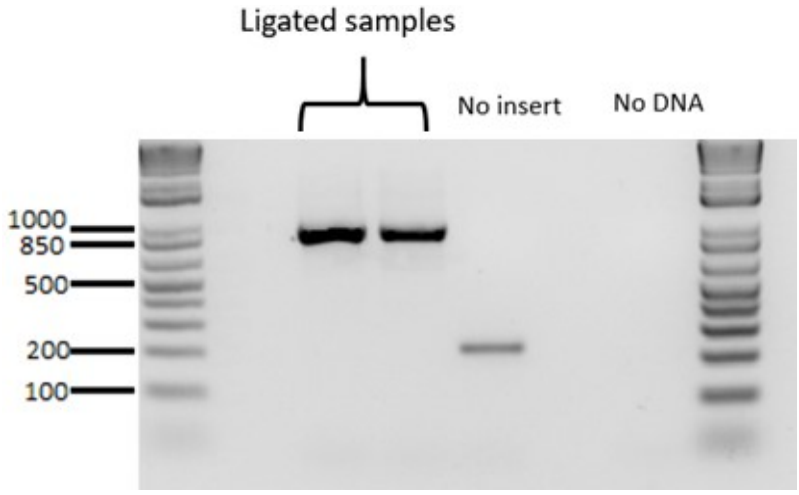


**Figure 20. 2% agarose gel analysis for PCR samples for OCX-32 insert ligated into pSMT3 plasmid, no insert control positive control and no template negative control.** The samples were amplified using GeneAMP PCR System 2400 (PerkinElmer) using pSMT3 primers designed using primer designing tool NCBI (**Table S2**).

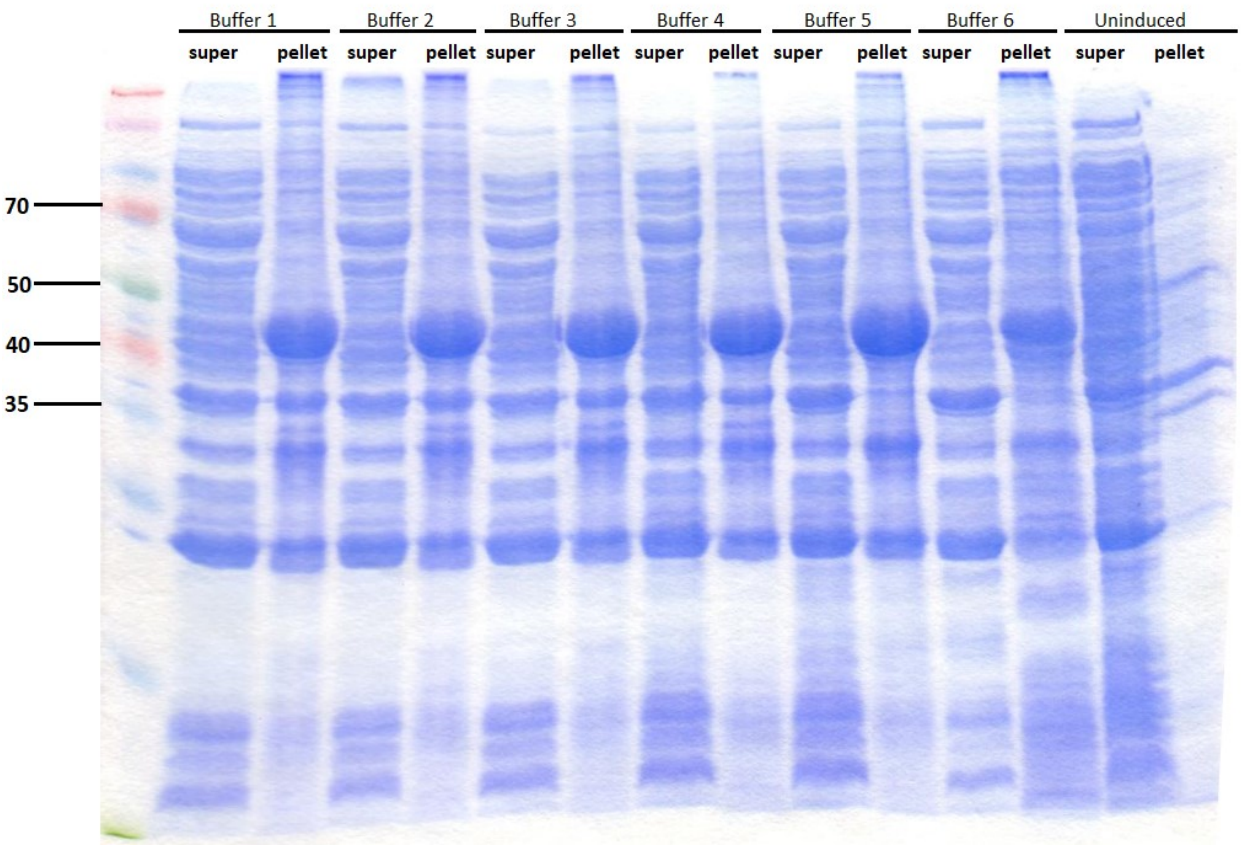


**Figure 21. Coomassie Blue-stained SDS-PAGE (12.5%) solubility analysis for *E. coli* Rosetta (1ml cultures) transformed with SUMO-OCX-32 haplotype A construct.** The solubility testing was done using BugBuster protein extraction reagent mixed with various buffers (**Table S1**). The bacteria were induced with 0.1mM IPTG at 15$^{o}$C for 6h. Super: supernatant following centrifuging of the total lysate, pellet: the pellet following centrifugation and dissolved in SDS. Uninduced: 1ml culture without IPTG induction, lysed with Bugbuster mix and centrifuged.

2.5 Dialysis refolding for GST-OCX-32

Protein purification using nickel affinity chromatography and refolding while bound to the column had very low yield (**Figure 15**). SDS-PAGE analysis of the protein subsequently eluted from the nickel affinity column under denaturing conditions showed large amounts of protein (**Figure 16**). Thus, the denatured recombinant protein was partially purified using the nickel affinity column and eluted without refolding. The denatured protein was slowly refolded using dialysis and showed a yield of 18.8% soluble with disulfide shuffling reagents including 20mM Tris-HCl, 0.5M NaCl, 0.1mM oxidized glutathione, 1mM reduced glutathione, 0.2mM EDTA, 0.5mM BME pH 7 (B1) (**Figure 22**). The soluble protein was tested against the Gram-positive *S. aureus* at concentrations up to 29.4 μg/ml and, paradoxically, showed faster growth of bacteria as the concentration of OCX-32 increased. The solubilizing buffer (B1) alone showed the highest bacterial growth inhibition (**Figure S5**). The components of the buffer were tested to find the constituent that was affecting growth. B1 with no EDTA (B2) showed the most similar growth compared to 20mM Tris-HCl, 0.5M NaCl alone (data not shown). When refolding dialysis was repeated using B2, the protein yield was 9.2% soluble with 8.18 μg/ml concentration in the supernatant (**Figure 23**). This recombinant protein was tested against Gram-positive *Bacillus cereus* and showed no dose-dependent inhibition of growth displayed by increase in lag time (**Figure S6**). The final $OD_{600}$ after 18h of monitoring showed a trend of dose-dependent inhibition of bacterial numbers with the highest concentration tested (6 μg/ml) displaying the lowest final absorbance (**Figure S6**). Different EDTA concentrations were tested to increase the yield of purified soluble recombinant protein without a non-specific effect on bacterial growth. Various concentrations of EDTA were added to dialysis buffer B2 (0-0.2mM EDTA) and tested

against *B. cereus.* From the concentrations tested, 0.02mM of EDTA was the highest that showed no inhibition of bacterial growth (**Figure S7**). Thus, the concentration of EDTA in the dialysis buffer was reduced to 0.02mM (B3). The GST-OCX-32 recombinant protein was refolded using B3 as a final buffer and showed a yield of 21.5% soluble with 30.8 μg/ml in the supernatant (**Figure 24**). The antimicrobial activity of this soluble refolded protein was tested against *B. cereus* and it showed a slight decrease in lag time (increase of bacterial growth) compared to negative controls (B3) and PBS (**Figure 25**). There was no difference in lag time between the two concentrations of GST-OCX-32 tested (11.55 μg/ml and 23.11 μg/ml) while their final $OD_{600}$ showed slight a dose-dependent decrease (**Figure 25**).

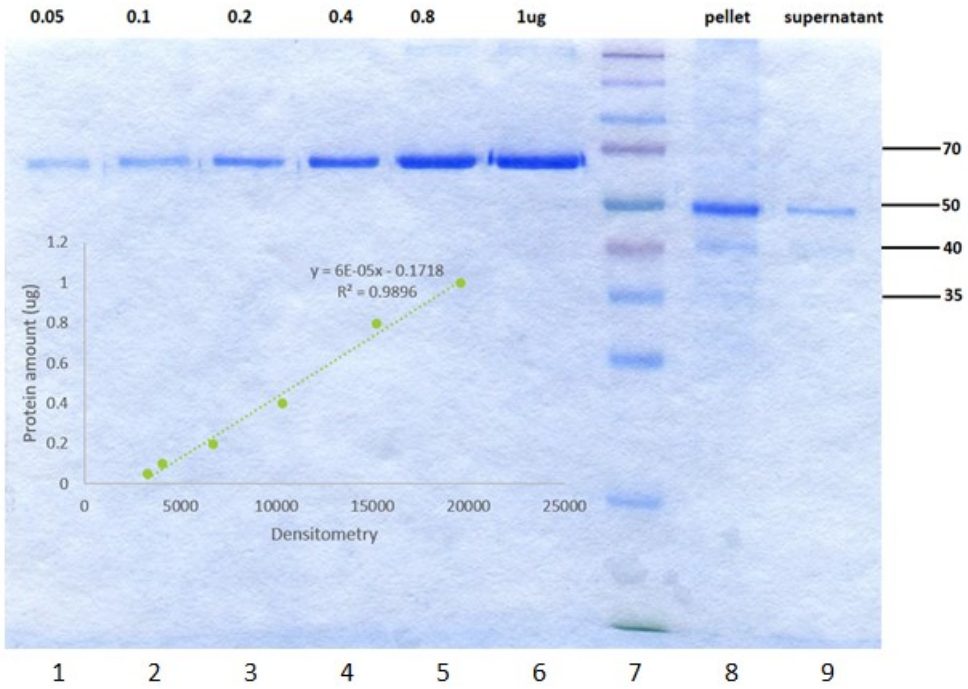


**Figure 22. SDS-PAGE analysis for dialysis refolding of GST-OCX-32 haplotype A.** The refolded protein at **lane 9** (supernatant) was solubilized in 20mM Tris-HCl, 0.5M NaCl, 0.1mM oxidized glutathione, 1mM reduced glutathione, 0.2mM EDTA, 0.5mM BME pH 7. The pellet (**lane 8**) following dialysis was resolubilized in 6M guanidine hydrochloride, ethanol precipitated and finally solubilized in loading buffer. **Lane 1-6** show known amounts of bovine serum albumin (BSA) used for calculating the standard curve.

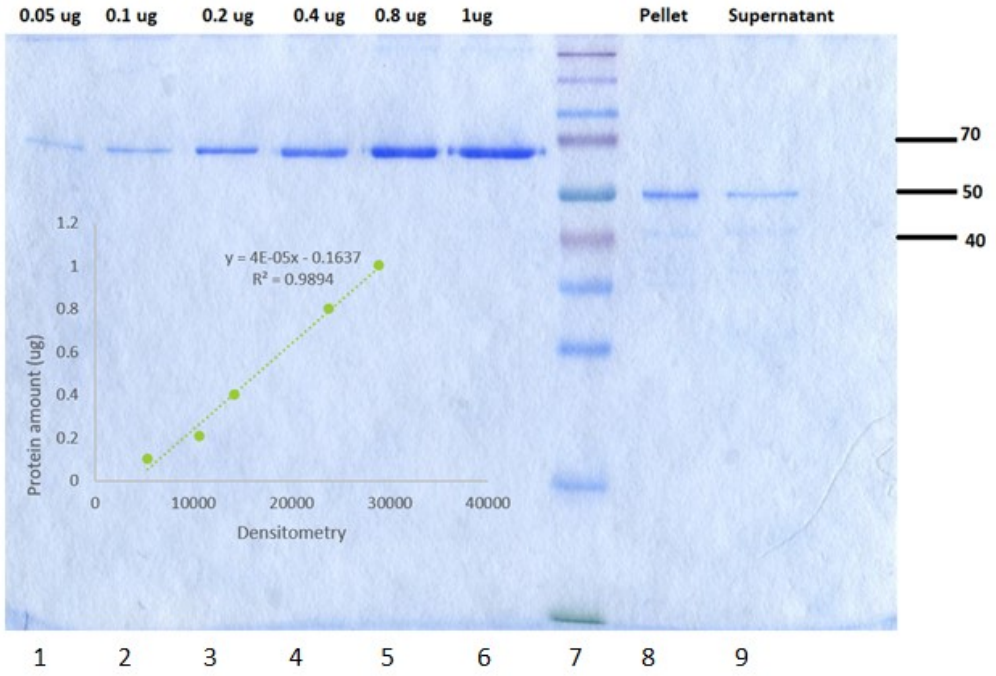


**Figure 23. SDS-PAGE analysis for dialysis refolding of GST-OCX-32 haplotype A.** The refolded protein at **lane 9** (supernatant) was solubilized in 20mM Tris-HCl, 0.5M NaCl, 0.1mM Oxidized Glutathione, 1mM reduced glutathione, 0.5mM BME pH 7 (No EDTA). The pellet (**lane 8**) following dialysis was resolubilized in 6M guanidine hydrochloride, ethanol precipitated and finally solubilized in loading buffer. **Lane 1-6** show known amounts of bovine serum albumin (BSA) used for calculating the standard curve.

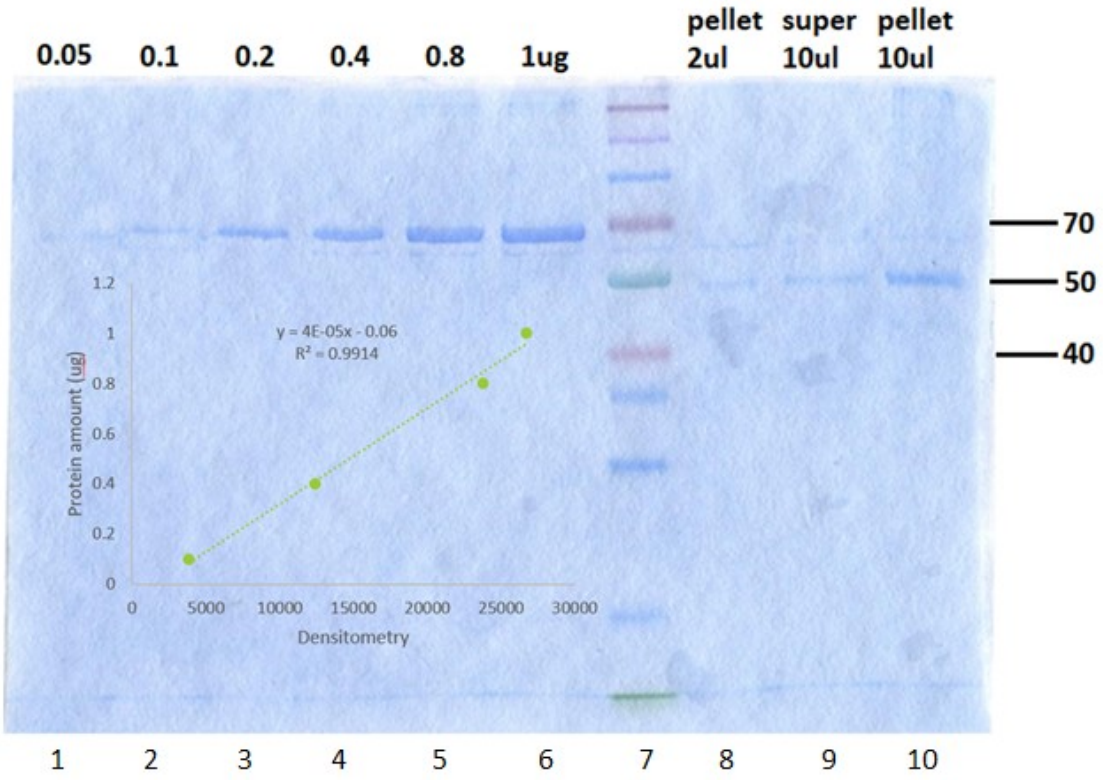


**Figure 24. SDS-PAGE analysis for dialysis refolding of GST-OCX-32 haplotype A.** The refolded protein at **lanes 8 and 9** (supernatant) was solubilized in 20mM Tris-HCl, 0.5M NaCl, 0.1mM oxidized glutathione, 1mM reduced glutathione, 0.02mM EDTA, 0.5mM BME pH 7. The pellet (**lane 10**) following dialysis was resolubilized in 6M guanidine hydrochloride, ethanol precipitated and finally solubilized in loading buffer. **Lane 1-6** show known amounts of bovine serum albumin (BSA) used for calculating the standard curve.

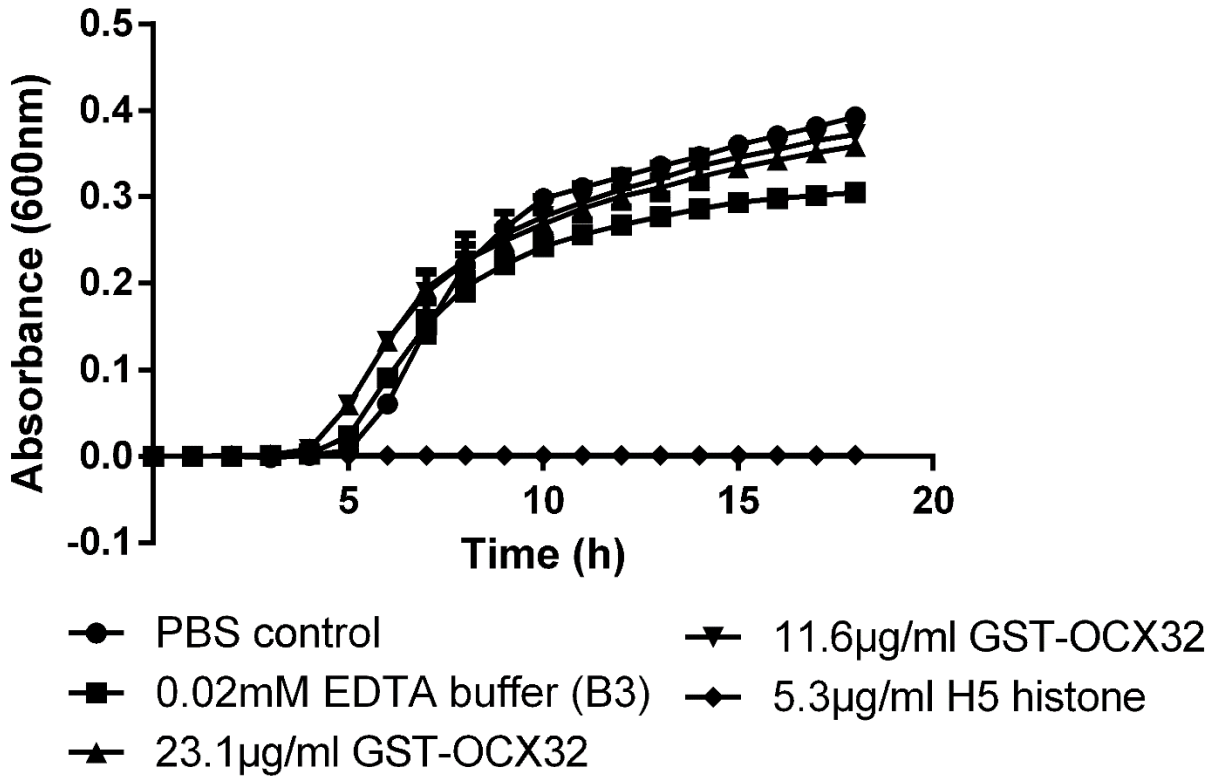


**Figure 25. Time-dependent growth of Gram-positive *B. cereus* under different conditions and at 2 concentrations of GST-OCX-32 haplotype A**. PBS, pH 7.4 was used as negative control of inhibition as well as buffer B3 (0.02mM EDTA). Histone H5 at 5.3 µg/ml was used as positive control for inhibition.

2.6 SUMO-OCX-32 dialysis refolding and antimicrobial activity test

Haplotype A 6xHis-SUMO-OCX-32-6xHis recombinant protein was overexpressed using *E. coli* Rosetta cells. Following solubilization of the protein from inclusion bodies using GnHCl, the recombinant OCX-32 was partially purified by nickel affinity chromatography under denaturing conditions. The denatured protein was refolded using dialysis by slowly diluting out the denaturant (**Figure 26**). The protein had a soluble yield of 98.5% and a final concentration of 763.0 μg/ml (total volume of 1ml refolded), according to densitometry analysis of the 42kDa band (**Figure 27**). The purity of the protein was 78.7% according to densitometry analysis comparing the 42kDa band with the total protein in the lane (**Figure 26**). Following purification, the SUMO-OCX-32 was tested against *B. cereus* to ascertain the presence of antimicrobial activity. The protein did not show any bacterial growth inhibition (increase in lag time) compared to control (**Figure 28**). For the assay, 4 μg/ml to 128 μg/ml were tested. This antimicrobial activity assay was repeated 3 times and showed similar results.

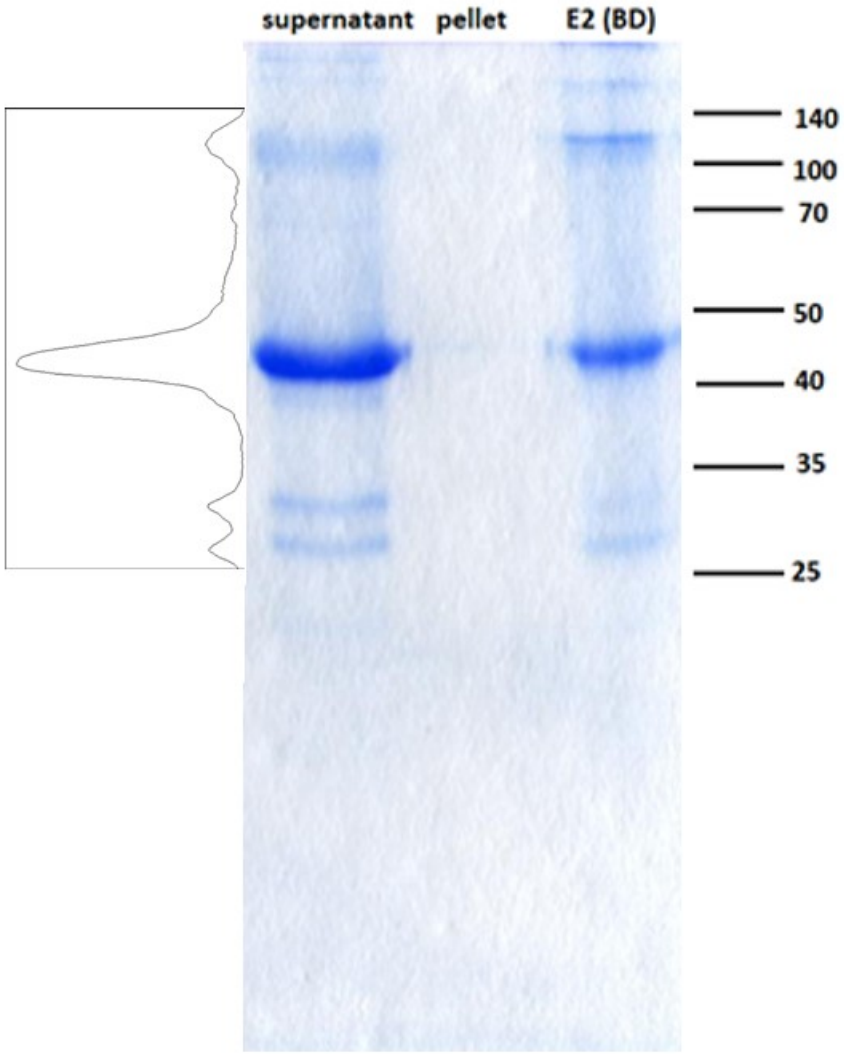


**Figure 26. SDS-PAGE analysis for dialysis refolding of SUMO-OCX-32 haplotype A.** The refolded protein (**supernatant**) was in a final dialysis buffer consisting of 20mM Tris-HCl, 0.5M NaCl, 0.1mM oxidized glutathione, 1mM reduced glutathione, 0.02mM EDTA, pH 7.0. The **pellet** following dialysis was resolubilized in 6M guanidine hydrochloride, ethanol precipitated and finally solubilized in loading buffer. **E2 (BD**) shows the starting material eluted from nickel affinity column under denaturing conditions, which was subsequently refolded by dialysis.

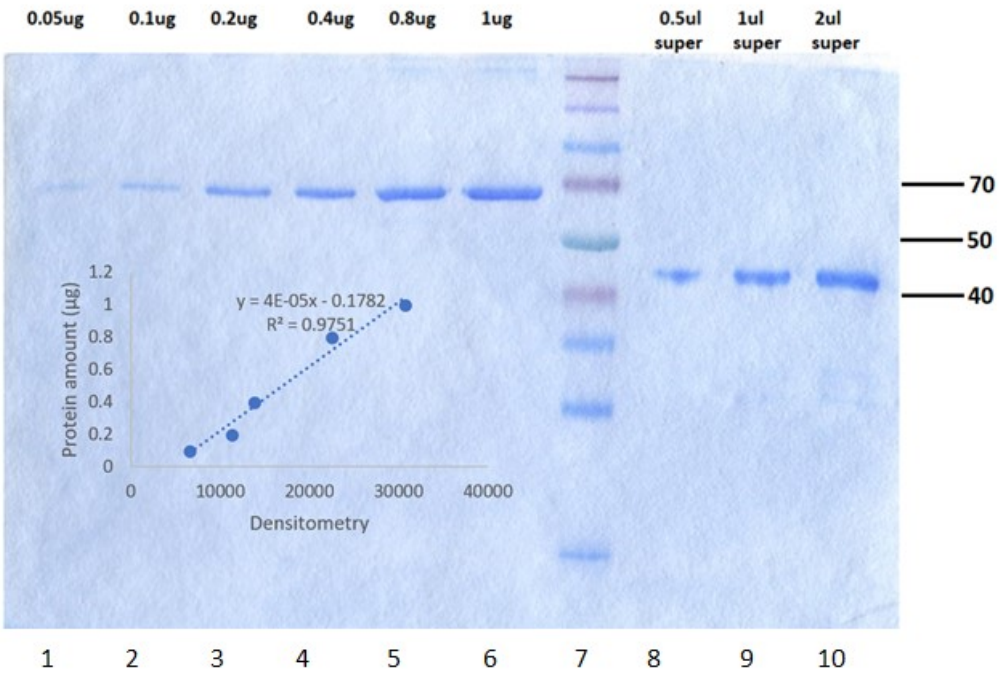


**Figure 27. SDS-PAGE analysis for dialysis refolding of SUMO-OCX-32 haplotype A.** The refolded protein (supernatant) was in a final dialysis buffer consisting of 20mM Tris-HCl, 0.5M NaCl, 0.1mM oxidized glutathione, 1mM reduced glutathione, 0.02mM EDTA, pH 7.0. Different volumes of the supernatant (**Lanes 8-10**) were loaded to avoid saturation for densitometry. **Lane 1-6** show known standards of bovine serum albumin (BSA) used for calculating the standard curve.

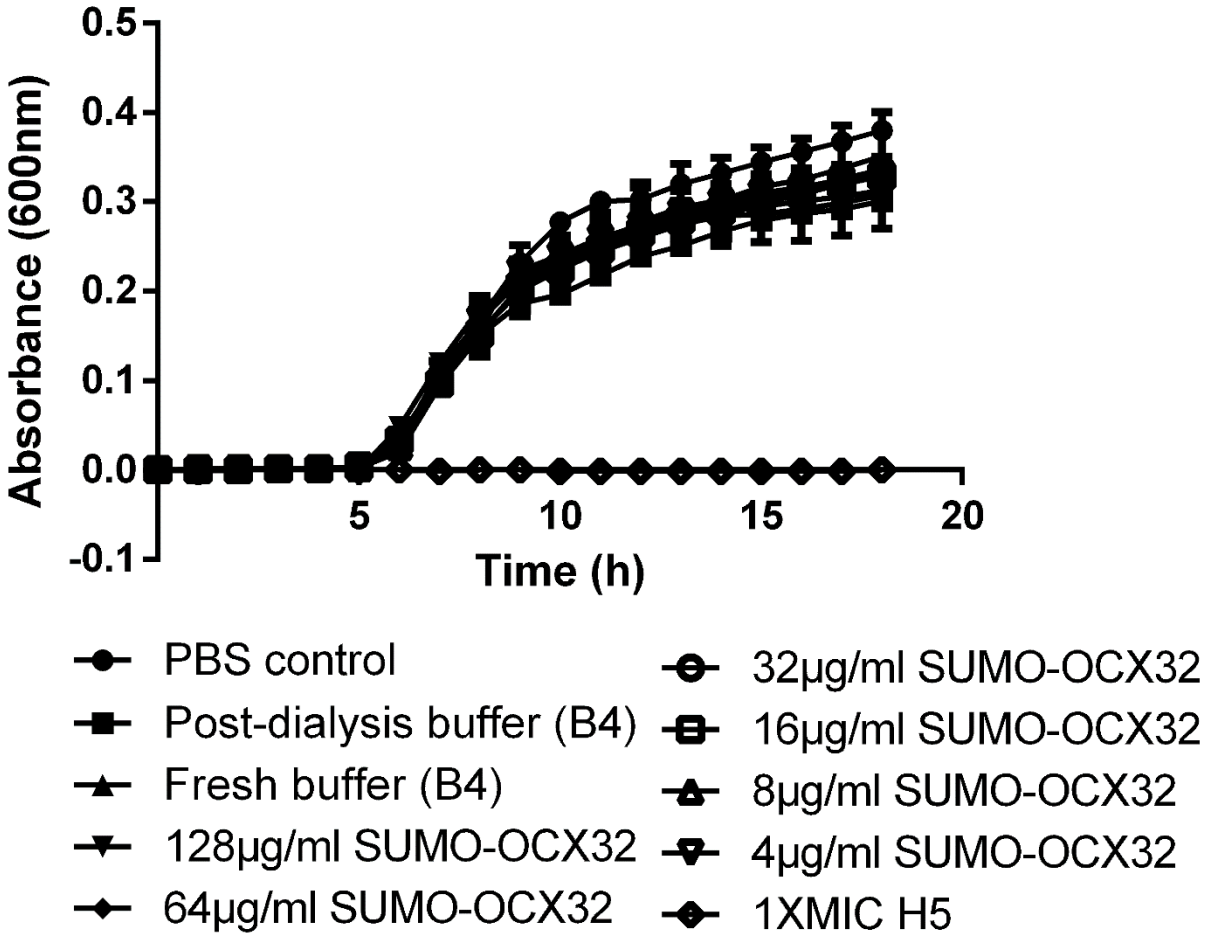


**Figure 28. Dose-dependent growth inhibition of Gram-positive *B. cereus* bacteria versus SUMO-OCX-32 haplotype A.** PBS pH 7.4 was used as negative control for inhibition. Post-dialysis buffer B4 (0mM BME) and fresh buffer B4 (0mM BME) were also evaluated as buffer controls. Histone H5 at 5.3 µg/ml was used as positive control for inhibition.

## Supplementary


**Figure S1. Proteomics analysis for all 5 haplotypes of 50kDa GST-OCX-32 recombinant protein band.** Yellow highlights indicate exclusive unique peptides. Green highlights on methionine residues indicate oxidation. Green highlights on asparagine and glutamine indicate deamidation.

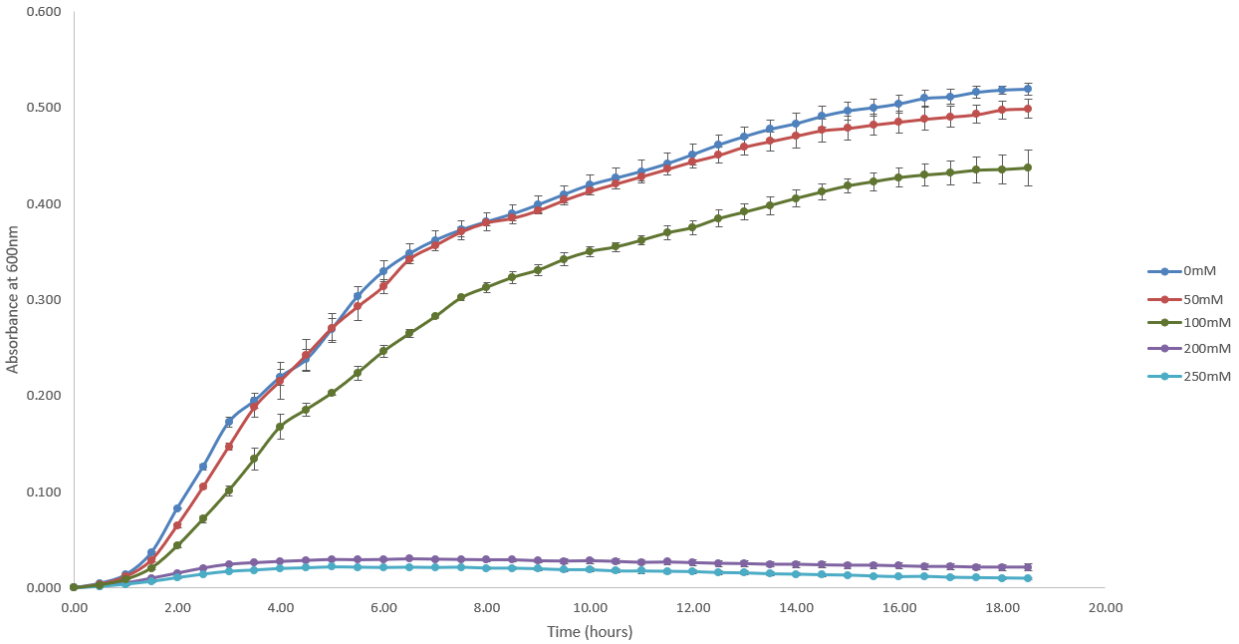


**Figure S2. Dose-dependent effect of imidazole on *Salmonella enterica* serovar Enteritidis growth.**

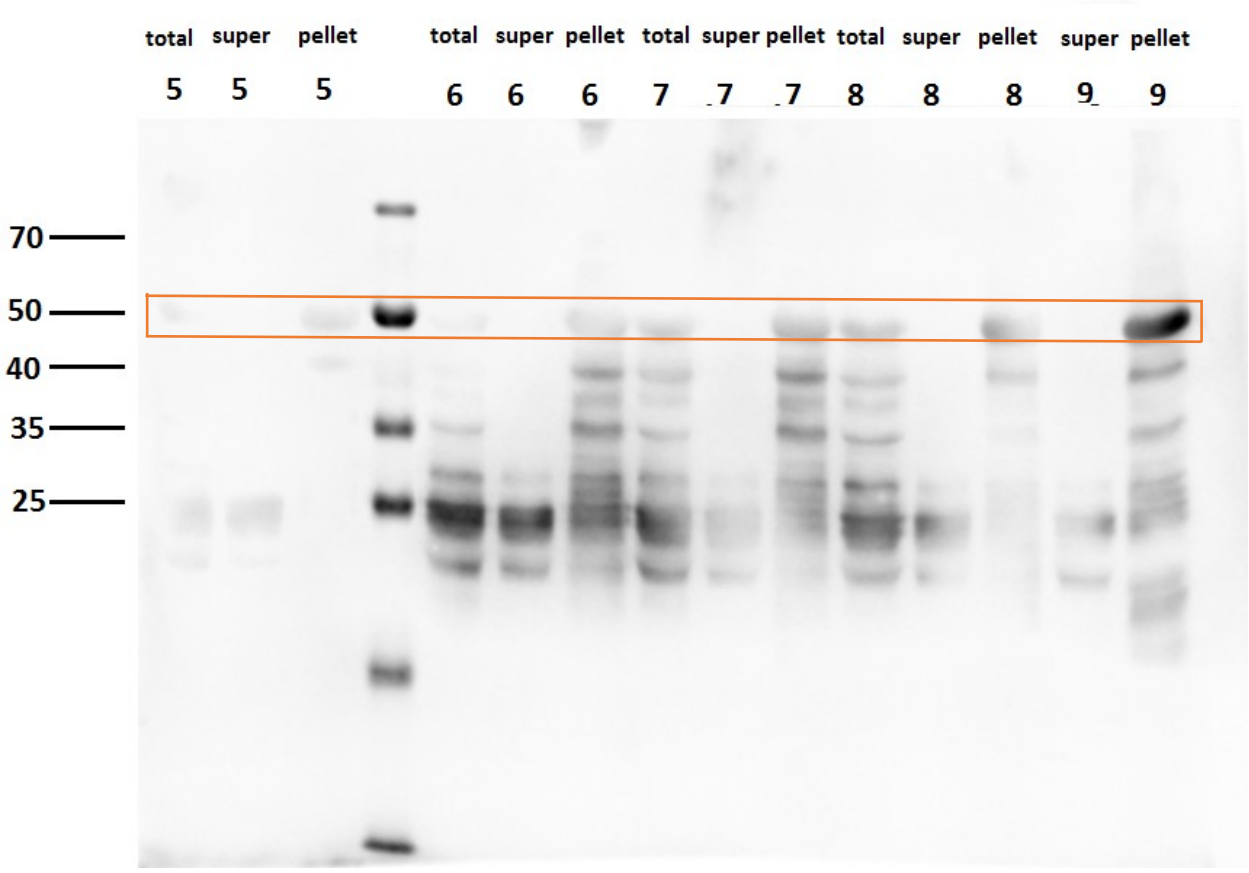


**Figure S3. Western blot analysis labelled with anti-GST antibody for E. coli Rosetta solubility test with various buffers (Table S1).** The outlined bands are the expected size for GST-OCX-32 recombinant protein. Total = total lysate prior to centrifuging, Super = supernatant following centrifugation of the lysate, Pellet= insoluble pellet following centrifugation of the lysate.

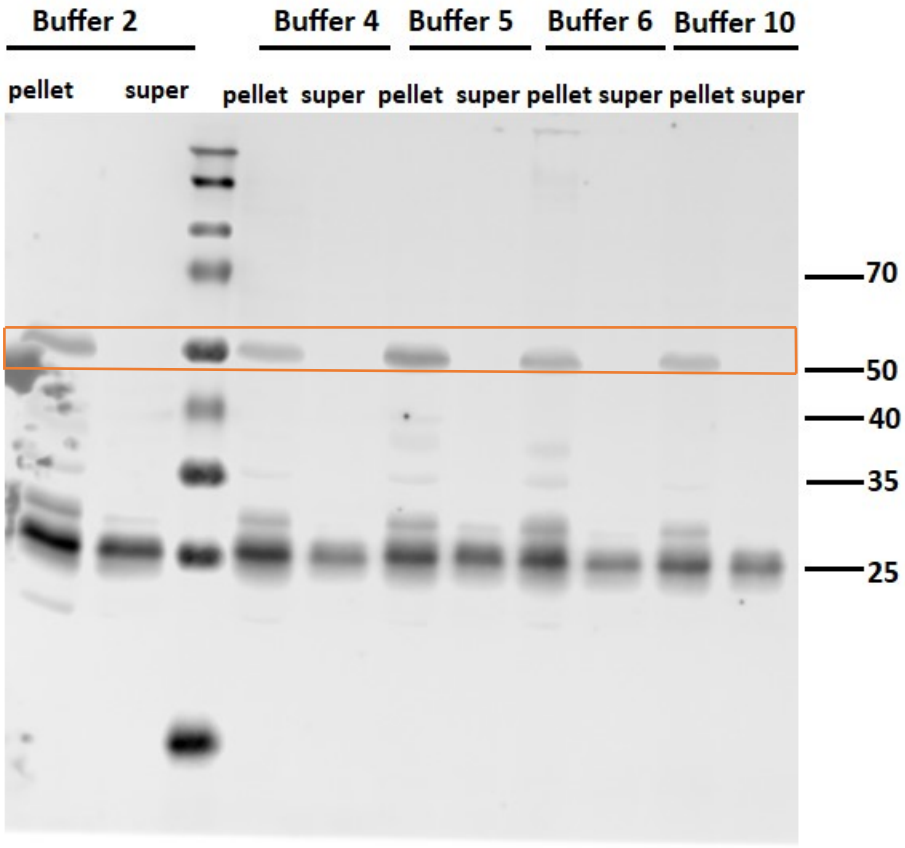


**Figure S4. Western blot analysis labelled with anti-GST antibody for *E. coli* RIL solubility test with various buffers (Table S1).** The outlined bands are the expected size for GST-OCX-32 recombinant protein. Pellet= insoluble pellet following centrifugation of the lysate, Super = supernatant following centrifugation of the lysate.

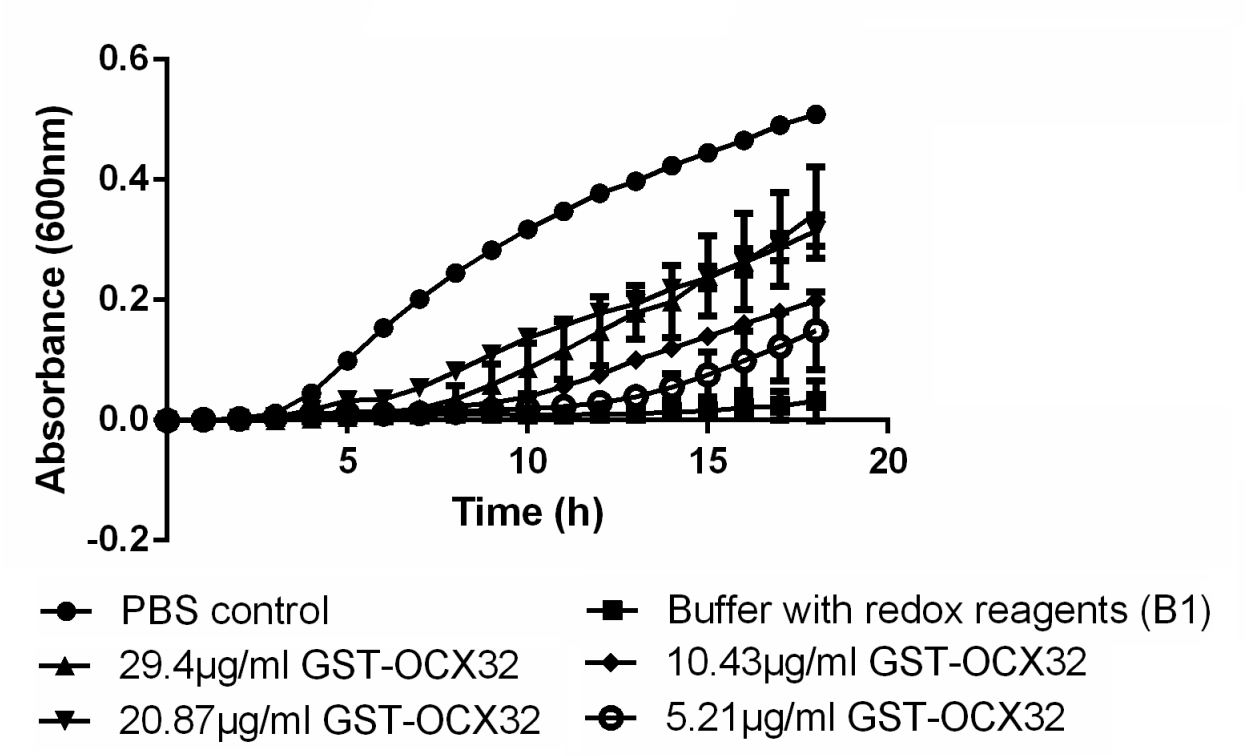


**Figure S5. Time-dependent growth of Gram-positive *S. aureus* bacteria in presence of GST-OCX-32 haplotype A.** The GST-OCX-32 was dissolved in 0.5M NaCl, 20mM Tris-HCl, 1mM reduced glutathione, 0.1mM oxidized glutathione, 0.2mM EDTA, 0.5mM BME, pH 7 **(B1).** This buffer was used as negative control of inhibition along with PBS pH 7.4.

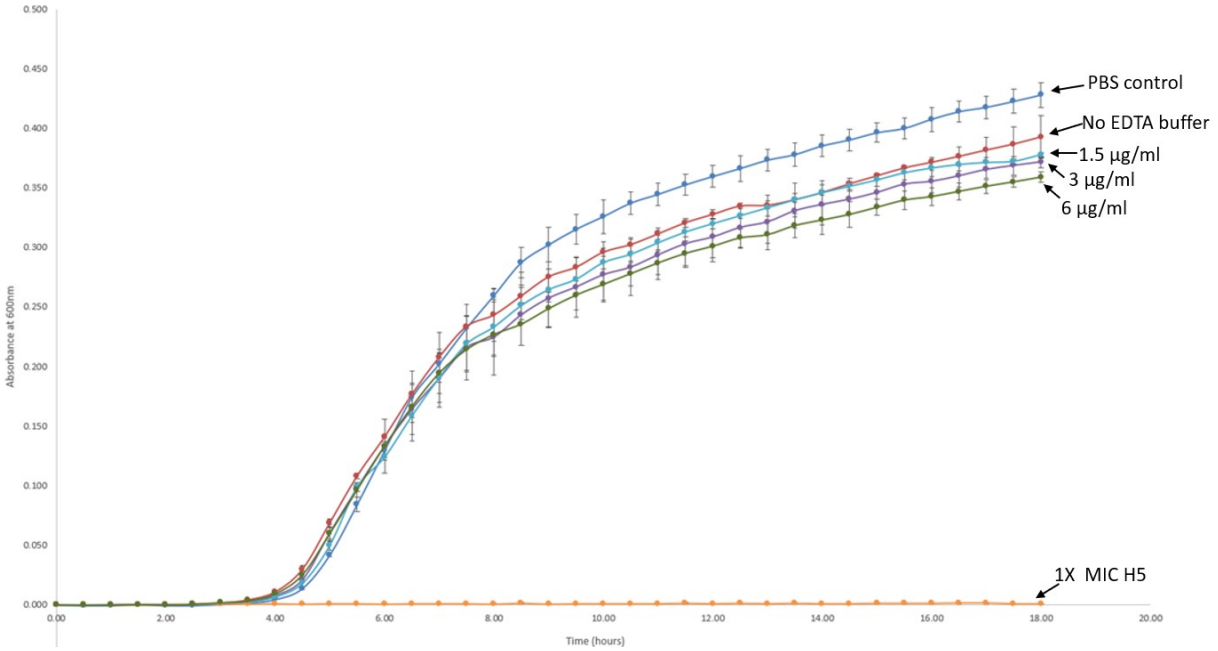


**Figure S6. Time-dependent growth of Gram-positive *B. cereus* bacteria in presence of GST-OCX-32 haplotype A.** The GST-OCX-32 was dissolved in 0.5M NaCl, 20mM Tris-HCl, 1mM reduced glutathione, 0.1mM oxidized glutathione, 0.5mM BME, pH 7 **(B2).** This buffer was used as negative control of inhibition along with PBS pH 7.4. Histone H5 was used as positive control of inhibition.

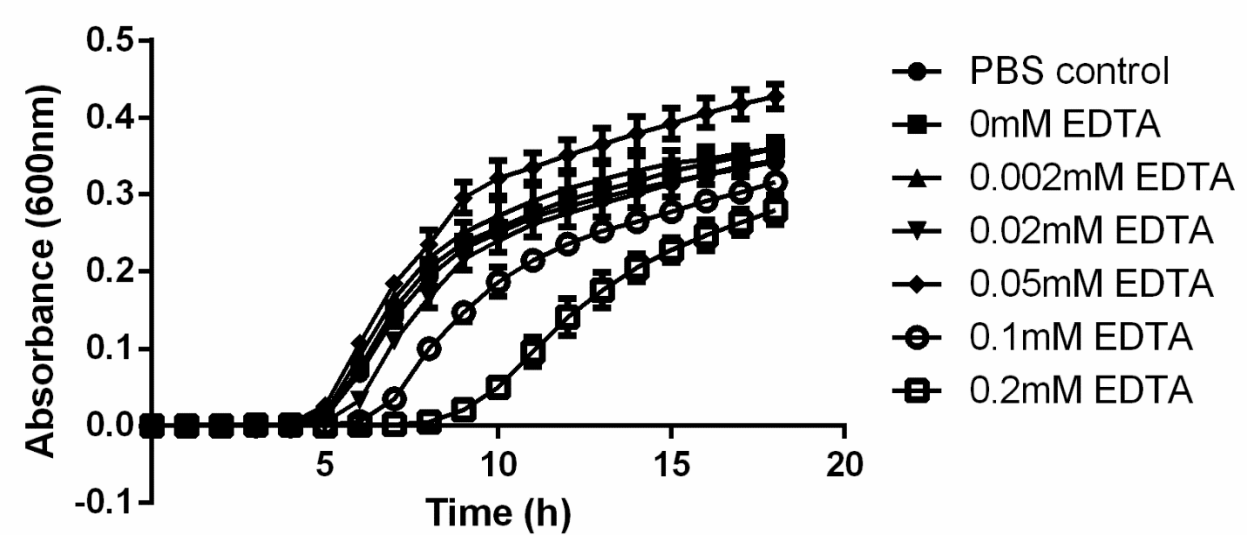


**Figure S7. Effect of EDTA on *B. cereus* growth.** The increasing EDTA concentrations in dialysis buffer (0.5M NaCl, 20mM Tris-HCl, 1mM reduced glutathione, 0.1mM oxidized glutathione, 0.5mM BME, pH 7) were evaluated PBS pH 7.4 was used as a negative control for inhibition.

**Table S1. Buffers used for Bugbuster mix**

| |
|---|
| 1. 50mM NaPi, 500mM NaCl, 5m, 10% glycerol, 1% Triton pH 7 |
| 2. 50mM Tris, 500mM NaCl, 10% glycerol, 1% Triton pH 7 |
| 3. 50mM HEPES, 500mM NaCl, 10% glycerol, 1% Triton pH 7 |
| 4. 50mM MES, 10% glycerol, 1% Triton pH 6.5 |
| 5. 1X PBS, 10% glycerol, 1% Triton pH 7 |
| 6. 50mM Tris, 150mM NaCl, pH 7 |
| 7. 50mM HEPES, 150mM NaCl, pH 7 |
| 8. 50mM Tris, 500mM NaCl, 10% glycerol, pH 7 |
| 9. 50mM HEPES, 500mM NaCl, 10% glycerol, pH 7 |
| 10. 50mM HEPES, 300mM NaCl, 10% glycerol, pH 7 |

**Table S2. Nucleotide sequence of PCR primers used for DNA sequencing and verification of ligation.** The PCR samples were denatured for 2min at 95$^{o}$C followed by 30 cycles of 30s at 95$^{o}$C, 30s at 60$^{o}$C, and 30s at 72$^{o}$C. Finally, it underwent final extension for 5min at 72$^{o}$C.

| | **Forward** | **Reverse** |
|---|---|---|
| **pGEX4T1 primer (GST)** | GGGCTGGCAAGCCACGTTTGGTG | CCGGGAGCTGCATGTGTCAGAGG |
| **pSMT3 primer (SUMO)** | GCGTTCGCTAAAAGACAGCG | AGGCTCTAGATTCGAAAGCGG |

# Chapter 4

# General Discussion

The Canadian poultry industry was worth $4.2 billion in 2016, with egg production accounting for $1.04 billion. Table eggs are the largest portion of the egg market at 73% with processed egg products representing the rest. Canadian per capita consumption was 238.8 eggs per year in 2016, which was a 2.7% increase from previous year. In addition, Canada exported $21.7 million worth of processed eggs in 2016 (AAFC, 2017). The poultry industry also includes broiler chickens grown for consumption. In Canada, the per capita consumption of chicken meat was 32.5kg in 2016. In addition, Canada also exported a total of 134.1 million kg of chicken products in 2016 alone (AAFC, 2017). Therefore, the poultry industry is a significant component of the dietary health of Canadians and of the Canadian economy.

**Antimicrobial proteins from broiler chickens**

One consequence of the size of the poultry industry is that it also produces large amounts of waste products. According to the environmental protection agency (EPA), blood from chicken processors accounts for their largest pollutant that enters the waste water treatment (EPA, 2002). Finding economical usages for blood from chicken processors could be very valuable since there are often imposed surcharges based on quantities of pollutants that enter the waste water (Garcia et al., 2016). This aspect was one component of our rationale to extract histones from chicken red blood cells. These RBCs are different from blood products of other livestock, since poultry RBCs are nucleated. Histones are well known to have antimicrobial activity and active histones or histone fragments have been isolated from various organisms such as mammalian, amphibian and fish species (Kawasaki and Iwamuro, 2008). In my study, the histones were tested against antibiotic-resistant and antibiotic-susceptible *S. aureus,* in both planktonic and biofilm forms (MRSA and MSSA). The project had several goals including:

determining the biofilm eradication concentration of the histone mixture against MSSA and MRSA, assessing the expression levels of AMP resistance genes that are upregulated in response to CAMPs, determining the kill kinetics of histone mixture against planktonic form of the two strains, and gaining insight into the mechanism histone bactericidal activity. For example, our study looked at several genes such as the *dlt* operon which induces D-alanylation of teichoic acids and *vraFG* which acts similarly to ABC transporter system to export the pore forming CAMPs such as histones (Rose-Martel et al., 2017). In my part of the project, the main goals were to assess the biofilm eradication concentration of the histones against MSSA and MRSA, to determine kill kinetics of the histone mixture against planktonic MSSA and MRSA, and to determine the interaction of histones with bacterial surfaces using SEM. The extracted histone mixture completely eradicated mature biofilms for the two strains (MSSA and MRSA) at relatively low concentrations (MSSA= 21±5 µg/ml, MRSA=23±5 µg/ml), compared to other CAMPs such as indolicidin, CAMA (cecropin (1-7)–melittin A (2-9) amide) and nisin that have MBEC values of 512, 5120, and 640 µg/ml, respectively, against MRSA (Mataraci and Dosler, 2012). The histone MBEC values for both strains were significantly higher than the previously determined MIC values for planktonic forms (Rose-Martel and Hincke, 2014). However, the MBEC to MIC ratio was not as high as similar cationic antimicrobial peptides such as indolicidin and nisin. These CAMPs are much less active against biofilm MRSA with 40 to 80-fold higher MBEC compared to MIC (Mataraci and Dosler, 2012). Similarly, traditional antibiotics also show very high biofilm eradication concentrations compared to their MIC for planktonic bacteria. For example, the *P. aeruginosa* biofilm inhibitory concentration is 256 µg/ml for the piperacillin/tazobactam combination compared to 4 µg/ml for planktonic bacteria (Moskowitz

et al., 2004). *S. aureus* shows a similar phenomenon with vancomycin; its MBEC is >256 µg/ml, versus a MIC of 1 µg/ml for its planktonic form (LaPlante and Mermel, 2009). In addition, we saw a significant reduction in growth at concentrations much lower than the MBEC ($p \leq 0.002$). MSSA was significantly reduced at histone mixture concentrations comparable to its MIC (8 µg/ml vs MIC of 6±1 µg/ml). MRSA showed significant reduction at 16 µg/ml or 2XMIC ($p \leq 0.0001$). Therefore, the histone mixture shows very strong activity against biofilms of both strains of *S. aureus* at concentrations that are similar to their MICs. Therefore, the histone mixture retained its activity even in the presence of the extracellular polymeric substance (EPS) in which the bacteria were embedded, that would hinder antibiotic penetration.

In order to determine the kinetics of biocidal activity of the histone mixture against planktonic MRSA and MSSA, time kill curves were performed. Another CAMP, indolicidin, was used as a positive control for inhibition. The histone mixture showed the most activity against MRSA, in that it eliminated >2 $\log_{10}$ of bacteria within 5 min at 1xMIC. MSSA showed lower susceptibility to the histones with only 0.5 $\log_{10}$ reduction in 5 min at the same concentration (1xMIC). Therefore, the resistance mechanism of the MRSA strain to methicillin is not protective against the histones mechanism of bacterial cell death. Indolicidin activity at 1XMIC was even more rapid with 5 min incubation leading to a ~6 $\log_{10}$ reduction in both strains. This may be due to the small size of indolicidin (13 aa) or its increased proportion of hydrophobic residues (38% tryptophan and 23% proline) compared to the average histones composition (16 kDa and 28-45% hydrophobicity) (Falla et al., 1996; Rose-Martel et al., 2017). Therefore, the kill kinetics study on planktonic MSSA and MRSA showed that histones can rapidly inhibit bacterial growth (within 5 min of exposure), with MRSA showing the greater susceptibility.

CAMPs mainly interact with bacteria through surface interactions such as pore formation or physical thinning of the cell membrane (Brogden, 2005). The histone mixture from chicken erythrocytes has been previously shown to interact with Gram-positive LTA as well as Gram-negative LPS (Rose-Martel and Hincke, 2014). Thus, a possible mechanism of action for the histone mixture against *S. aureus* is bacterial membrane damage. The MRSA biofilm was visualized using scanning electron microscopy to identify visible damage on the bacterial surface. The bacterial cells encased in the biofilm appeared smooth and fully spherical when treated with sterile water. The bacteria incubated with 128 µg/ml histones showed numerous amounts of bacterial surface damage, such as signs of blebbing, pore formation as well as cell collapse. As predicted, the histones affect the bacterial membranes similarly to other CAMPs such as LL-37 and magainins (Brogden, 2005).

Overall, the histone mixture from chicken erythrocytes has shown potent activity against biofilm forms of MSSA and MRSA. This can be very beneficial in future treatments due to the increased prevalence of antibiotic resistance of many pathogens as well as the difficulty in treating mature biofilms. In addition, a possible mechanism was studied through how the histone mixture affects the bacterial surface. The bacteria showed clear signs of damage following exposure to histones. Thus, one possible mechanism of histones affecting biofilm could be membrane damage, which could provide a point of entry for histone molecules to cause internal cell damage. Moreover, the kinetics of biocidal activity against planktonic *S. aureus* showed that there is significant reduction of bacteria within 5 min of exposure to the histones. Therefore, the histone mixture from chicken RBCs showed eradication activity at relatively low concentrations compared to other CAMPs that require >100µg/ml to completely

eradicate biofilms. Therefore, our data demonstrates that histones may become a good alternative to conventional antibiotics in treating antibiotic-resistant strains of *S. aureus* in both planktonic and biofilm forms.

**Increasing eggshell antimicrobial protection through selective expression of a cuticle protein**

Egg-associated infections are very serious in such a large industry, which includes table eggs and processed eggs that enter the market as baked goods, mayonnaise, various types of pasta and noodles etc. One of the most dangerous pathogens that affects eggs in the United States is *Salmonella enterica* serovar Enteritidis (CDC, 2017b). Since the avian egg is essential for reproductive success, it has many natural protective elements. The integrity of the eggshell, which is made up of multiple layers, is a key factor. The cuticle is the surface layer which is the first line of defence as well as protection against dehydration of the egg contents. The cuticle contains proteins including ovocalyxin-32 (Jonchère et al., 2010). One of the main goals of my project was to express and purify this protein which has previously been shown to have antimicrobial activity (Xing et al., 2007). Thus, I worked on expressing recombinant versions of 5 haplotypes of the OCX-32 protein that are naturally occurring in commercial egg-laying flocks. The protein was expressed in *E. coli* and various purification methods were attempted. The largest barrier that I encountered was obtaining soluble protein, either due to the nature of *E. coli* as a protein expression system and its lack of post-translational modification, or due to the intrinsic nature of the recombinant protein. The original recombinant protein contained glutathione-S-transferase (GST) at the N-terminus. This tag was included to enhance solubility of the fusion partner and help with purification through binding with glutathione agarose (Costa et al., 2014). The recombinant protein also contained a histidine tag at the C-terminus of

the OCX-32 which served as another purification method through nickel affinity chromatography. This chromatographic method is based on immobilized metal ions, such as nickel or cobalt, that act as ligands to bind the imidazole ring in histidine residues; it is possible to enrich the protein up to 100-fold through a single pass (Pierce Protein methods, 2011).

Many issues were explored to prepare soluble recombinant OCX-32. The expression conditions were first changed to produce as much protein as possible in the soluble fraction. This was done through optimizing the induction concentration, temperature, and time. This method showed that the IPTG concentration could be halved while retaining high expression levels. From the various concentrations tested, a mid-range concentration of 0.5mM showed highest amounts of induced protein even compared to 1mM. This approach also helped to minimize degradation of the target protein due to the effects of expressing a foreign protein in the bacteria. When bacteria are induced to produce such large quantities of non-essential protein, the limited bacterial resources cannot meet the demand and the bacterial growth rate is decreased (Malakar and Venkatesh, 2012). This reduction in the growth rate is most evident during the early exponential phase (Malakar and Venkatesh, 2012). Thus, for this study, the bacteria were not induced until they attained $OD_{600}$ = 0.5, in order to allow bacteria to reach sufficient numbers without the burden of expressing large quantities of foreign protein. Through this optimization process, we found that a reduced induction temperature (15$^{o}$C) allowed bacterial expression to progress slowly and with less degradation. This was compared to 22$^{o}$C and 30$^{o}$C. Lastly, incubation times were also optimized to produce as much protein as possible at the lower temperature without leading to degradation. Induction for long periods can be stressful for the bacteria due to hijacking of translation machinery and may even lead to

cell death. However, if the growth is not conducted for sufficient duration, the quantity of expressed protein can also suffer. Thus, a wide range of growth times were evaluated, ranging from 1h to 18h. The longest incubation period expressed the highest amount of protein. However, degradation was also clearly higher compared to shorter incubation periods. Incubation period of 6h showed highest protein expression with minimal proteolytic degradation compared to 12h and 18h. Therefore, in all subsequent experiments, the recombinant protein was expressed using 0.5mM IPTG for 6h at 15$^{o}$C.

Following optimization of protein expression, the quantity of soluble protein obtained was still too low to perform any antimicrobial activity assay. The majority of heterologous proteins are often packaged into inclusion bodies. This aggregation is even more probable when the protein being over-expressed contains multiple cysteine residues that require formation of disulfide bridges for native conformation (Butt et al., 2005). Inclusion bodies contain mostly the incorrectly folded protein and can form aggregates in the cytosol or the periplasmic space (Singh et al., 2015). The inclusion bodies can sometimes aggregate to such a large degree that they are visible under light microscope (Butt et al., 2005). These inclusion bodies present a lot of problems in terms of solubility of the expressed protein, since they often require denaturation to dissolve. However, they can also act as a form of purification step, since they are relatively easy to separate from the rest of the bacterial proteins through cell lysis and centrifugation. Other bacterial proteins that can co-precipitate with the inclusion bodies may require further washes, with low concentration of denaturant such as urea as well as detergents, to remove (Vallejo and Rinas, 2004). Therefore, the conditions developed for the optimization process (15$^{o}$C incubation for 6h with 0.5mM IPTG) were used to express

recombinant OCX-32 and purify it from the inclusion bodies. This allowed a much larger starting concentration of protein since most of the over-expressed protein was found to be aggregated into inclusion bodies. The inclusion bodies were washed, purified, and then fully dissolved in denaturing conditions. The soluble recombinant protein was bound to the metal ion affinity resin via its 6xhistidine tag. The protein refolding was attempted while the OCX-32 was bound to the nickel affinity column. This allowed some of the protein to be successfully refolded. However, the quantity of soluble protein obtained was very low and could not be pooled together from different batches due to protein losses during attempts to concentrate with spin-filters. We assessed where protein was being lost, since the starting denatured protein quantities were >1mg/ml and the resulting soluble protein was <50µg from 200ml of starting culture. We found that the problem was precipitation within the metal ion affinity column; most of the protein was precipitating when the denaturant was removed within a relatively short time. Thus, the rate of removal of denaturant had to be much slower. The slower refolding would require much longer incubation periods and buffer volumes compared to producing soluble protein from the initial culture.

In order to explore other avenues prior to committing to the slower refolding, we also assessed using an alternative bacterial expression strain to provide rare tRNAs that standard *E. coli* does not normally express. In addition, a strain that increases disulfide bond formation through mutations in two of its genes was evaluated. These strains would produce some fraction of the recombinant protein in soluble form and eliminate the need for denaturation. However, neither strategy produced the GST-OCX-32 recombinant protein in soluble form.

Thus, alternative methods were required to change the recombinant protein and force it into soluble fraction. Another protein tag, small ubiquitin-like modifier (SUMO), was tested in order to decrease the size of the tag and increase solubility. The small ubiquitin-like modifier (SUMO) tag is known to enhance solubility as well as stability of the fusion protein (Kong and Guo, 2011). Following this change, the new recombinant protein was expressed in both *E. coli* Rosetta as well as Origami 2. However, even with the change in fusion partner, the SUMO-OCX-32 recombinant protein was still aggregating in inclusion bodies. The only changes that were apparent compared to the GST-OCX-32 recombinant protein was that the new tag enhanced total expression levels and led to much higher recombinant protein quantities while using same culture conditions and starting amounts. Therefore, we had to resort to slower refolding of this protein extracted from inclusion bodies to obtain sufficient protein for antimicrobial activity assay.

The above trials showed that the recombinant protein was not being solubilized even following changes to buffer, strain, and protein tag. Thus, the inclusion bodies were used to isolate recombinant protein. Following isolation of the inclusion bodies, a correct redox environment is required to form the correct disulfide bonds while the denaturant is removed. The redox environment can be provided by adding low concentrations of oxidized and reduced glutathione (Okumura et al., 2011). The denaturant can be slowly diluted out using other methods instead of the step-wise reduction used in on-column refolding. However, the protein may precipitate in the intermediate folding steps due to non-native interactions between hydrophobic residues (Vallejo and Rinas, 2004). One way to remove the denaturant is through dialysis. The protein can be directly dissolved in the denaturant and then the concentration of

the denaturant is reduced through slow dilution. This can be a good method since the protein of interest is dissolved in larger volume and thus starting concentration is low, which minimizes aggregation. However, it can also have disadvantages since the protein will need to be re-concentrated later for use in functional testing. In addition, the amounts of buffer used can be quite large. One alternative to this method is using dialysis tubing to retain the denatured protein while removing the denaturant by dialysis. This must be done slowly since the protein is much more concentrated in the dialysis bag than in the previous method of direct dilution. This approach of using dialysis bag was chosen going forward since it would eliminate the steps of re-concentrating the protein which can lead to further losses.

The slow refolding through dialysis was first conducted using the original recombinant protein, GST-OCX-32-6XHis. In addition to denaturant, oxidized and reduced glutathione, the buffer also contained 0.2mM EDTA and 0.5mM BME. EDTA chelates divalent cations such as nickel which can leach from the affinity chromatography and lead to His-tag mediated aggregation. EDTA also chelates other trace divalent cations that could interfere with the refolding process. BME reduces any misfolded disulfide bonds, which are especially problematic in the early stages of the refolding. Following reduction of the denaturant within a brief period of hours (3-8h), the soluble protein obtained was still very low (<40µg). The protein precipitated heavily during the last stages of refolding. Small quantities of the soluble recombinant protein were however tested for antimicrobial activity. It was found that certain buffer components that enhanced refolding, such as EDTA, inhibited bacterial growth by themselves. Therefore, the EDTA concentration was reduced 10-fold. Following this change of EDTA, the refolded protein yield was similar: 18.8% compared 21.5%. This showed that more than 80% of our starting protein in

inclusion bodies were precipitating. Thus, it was evident that GST as a protein tag was not enhancing the refolding or solubility of the fusion partner.

However, SUMO has been shown to enhance protein refolding without prior solubility enhancement in the absence of denaturant (Kong and Guo, 2011). Thus, the SUMO-OCX-32 recombinant protein was denatured and refolded using dialysis. The new recombinant protein showed almost complete solubility (>98%) after diluting out the denaturant by dialysis. The higher solubility amounts could be due to the structure of the SUMO tag which has a hydrophobic core and hydrophilic surface that allows it to act as a detergent towards its partner (Butt et al., 2005; Kong and Guo, 2011). This may indicate that the SUMO tag is enhancing protein solubility similar to its original role in eukaryotes as a chaperone in protein folding (Butt et al., 2005). The SUMO may act as a nucleation site for protein refolding similarly to ubiquitin and thus help the fusion partner to refold correctly (Khorasanizadeh et al., 1996). The refolded SUMO-OCX-32 recombinant protein was tested against a major food pathogen, *Bacillus cereus*. The rOCX-32 did not show antimicrobial activity against this pathogen when tested up to 128µg/ml, possibly due to failure to retain activity following denaturation and subsequent refolding with improper disulfide bond formation. Thus, the buffer conditions could be affecting the refolded protein and preventing the formation of a correct native conformation. The haplotype that was tested could also have very low activity compared to the remaining 4 haplotypes. Hence, in the future, it will be necessary to also test the antimicrobial activity of the remaining haplotypes following expression and refolding. If antimicrobial activity against antibiotic susceptible food pathogens is detected, OCX-32 will be tested against antibiotic resistant strains. This includes antibiotic resistant *Salmonella* serovars Typhimurium and

Enteritidis. If the protein provides potent activity, it could be exploited in therapeutic applications. Further purification of the refolded protein may also prove beneficial since it is currently only ~80% pure. The removal of other contaminants may increase the activity of our protein of interest. This could be done through nickel affinity chromatography and elution at various concentrations of imidazole to separate the different sized contaminants. It can also be done through size-exclusion chromatography (SEC) since the difference in molecular weight between the contaminants and the recombinant protein is sufficient (rOCX-32 = 42kDa vs main contaminants ≅ 30kDa). However, since this difference in size is lower than two-fold, multiple passes through the SEC would probably be required for necessary resolution. Moreover, the SUMO tag could be affecting the activity of the OCX-32, and could be removed using the internal cleavage site, Ulp1. The subsequent separation of the SUMO and OCX-32 moieties might prove challenging as both contain histidine tag. Therefore, SEC may be required or nickel affinity chromatography with range of imidazole concentrations for eluting out the two components. Alternatively, the expression construct could be redesigned to delete the N-terminal His-tag associated with the SUMO. This would simplify separation of the tag from the target protein.

Overall, the OCX-32 fusion protein shows great difficulty in solubilization even following changes in bacterial strain, protein tag, and using various buffers. The on-column refolding step was associated with a large amount of precipitation, which could be due to rapid decrease of urea or to changing from guanidine hydrochloride to urea. Slow refolding of the recombinant OCX-32 using dialysis showed some promise in terms of obtaining protein for antimicrobial activity testing. The dialysis refolding for SUMO-OCX-32 showed very high solubility (>98%) and

generated large quantities of protein in soluble form. However, the solubilized protein failed to show antimicrobial activity. This could have been due to (1) incorrect refolding which did not retain activity of the protein, (2) the haplotype tested does not have antimicrobial activity, (3) the SUMO or its constituent histidine tag affects the activity of ovocaxlyin-32. These possible issues would have to be tested in future studies. The cDNA for the remaining haplotypes will need to be ligated into the SUMO plasmid to express the different recombinant proteins. In addition, the SUMO tag could also be cleaved from purified recombinant protein using Ulp1 protease to test the potential antagonistic effects of SUMO.

In the studies reported here, two dramatically different approaches were taken. Isolation of an antimicrobial histone mixture from an abundant starting material proved to be highly successful and promising. On the other hand, expression of a soluble recombinant protein for functional assessment proved to be highly problematic and required great investment of time and energy to prepare a soluble protein for testing. Further developmental work will be necessary to determine if this approach is a viable strategy.

## References


AAFC (2017). Canada's table and processed egg industry. Available at: http://www.agr.gc.ca/eng/industry-markets-and-trade/market-information-by-sector/poultry-and-eggs/poultry-and-egg-market-information/table-and-processed-eggs/?id=1384971854396. Accessed 20 November 2017

Ahmed, T.A.E., Suso, H.-P., and Hincke, M.T. (2017). In-depth comparative analysis of the chicken eggshell membrane proteome. J. Proteomics *155*: 49–62.

Akira, S. (2001). Toll-like Receptors and Innate Immunity. Adv. Immunol. *78*: 1–56.

Band, V.I., and Weiss, D.S. (2015). Mechanisms of Antimicrobial Peptide Resistance in Gram-Negative Bacteria. Antibiot. (Basel, Switzerland) *4*: 18–41.

Berrang, M.E., Cox, N.A., Frank, J.F., and Buhr, R.J. (1999). Bacterial Penetration of the Eggshell and Shell Membranes of the Chicken Hatching Egg: A Review. J. Appl. Poult. Res. *8*: 499–504.

Bjarnsholt, T., Ciofu, O., Molin, S., Givskov, M., and Høiby, N. (2013). Applying insights from biofilm biology to drug development — can a new approach be developed? Nat. Rev. Drug Discov. *12*: 791–808.

Blattner, F.R., Plunkett, G., Bloch, C.A., Perna, N.T., Burland, V., Riley, M., et al. (1997). The complete genome sequence of Escherichia coli K-12. Science *277*: 1453–62.

Board, R., and Tranter, H.S. (1986). The microbiology of eggs. In Egg Science and Technology, O.J.C. W.J Stadelman, ed. (Westport, CT: AVI Publishing Company), p.

Brinkmann, V., and Zychlinsky, A. (2012). Neutrophil extracellular traps: Is immunity the second function of chromatin? J. Cell Biol. *198*: 773–783.

Brogden, K.A. (2005). Antimicrobial peptides: pore formers or metabolic inhibitors in bacteria? Nat. Rev. Microbiol. *3*: 238–250.

Bruce, J., and Drysdale, E.M. (1994). Trans-shell transmission. In Microbiology of the Avian Egg, (Boston, MA: Springer US), pp 63–91.

Butt, T.R., Edavettal, S.C., Hall, J.P., and Mattern, M.R. (2005). SUMO fusion technology for difficult-to-express proteins. Protein Expr. Purif. *43*: 1–9.

BVTech Plasmid (2017). Plasmid map of pGEX-4T-1. Available at: http://www.biovisualtech.com/bvplasmid/pGEX-4T-1.htm. Accessed 28 October 2017

CDC (2013a). Antibiotic Resistance Threats in the United States, 2013. Available at: https://www.cdc.gov/drugresistance/threat-report-2013/index.html. Accessed 17 February 2018

CDC (2013b). Untreatable: Report by CDC details today's drug-resistant health threats. Available at: https://www.cdc.gov/media/releases/2013/p0916-untreatable.html. Accessed 2 November 2017

CDC (2016a). How Influenza (Flu) Vaccines Are Made. Available at: https://www.cdc.gov/flu/protect/vaccine/how-fluvaccine-made.htm. Accessed 1 November 2017

CDC (2016b). Superbugs threaten hospital patients. Available at: https://www.cdc.gov/media/releases/2016/p0303-superbugs.html. Accessed 2 November 2017

CDC (2017a). Biggest Threats | Antibiotic/Antimicrobial Resistance | CDC. Available at: https://www.cdc.gov/drugresistance/biggest_threats.html. Accessed 30 October 2017

CDC (2017b). Salmonella and Food. Available at: https://www.cdc.gov/features/salmonella-food/index.html. Accessed 23 November 2017

Centers for Disease Control and Prevention (2016). General Information | MRSA | CDC. Available at: https://www.cdc.gov/mrsa/community/index.html. Accessed 18 November 2017

CFIA (2013). Food-Related Illnesses. Available at: https://www.canada.ca/en/health-canada/services/food-nutrition/food-safety/food-related-illnesses.html. Accessed 27 November 2017

Ciofu, O., Rojo-Molinero, E., Macià, M.D., and Oliver, A. (2017). Antibiotic treatment of biofilm infections. APMIS *125*: 304–319.

Cohen, W.D. (1982). The cytomorphic system of anucleate non-mammalian erythrocytes. Protoplasma *113*: 23–32.

Conly, J., and Johnston, B. (2005). Where are all the new antibiotics? The new antibiotic paradox. Can. J. Infect. Dis. Med. Microbiol. = J. Can. Des Mal. Infect. La Microbiol. Medicale *16*: 159–60.

Cordeiro, C.M.M., Esmaili, H., Ansah, G., and Hincke, M.T. (2013). Ovocalyxin-36 is a pattern recognition protein in chicken eggshell membranes. PLoS One *8*: e84112.

Costa, S., Almeida, A., Castro, A., and Domingues, L. (2014). Fusion tags for protein solubility, purification and immunogenicity in Escherichia coli: the novel Fh8 system. Front. Microbiol. *5*: 63.

Dominguez-Vera, J.M., Gautron, J., Garcia-Ruiz, J.M., and Nys, Y. (2000). The effect of avian uterine fluid on the growth behavior of calcite crystals. Poult. Sci. *79*: 901–7.

Dunn, I.C., Joseph, N.T., Bain, M., Edmond, A., Wilson, P.W., Milona, P., et al. (2009). Polymorphisms in eggshell organic matrix genes are associated with eggshell quality measurements in pedigree Rhode Island Red hens. Anim. Genet. *40*: 110–114.

EPA (2002). Development Document for the Proposed Effluent Limitations Guidelines and Standards for the Meat and Poultry Products Industry Point Source Category (40 CFR 432) (Washington, D.C.: DIANE Publishing).

Falla, T.J., Karunaratne, D.N., and Hancock, R.E. (1996). Mode of action of the antimicrobial peptide indolicidin. J. Biol. Chem. *271*: 19298–303.

Flemming, H.-C., Neu, T.R., and Wozniak, D.J. (2007). The EPS matrix: the "house of biofilm cells". J. Bacteriol. *189*: 7945–7.

Flemming, H.-C., and Wingender, J. (2010). The biofilm matrix. Nat. Rev. Microbiol. *8*: 623–33.

Fulton, J.E., Soller, M., Lund, A.R., Arango, J., and Lipkin, E. (2012a). Variation in the ovocalyxin-32 gene in commercial egg-laying chickens and its relationship with egg production and egg quality traits. Anim. Genet. *43*: 102–113.

Fulton, J.E., Soller, M., Lund, A.R., Arango, J., and Lipkin, E. (2012b). Variation in the ovocalyxin-32 gene in commercial egg-laying chickens and its relationship with egg production and egg quality traits. *43*: 102–113.

Gantois, I., Ducatelle, R., Pasmans, F., Haesebrouck, F., Gast, R., Humphrey, T.J., et al. (2009).

Mechanisms of egg contamination by *Salmonella* Enteritidis. FEMS Microbiol. Rev. *33*: 718–738.

Garcia, R.A., Nieman, C.M., Haylock, R.A., Rosentrater, K.A., and Piazza, G.J. (2016). The effect of chicken blood and its components on wastewater characteristics and sewage surcharges. Poult. Sci. *95*: 1950–1956.

Gautron, J., Hincke, M.T., Mann, K., Panhéleux, M., Bain, M., McKee, M.D., et al. (2001). Ovocalyxin-32, a Novel Chicken Eggshell Matrix Protein. J. Biol. Chem. *276*: 39243–39252.

Gavazzi, G., Herrmann, F., and Krause, K.-H. (2004). Aging and Infectious Diseases in the Developing World. Clin. Infect. Dis. *39*: 83–91.

GE Healthcare Life Sciences (2017). HiTrap Chelating HP immobilized metal affinity chromatography columns - GE Healthcare.

Gole, V.C., Chousalkar, K.K., Roberts, J.R., Sexton, M., May, D., Tan, J., et al. (2014). Effect of egg washing and correlation between eggshell characteristics and egg penetration by various Salmonella Typhimurium strains. PLoS One *9*: e90987.

Götting, M., and Nikinmaa, M. (2015). More than hemoglobin - the unexpected diversity of globins in vertebrate red blood cells. Physiol. Rep. *3(2)*: e12284.

Hannig, G., and Makrides, S.C. (1998). Strategies for optimizing heterologous protein expression in Escherichia coli. Trends Biotechnol. *16*: 54–60.

Health Canada, and Public Health Agency of Canada (2014). Impacts of antibiotic resistance.

Hincke, M.T., Gautron, J., Mann, K., Panhéleux, M., McKee, M.D., Bain, M., et al. (2003). Purification of ovocalyxin-32, a novel chicken eggshell matrix protein. Connect. Tissue Res. *44 Suppl 1*: 16–9.

Hincke, M.T., Nys, Y., Gautron, J., Mann, K., Rodriguez-Navarro, A.B., and McKee, M.D. (2012). The eggshell: structure, composition and mineralization. Front. Biosci. (Landmark Ed. *17*: 1266–80.

Hirsch, J.G. (1958). Bactericidal action of histone. J. Exp. Med. *108*: 925–44.

Høiby, N., Bjarnsholt, T., Givskov, M., Molin, S., and Ciofu, O. (2010). Antibiotic resistance of bacterial biofilms. Int. J. Antimicrob. Agents *35*: 322–332.

Hughey, V.L., and Johnson, E.A. (1987). Antimicrobial activity of lysozyme against bacteria involved in food spoilage and food-borne disease. Appl. Environ. Microbiol. *53*: 2165–70.

Iannotti, L.L., Lutter, C.K., Bunn, D.A., and Stewart, C.P. (2014). Eggs: the uncracked potential for improving maternal and young child nutrition among the world's poor. Nutr. Rev. *72*: 355–368.

Jodoin, J. (2017). Histone H5: Bioinspiration for novel antimicrobial peptides. University of Ottawa.

Jonchère, V., Réhault-Godbert, S., Hennequet-Antier, C., Cabau, C., Sibut, V., Cogburn, L.A., et al. (2010). Gene expression profiling to identify eggshell proteins involved in physical defense of the chicken egg. BMC Genomics *11*: 57.

Kawasaki, H., and Iwamuro, S. (2008). Potential roles of histones in host defense as antimicrobial agents. Infect. Disord. Drug Targets *8*: 195–205.

Keller, L.H., Benson, C.E., Krotec, K., and Eckroade, R.J. (1995). Salmonella enteritidis colonization of the reproductive tract and forming and freshly laid eggs of chickens. Infect. Immun. *63*: 2443–9.

Khorasanizadeh, S., Peters, I.D., and Roder, H. (1996). Evidence for a three-state model of protein folding from kinetic analysis of ubiquitin variants with altered core residues. Nat. Struct. Biol. *3*: 193–205.

Kong, B., and Guo, G.L. (2011). Enhanced In Vitro Refolding of Fibroblast Growth Factor 15 with the Assistance of SUMO Fusion Partner. PLoS One *6*: e20307.

Kulshreshtha, G., Rodriguez-Navarro, A., Sanchez-Rodriguez, E., Diep, T., and Hincke, M.T. (2018). Cuticle and pore plug properties in the table egg. Poult. Sci.

LaPlante, K.L., and Mermel, L.A. (2009). In vitro activities of telavancin and vancomycin against biofilm-producing Staphylococcus aureus, S. epidermidis, and Enterococcus faecalis strains. Antimicrob. Agents Chemother. *53*: 3166–9.

Lodise, T.P., and McKinnon, P.S. (2007). Burden of Methicillin-Resistant *Staphylococcus aureus* : Focus on Clinical and Economic Outcomes. Pharmacotherapy *27*: 1001–1012.

Lyon, B.R., and Skurray, R. (1987). Antimicrobial resistance of Staphylococcus aureus: genetic basis. Microbiol. Rev. *51*: 88–134.

Maeda, H., and Yamamoto, T. (1996). Pathogenic mechanisms induced by microbial proteases in microbial infections. Biol. Chem. Hoppe. Seyler. *377*: 217–26.

Malakar, P., and Venkatesh, K. V. (2012). Effect of substrate and IPTG concentrations on the burden to growth of Escherichia coli on glycerol due to the expression of Lac proteins. Appl. Microbiol. Biotechnol. *93*: 2543–2549.

Marcq, C., Théwis, A., Portetelle, D., and Beckers, Y. (2013). Refinement of the production of antigen-specific hen egg yolk antibodies (IgY) intended for passive dietary immunization in animals. A review. Biotechnol. Agron. Société Environ. *17*: 483–493.

Mataraci, E., and Dosler, S. (2012). In Vitro Activities of Antibiotics and Antimicrobial Cationic Peptides Alone and in Combination against Methicillin-Resistant Staphylococcus aureus Biofilms. Antimicrob. Agents Chemother. *56*: 6366–6371.

Matsuzaki, K. (1999). Why and how are peptide-lipid interactions utilized for self-defense? Magainins and tachyplesins as archetypes. Biochim. Biophys. Acta *1462*: 1–10.

Moskowitz, S.M., Foster, J.M., Emerson, J., and Burns, J.L. (2004). Clinically feasible biofilm susceptibility assay for isolates of Pseudomonas aeruginosa from patients with cystic fibrosis. J. Clin. Microbiol. *42*: 1915–22.

NCBI (2017). RARRES1 retinoic acid receptor responder 1 [ Gallus gallus (chicken) ]. Available at: https://www.ncbi.nlm.nih.gov/gene?cmd=retrieve&list_uids=395209. Accessed 27 November 2017

Neu, H.C. (1992). The crisis in antibiotic resistance. Science (80-. ). *257*: 1064–1074.

NIH (2016). Gram-negative Bacteria. Available at: https://www.niaid.nih.gov/research/gram-negative-bacteria. Accessed 17 February 2018

O'Toole, G., Kaplan, H.B., and Kolter, R. (2000). Biofilm Formation as Microbial Development. Annu. Rev. Microbiol. *54*: 49–79.

Okumura, M., Saiki, M., Yamaguchi, H., and Hidaka, Y. (2011). Acceleration of disulfide-coupled protein folding using glutathione derivatives. FEBS J. *278*: 1137–1144.

Park, C.B., Yi, K.-S., Matsuzaki, K., Kim, M.S., and Kim, S.C. (2000). Structure-activity analysis of buforin II, a histone H2A-derived antimicrobial peptide: The proline hinge is responsible for the cell-penetrating ability of buforin II. Proc. Natl. Acad. Sci. *97*: 8245–8250.

Patrick, M.E., Adcock, P.M., Gomez, T.M., Altekruse, S.F., Holland, B.H., Tauxe, R. V., et al. (2004). *Salmonella* Enteritidis Infections, United States, 1985–1999. Emerg. Infect. Dis. *10*: 1–7.

Peschel, A., and Sahl, H.-G. (2006). The co-evolution of host cationic antimicrobial peptides and microbial resistance. Nat. Rev. Microbiol. *4*: 529–536.

Peterson, C.L., and Hansen, J.C. (2008). Chicken erythrocyte histone octamer preparation. CSH Protoc. *2008*: pdb.prot5112.

Pierce Protein methods (2011). His-tagged Proteins–Production and Purification. Available at: https://www.thermofisher.com/ca/en/home/life-science/protein-biology/protein-biology-learning-center/protein-biology-resource-library/pierce-protein-methods/his-tagged-proteins-production-purification.html. Accessed 26 November 2017

Pierce Protein Methods (2017). GST-tagged Proteins–Production and Purification. Available at: https://www.thermofisher.com/ca/en/home/life-science/protein-biology/protein-biology-learning-center/protein-biology-resource-library/pierce-protein-methods/gst-tagged-proteins-production-purification.html. Accessed 6 November 2017

Promega (2017). GoTaq® Green Master Mix Protocol. Available at: https://www.promega.ca/resources/protocols/product-information-sheets/g/gotaq-green-master-mix-m712-protocol/. Accessed 29 November 2017

Public Health Agency of Canada (2016). Infographic: Food-related illnesses, hospitalizations and deaths in Canada. Available at: https://www.canada.ca/en/public-health/services/publications/food-nutrition/infographic-food-related-illnesses-hospitalizations-deaths-in-canada.html. Accessed 17 February 2018

Ramachandran, G. (2014). Gram-positive and gram-negative bacterial toxins in sepsis: a brief review. Virulence *5*: 213–8.

Rosano, G.L., and Ceccarelli, E.A. (2014). Recombinant protein expression in Escherichia coli : advances and challenges. *5*: 1–17.

Rose-martel, M., Du, J., and Hincke, M.T. (2012). Proteomic analysis provides new insight into the chicken eggshell cuticle. J. Proteomics *75*: 2697–2706.

Rose-Martel, M., and Hincke, M.T. (2014). Antimicrobial histones from chicken erythrocytes bind bacterial cell wall lipopolysaccharides and lipoteichoic acids. Int. J. Antimicrob. Agents *44*: 470–472.

Rose-Martel, M., and Hincke, M.T. (2017). The Eggshell Proteome Yields Insight Into Its Antimicrobial Protection. In Egg Innovations and Strategies for Improvements, (Elsevier), pp 157–163.

Rose-Martel, M., Kulshreshtha, G., Ahferom Berhane, N., Jodoin, J., and Hincke, M.T. (2017). Histones from Avian Erythrocytes Exhibit Antibiofilm activity against methicillin-sensitive and methicillin-resistant Staphylococcus aureus. Sci. Rep. *7*: 45980.

Sass, V., Pag, U., Tossi, A., Bierbaum, G., and Sahl, H.-G. (2008). Mode of action of human β-defensin 3 against Staphylococcus aureus and transcriptional analysis of responses to defensin challenge. Int. J. Med. Microbiol. *298*: 619–633.

Scallan, E., Hoekstra, R.M., Angulo, F.J., Tauxe, R. V, Widdowson, M.-A., Roy, S.L., et al. (2011). Foodborne illness acquired in the United States--major pathogens. Emerg. Infect. Dis. *17*: 7–15.

Schloss, P.D., and Handelsman, J. (2004). Status of the microbial census. Microbiol. Mol. Biol. Rev. *68*: 686–91.

Schwartz, S.O., and Stansbury, F. (1954). Significance of nucleated red blood cells in peripheral blood; analysis of 1,496 cases. J. Am. Med. Assoc. *154*: 1339–40.

Scott, M.G., Gold, M.R., and Hancock, R.E. (1999). Interaction of cationic peptides with lipoteichoic acid and gram-positive bacteria. Infect. Immun. *67*: 6445–53.

Simor, A.E., Gilbert, N.L., Gravel, D., Mulvey, M.R., Bryce, E., Loeb, M., et al. (2010). Methicillin-Resistant Staphylococcus aureus Colonization or Infection in Canada: National Surveillance and Changing Epidemiology, 1995–2007. Infect. Control Hosp. Epidemiol. *31*: 348–356.

Singh, A., Upadhyay, V., Upadhyay, A.K., Singh, S.M., and Panda, A.K. (2015). Protein recovery from inclusion bodies of Escherichia coli using mild solubilization process. Microb. Cell Fact. *14*: 41.

Sparks, N.H.C., and Board, R.G. (1984). Cuticle, shell porosity and water uptake through hens' eggshells. Br. Poult. Sci. *25 (2)*:267-276.

Stewart, P.S., and Costerton, J.W. (2001). Antibiotic resistance of bacteria in biofilms. Lancet (London, England) *358*: 135–8.

Supuran, C.T. (2012). Inhibition of bacterial carbonic anhydrases and zinc proteases: from orphan targets to innovative new antibiotic drugs. Curr. Med. Chem. *19*: 831–44.

Travis, J., and Potempa, J. (2000). Bacterial proteinases as targets for the development of second-generation antibiotics. Biochim. Biophys. Acta *1477*: 35–50.

Vallejo, L., and Rinas, U. (2004). Strategies for the recovery of active proteins through refolding of bacterial inclusion body proteins. Microb. Cell Fact. *3*: 11.

Wellman-Labadie, O., Picman, J., and Hincke, M.T. (2008). Antimicrobial activity of cuticle and outer eggshell protein extracts from three species of domestic birds. Br. Poult. Sci. *49*: 133–143.

WHO (2017). WHO | Antimicrobial resistance (World Health Organization). Available at: http://www.who.int/mediacentre/factsheets/fs194/en/. Accessed 30 October 2017

Xing, J., Wellman-labadie, O., Gautron, J., and Hincke, M.T. (2007). Recombinant eggshell ovocalyxin-32 : Expression , purification and biological activity of the glutathione S -transferase fusion protein. *147*: 172–177.

Yeaman, M.R., and Yount, N.Y. (2003). Mechanisms of Antimicrobial Peptide Action and Resistance. Pharmacol. Rev. *55*: 27–55.

Zasloff, M. (2002). Antimicrobial peptides of multicellular organisms. Nature *415*: 389–395.

Zasloff, M., Martin, B., and Chen, H.C. (1988). Antimicrobial activity of synthetic magainin peptides and

several analogues. Proc. Natl. Acad. Sci. U. S. A. *85*: 910–3.

Zentner, G.E., and Henikoff, S. (2013). Regulation of nucleosome dynamics by histone modifications. Nat. Struct. Mol. Biol. *20*: 259–266.